



**ATORVASTATIN INDUCES APOPTOSIS VIA THE PI3K/AKT  
SIGNALLING PATHWAY IN HUMAN HEPATOCELLULAR  
CARCINOMA (HEPG2) CELLS**

**By**

**TASKEEN FATHIMA DOCRAT**

*Bsc. B. Med Sc. (Hons) University of KwaZulu-Natal*

*Submitted in fulfillment of the requirements for the degree of Master of Medical  
Science (Medical Biochemistry), School of Laboratory Medicine and Medical  
Sciences, College of Health Sciences, University of KwaZulu-Natal*

**2016**

## DECLARATION

I, Miss Taskeen Fathima Docrat, declare as follows:

That the work described in this thesis has not been submitted to UKZN or other tertiary institution for purposes of obtaining an academic qualification, whether by myself or any other party. The use of work by others has been duly acknowledged in the text.

That my contribution to the project was as follows: all laboratory experiments, analysis of data and writing of thesis was done individually.

That the contributions of others to the project were as follows:

- a) Professor A.A. Chaturgoon is the primary supervisor. The concepts of the project were formulated by him. He was involved in laboratory guidance, and editing of thesis.
- b) Dr S. Nagiah is the co-supervisor. She has also assisted in developing the concepts of the project. She has been involved in lab work as well as editing of the thesis.

Signed:



Date: 12/ 12/ 2016

---

---

**DEDICATION**

**In Loving Memory of My Father,**

**Aboobaker Docrat**

*(27/03/1952 - 06/07/2006)*

## **ACKNOWLEDGEMENTS**

### **God**

First and above all, I praise God for providing me with this opportunity and granting me the capability to proceed successfully.

### **My mum**

You have always been my pillar of strength, for all that you do for me, the constant motivation, encouragement, love and support, I am eternally grateful. Without you I would not be where I am today.

### **Professor A.A. Chuturgoon**

I thank you for giving me the opportunity of being a part of Medical Biochemistry; I have grown under your care. I am grateful for the thoughtful guidance, motivation and constructive criticism. Unlike most professors who teach their students to find the right answers, you've taught us to ask the right questions. You are a true inspiration. As one would remember a brilliant student, I will always remember my brilliant professor.

### **Dr S. Nagiah**

I could not have asked for a better mentor, you add character and legacy to the walls of this department that would have been just a brick and mortar structure. I am deeply grateful for all the friendly assistance, valuable advice, insightful discussion and your support throughout the duration of my study. Thank you for believing in me. I hope you reach great heights of success.

### **Miss D.B Naidoo**

I would like to express my gratitude towards you for the laboratory assistance and support you have given me during my study. You have moulded me into a better young scientist. I wish you well for your future.

### **My loved ones**

To my siblings and loved ones, I appreciate having you all in my life; words cannot describe how lucky I am.

### **My friends**

I could not have asked for a better group of friends to share my postgraduate study with, Miss S. Dhani, Miss L. Gungatharan, Miss T. Ghazi Miss L. Shunmugam, Miss N. Devnarain, Miss D. Moodley, and Mr N. Sheik Abdul. I thank you all for your support, laboratory assistance and the good memories we have created.

### **The PhD students and staff of Medical Biochemistry**

I would like to express my sincere appreciation to Dr C. Tiloke and Miss S. Raghubeer for their patience and assistance in the laboratory, Mrs N. Needhi for all the technical assistance and thoughtful guidance, and Ms R. Myburg for the warm encouragement and motherly advice. To the rest of the staff, Master, and PhD students, thank you for the support and assistance.

### **The National Research Foundation and College of Health Science, UKZN**

I would like to thank NRF and CHS for the scholarship and funding of this study.

## PRESENTATIONS

Atorvastatin induces apoptosis via the PI3K/Akt signalling pathway in Human Hepatocellular Carcinoma (HepG2) cells.

T. F., Docrat, S., Nagiah, and A.A. Chuturgoon

College of Health Sciences Research Symposium, University of KwaZulu-Natal, Durban, South Africa (11-12 September 2016)

## TABLE OF CONTENTS

<b>DECLARATION</b> .....	<b>i</b>
<b>DEDICATION</b> .....	<b>ii</b>
<b>ACKNOWLEDGEMENTS</b> .....	<b>iii</b>
<b>PRESENTATIONS</b> .....	<b>v</b>
<b>LIST OF FIGURES</b> .....	<b>ix</b>
<b>LIST OF ABBREVIATIONS</b> .....	<b>xi</b>
<b>ABSTRACT</b> .....	<b>xvii</b>
<b>CHAPTER ONE</b> .....	<b>1</b>
<b>1.1 INTRODUCTION</b> .....	<b>1</b>
<b>1.1.1 Study Rationale and aims</b> .....	<b>2</b>
<b>1.1.2 Aim</b> .....	<b>3</b>
<b>1.1.3 Objectives of this study were designed to:</b> .....	<b>3</b>
<b>1.1.4 Hypothesis</b> .....	<b>3</b>
<b>1.2 LITERATURE REVIEW</b> .....	<b>4</b>
<b>1.2.1 Statins</b> .....	<b>4</b>
<b>1.2.1.1 Mode of action of statins in Coronary Artery Disease</b> .....	<b>5</b>
<b>1.2.1.2 Mechanism of action of statins and cancer</b> .....	<b>5</b>
<b>1.2.1.3 Epidemiological link between HMG-CoA reductase inhibitors and cancer</b> ..	<b>6</b>
<b>1.2.1.4 Biochemical effects of statins</b> .....	<b>7</b>
<b>1.2.2 Liver cancer</b> .....	<b>8</b>
<b>1.2.2.1 HepG2 cells</b> .....	<b>8</b>
<b>1.2.3 Reactive oxygen species (ROS)</b> .....	<b>9</b>
<b>1.2.3.1 Free Radicals</b> .....	<b>9</b>
<b>1.2.3.2 Antioxidants</b> .....	<b>9</b>
<b>1.2.3.3 Cytochrome P450 3A4</b> .....	<b>10</b>
<b>1.2.4 Apoptosis</b> .....	<b>11</b>
<b>1.2.4.1 The intrinsic pathway of apoptosis</b> .....	<b>12</b>
<b>1.2.4.2 The extrinsic pathway of apoptosis</b> .....	<b>13</b>
<b>1.2.5 Necrosis</b> .....	<b>15</b>
<b>1.2.6 Role of PI3K/Akt signalling pathway in apoptosis and cell survival</b> .....	<b>15</b>
<b>1.2.7 Forkhead Box (FOXOs), c-Myc and the cell cycle</b> .....	<b>16</b>
<b>1.2.8 PI3K/Akt and cell cycle progression</b> .....	<b>18</b>

1.2.8.1	PI3K/Akt and NF- $\kappa$ B .....	19
1.2.8.2	PI3K/Akt and p53 crosstalk .....	19
1.2.9	Inflammatory status and cytokines.....	20
CHAPTER 2	.....	21
2.1	Materials and methods.....	21
2.1.1	Materials .....	21
2.2	Cell culture and maintenance.....	22
2.3	Atorvastatin preparation.....	23
2.4	Cell proliferation and metabolic activity.....	24
2.4.1	MTT assay.....	24
2.4.2	Treatment for subsequent assays.....	26
2.4.3	The ATP quantification assay .....	26
2.5	Oxidative status .....	28
2.5.1	The thiobarbituric acid reactive substance assay.....	28
2.5.2	The Griess assay .....	29
2.5.3	GSH-Glo <sup>TM</sup> Glutathione assay .....	30
2.5.4	Cytochrome-P <sub>450</sub> 3A4 assay kit.....	31
2.6	Cellular Death.....	32
2.6.1	The lactate dehydrogenase assay .....	32
2.6.2	Analysis of caspase activity.....	33
2.6.3	Enzyme-linked immunosorbent assay (ELISA) .....	34
2.7	Western Blotting.....	36
2.7.1	Protein extraction, quantification and standardisation .....	36
2.7.2	SDS-PAGE .....	38
2.7.3	Protein transfer .....	38
2.7.4	Immuno-Blotting.....	39
2.7.5	Quantification of band density using Chemiluminescence.....	40
2.7.6	Membrane re-probing.....	40
2.8	Statistical Analysis.....	40
CHAPTER THREE	.....	41
RESULTS	.....	41
3.1	Cell proliferation and metabolic activity.....	41
3.1.1	Cell Viability .....	41
3.1.2	Intracellular ATP levels.....	42



3.2	Oxidative status .....	42
3.2.1	Lipid Peroxidation.....	42
3.2.2	Level of nitrates and nitrites.....	43
3.2.3	Glutathione concentration .....	44
3.2.4	Cytochrome P450 3A4 Activity .....	45
3.3	Cellular Death.....	46
3.3.1	Extracellular LDH level.....	46
3.3.2	Analysis of caspases.....	47
3.3.3	Cytokine analysis.....	48
3.4	Western Blotting.....	49
CHAPTER FOUR.....		53
DISCUSSION .....		53
CHAPTER FIVE.....		58
5.1	Limitations of study .....	58
5.2	CONCLUSION.....	58
REFERENCES .....		59
APPENDIX 1 .....		68
MTT RAW DATA.....		68
APPENDIX 2 .....		68
GSH standards .....		68
APPENDIX 3 .....		70
ELISA standards- TNF- $\alpha$ .....		70
ELISA standards- IL-6.....		71
ELISA standards- IL-1 $\beta$ .....		72
ELISA standards- IL-10.....		73
APPENDIX 4.....		75
Protein quantification and standardisation .....		75

## LIST OF FIGURES

### CHAPTER 1

<b>Figure 1.1:</b> Chemical structure of Atorvastatin. (Kracun et al., 2009).....	4
<b>Figure 1.2:</b> Mechanism of action of Atorvastatin: inhibits cholesterol synthesis (prepared by author: Docrat, 2016). HMG-CoA: 3-hydroxy-3-methyl-glutaryl-coenzyme A, HMGCR: 3-hydroxy-3-methyl-glutaryl-coenzyme A reductase, PP: Pyrophosphate, ROS: Reactive oxygen species, eNOS: endothelial nitric oxide synthase, NADPH: Nicotinamide adenine dinucleotide phosphate.....	6
<b>Figure 1.3:</b> Antioxidant activity of GSH (prepared by author: Docrat, 2016) .....	10
<b>Figure 1.4:</b> Schematic representations of the main molecular pathways leading to apoptosis (Favaloro et al., 2012) .....	13
<b>Figure 1.5:</b> Induction of apoptosis in malignant cells due to novel chemotherapeutic agents that act in a specific manner (Wong et al., 2002).....	14
<b>Figure 1.6:</b> Inhibitory effect of statins on mevalonate and its downstream effects on PI3K/AKT signalling pathway (prepared by author: Docrat, 2016).....	16
<b>Figure 1.7:</b> Cell cycle regulation (prepared by author: Docrat, 2016) .....	18

### CHAPTER 2

<b>Figure 2.1:</b> A summary of methodology used in all experiments in the study (prepared by author: Docrat, 2016) .....	22
<b>Figure 2.2:</b> Trypan Blue dye exclusion method (prepared by author: Docrat, 2016) .....	23
<b>Figure 2.3:</b> Preparation of Atorvastatin from crystalline to amorphous form (PACE- Physician's Academy for Cardiovascular Education, 2016) .....	24
<b>Figure 2.4:</b> Principle of MTT assay (prepared by author: Docrat, 2016).....	25
<b>Figure 2.6:</b> Luciferase reaction where mono-oxygenation of luciferase occurs (prepared by author: Docrat, 2016) .....	27
<b>Figure 2.7:</b> Principle of TBARS assay (prepared by author: Docrat, 2016) .....	28
<b>Figure 2.8:</b> Principle of Griess reaction .....	29
<b>Figure 2.9:</b> Overview of GSH-Glo™ Glutathione Assay principle (prepared by author: Docrat, 2016). .....	30
<b>Figure 2.10:</b> Reaction involved in the P450-Glo™ assay (prepared by author: Docrat, 2016) .	32
<b>Figure 2.11:</b> Principle of LDH cytotoxicity assay (prepared by author: Docrat, 2016). .....	33
<b>Figure 2.12:</b> Overview of the caspase activity assay (prepared by author: Docrat, 2016).....	34
<b>Figure 2.13:</b> Serial dilutions for preparation of standards (prepared by author: Docrat, 2016).	35
<b>Figure 2.14:</b> ELISA Assay principle outlining configuration (prepared by author: Docrat, 2016) .....	36
<b>Figure 2.15:</b> Principle of BCA Assay (prepared by author: Docrat, 2016).....	37
<b>Figure 2.16:</b> Gel sandwich assembly (Bio-Rad laboratories, inc., 2016).....	39

### CHAPTER 3

<b>Figure 3.1:</b> A dose-dependent decline in HepG2 cell viability following Ato treatment (48hr). .....	41
---	----

<b>Figure 3.2:</b> Level of intracellular ATP was significantly reduced in Ato-treated cells when compared to control cells (** $p \leq 0.005$ ). RLU: relative light units .....	42
<b>Figure 3.3:</b> Level of malondialdehyde in Ato-treated cells is significantly reduced ( $p \leq 0.05$ ). 43	
<b>Figure 3.4:</b> Extracellular nitrite and nitrate levels were increased in cells exposed to Ato (** $p \leq 0.005$ ).....	44
<b>Figure 3.5:</b> Glutathione concentrations significantly decreased in HepG2 cells after exposure to Ato (** $p \leq 0.005$ ).....	45
<b>Figure 3.6:</b> CYP3A4 activity in HepG2 cells was significantly induced by Ato in comparison to the control ( $p \leq 0.05$ ). RLU: relative light units. Dex: Dexamethasone.....	46
<b>Figure 3.7:</b> Level of extracellular LDH in ato treated cells (** $p \leq 0.005$ ). OD: Optical density. 47	
<b>Figure 3.8:</b> Caspase- 3/7 (** $p \leq 0.005$ ), and -9 activities were significantly increased (** $p \leq 0.0001$ ), and capase-8 activity was significantly decreased in Ato treated cells (** $p \leq 0.005$ ). RLU: relative light units.....	48
<b>Figure 3.9:</b> Mean cytokine concentration of (A) TNF- $\alpha$ was significantly decreased ( $p \leq 0.05$ ), however IL-6 was elevated significantly (B) (** $p \leq 0.01$ ).....	49
<b>Figure 3.10:</b> Protein expression of (A) pAKT (** $p \leq 0.005$ ), and (B) AKT ( $p \leq 0.05$ ) in HepG2 cells was significantly decreased following ato exposure. RBD: Relative band density .....	50
<b>Figure 3.11:</b> Protein expression of (A) pGSK3-( $\alpha/\beta$ ) ( $p \leq 0.05$ ) and (B) p53 (** $p \leq 0.005$ ) was significantly increased by Atorvastatin. RBD: Relative band density .....	51
<b>Figure 3.12:</b> Protein expression of (A) NF- $\kappa$ B ( $p \leq 0.05$ ) and (B) IKK- $\beta$ ( $p \leq 0.05$ ) in treated cells. RBD: Relative band density.....	52

## **APPENDIX**

<b>Figure 1:</b> Standard curve generated from GSH standards.....	69
<b>Figure 2:</b> Standard curve generated from TNF- $\alpha$ standards.....	70
<b>Figure 3:</b> Standard curve generated from IL-6 standards.....	71
<b>Figure 4:</b> Standard curve generated from IL-1 $\beta$ standards.....	72
<b>Figure 5:</b> No significant change in IL-1 $\beta$ between control and treated cells .....	73
<b>Figure 6:</b> Standard curve generated from IL-10 standards.....	74
<b>Figure 7:</b> No significant change in IL-10 between control and treated cells.....	75
<b>Figure 8:</b> Standard curve generated from BSA standards .....	76

## LIST OF ABBREVIATIONS

AIF	Apoptosis-Inducing Factor
Akt	Protein Kinase B
APS	Ammonium persulphate
Ato	Atorvastatin
ATP	Adenosine triphosphate
Apaf-1	Apoptotic protease activating factor-1
BCA	Bicinchoninic acid
BHT	Butylated hydroxytoluene
BMI	Body mass index
BSA	Bovine serum albumin
CAD	Caspase Activated DNase
CCM	Complete culture medium
CDK	Cyclin-dependent kinase
CKI	Cyclin-dependent kinase inhibitor
CRP	C-reactive protein
$\text{Cu}^+$	Cuprous ion
$\text{Cu}^{2+}$	Cupric ion
$\text{CuSO}_4$	Copper sulphate
$\text{CYP}_{450}$	Cytochrome $\text{P}_{450}$
CYP2C8	Cytochrome $\text{P}_{450}$ 2C8
CYP3A4	Cytochrome $\text{P}_{450}$ 3A4
DED	Death effector domain

Dex	Dexamethasone
DD	Death domain
dH <sub>2</sub> O	Deionised water
DISC	Death inducing signalling complex
DMSO	Dimethyl sulphoxide
DR3	Death Receptor-3
EDTA	Ethylenediaminetetraacetic acid
ELISA	Enzyme-linked immunosorbent assay
EMEM	Eagle's minimum essential medium
eNOS	Endothelial nitric oxide synthase
ETC	Electron transport chain
FADD	Fas associated death domain
Fas-L	Fas ligand
Fas-R	Fas-receptor
FCS	Foetal calf serum
FoxO	Forkhead box O
FPP	Farnesyl pyrophosphate
GGPP	Geranylgeranyl pyrophosphate
GPx	Glutathione peroxidase
GR	Glutathione reductase
GSH	Glutathione
GSK-3( $\alpha/\beta$ )	Glycogen synthase kinase-3 alpha/beta
GSSG	Glutathione disulphide

GST	Glutathione- S- transferase
GTP	Guanosine triphosphate
h	Hours
H <sub>2</sub> O <sub>2</sub>	Hydrogen peroxide
H <sub>3</sub> PO <sub>4</sub>	Phosphoric acid
HCC	Hepatocellular carcinoma
HCl	Hydrochloric acid
HDL	High-density lipoprotein
HMG-CoA	3-hydroxy-3-methyl-glutaryl-coenzyme-A
HMGCR	3-hydroxy-3-methyl-glutaryl-coenzyme-A reductase
HRP	Horseradish peroxidase
IAP	Inhibitor of apoptosis protein
IC <sub>50</sub>	Median inhibition concentration
IκB	Inhibitor of kappa-B
IKK	Inhibitor or kappa-B kinase
IKK- β	Inhibitor of nuclear factor kappa-B kinase subunit beta
IL-1	Interleukin-1
IL-6	Interleukin-6
IL-8	Interleukin-8
LDH	Lactate dehydrogenase assay
LDL	Low density lipoprotein
MDA	Malondialdehyde
Mdm2	Murine double minute 2

Mg <sup>2+</sup>	Magnesium ions
Mt	Mitochondrial
MTT	3-(4, 5-Dimethylthiazol-2-yl)-2,5-Diphenyltetrazolium Bromide
NADPH	Nicotinamide adenine dinucleotide phosphate
NEDD	Naphthylethylenediamine dihydrochloride
NF κB	Nuclear factor kappa B
NO·	Nitric oxide
NO <sub>2</sub> <sup>-</sup>	Nitrite
NOS	Nitric oxide synthase
O <sub>2</sub> <sup>-</sup>	Superoxide
OD	Optical densities
OXPHOS	Oxidative phosphorylation
pAKT	Phosphorylated protein kinase B
PBS	Phosphate buffer saline
PDPK1	Phosphatidylinositol dependent protein kinase 1
pGSK-3(α/β)	Phosphorylated glycogen synthase kinase-3 alpha/beta
PI3K	Phosphoinositide 3-kinase
PIP <sub>2</sub>	Phosphatidylinositol-4, 5-biphosphate
PIP <sub>3</sub>	Phosphatidylinositol-3, 4, 5-triphosphate
PKB	Protein kinase B
PTEN	Phosphatase and tensin homologue
RBD	Relative band density
RIP	Receptor interacting protein

RLU	Relative light units
ROS	Reactive oxygen species
SDS-PAGE	Sodium dodecyl sulphate polyacrylamide gel electrophoresis
Smac/DIABLO	Second mitochondria-derived activator of caspase/direct inhibitor of apoptosis-binding protein with low pI
SOD	Superoxide dismutase
SULF	Sulfanilamide
TBA	Thiobarbituric acid
TBARS	Thiobarbituric acid reactive substances
TBS	Tris-buffered saline
TEMED	Tetramethylethylenediamine
TMB	3, 3', 5, 5'-tetramethylbenzidine
TNF- $\alpha$	Tumour necrosis factor alpha
TNF-R1	TNF- $\alpha$ receptor 1
TRADD	TNF-R1 associated DD
TRAIL	TNF-related apoptosis-inducing ligand
VCl <sub>3</sub>	Vanadium (III) Chloride



## ABSTRACT

Within the past decade, the use of statins as a potential cancer treatment has been investigated. However, the molecular mechanisms involved in their anti-oxidant, anti-proliferative and anti-cancer effects remain elusive. In our study, we investigated the involvement of downstream mevalonate products that mediate the anti-oxidant and anti-proliferative effects of Atorvastatin (Ato) in hepatocellular carcinoma, HepG2 cells. A more soluble form of Ato was prepared and the cells were treated with 678.8 $\mu$ g/ml (IC<sub>50</sub>) for 48hrs (MTT assay). The effect of Ato on cell viability and metabolic activity was determined using MTT and ATP assays; oxidative status using TBARS, Griess, GSH and CYP3A4 assays; cellular death using LDH, ELISA, and caspase -3/7, -8, and 9 activity. Additionally, protein expression of pAKT, AKT, pGSK3-( $\alpha/\beta$ ), p53, NF- $\kappa$ B, and IKK- $\beta$  was assessed by western blotting. Ato induced a dose-dependent decrease in cell viability with a concomitant depletion of intracellular ATP levels ( $p=0.005$ ). Interestingly, Ato significantly decreased lipid peroxidation ( $p=0.0097$ ) whilst increasing nitrite levels ( $p=0.001$ ). Atorvastatin significantly decreased glutathione levels ( $p=0.0003$ ), whereas the enzyme activity of CYP3A4 was significantly increased ( $p=0.0079$ ). Collectively, these results demonstrate the anti-oxidant properties of Ato. The anti-proliferative, cytotoxic, and apoptotic effects of Ato were depicted by a significant increase in LDH levels ( $p=0.0002$ ), induction of the intrinsic apoptotic pathway evidenced by a significant elevation in -9 activity ( $p<0.0001$ ) and caspase-3/7 ( $p=0.0003$ ), a significant decrease in Caspase-8 activity ( $p=0.0025$ ) and TNF- $\alpha$  concentration ( $p=0.0105$ ), and a significant increase in IL-6 concentration ( $p=0.0012$ ) which correlates with the significant reduction in NF- $\kappa$ B protein expression ( $p=0.013$ ). Protein expression of pGSK3-( $\alpha/\beta$ ) ( $p=0.0338$ ), and p53 ( $p=0.0032$ ), were significantly up-regulated; whereas protein expression of pAKT ( $p=0.0035$ ), AKT ( $p=0.0077$ ), and IKK- $\beta$  ( $p=0.0094$ ) were significantly reduced. In conclusion our data shows that Ato possesses anti-oxidant, anti-proliferative, cytotoxic and pro-apoptotic effects in HepG2 cells.

## CHAPTER ONE

### 1.1 INTRODUCTION

Statins are a well-known class of drugs used in the treatment of lipid-associated disorders, specifically hypercholesterolemia. They function by impeding cholesterol synthesis via inhibition of the key enzyme in the pathway, 3-hydroxy-3-methyl-glutaryl-coenzyme-A reductase (HMGCR) (Chan et al., 2003b). It is through this mechanism that statins have the ability to reduce the risk of stroke, myocardial infarction and death (Strandberg et al., 2004). The pleiotropic effects of statins include, improvement of endothelial dysfunction, improve atherosclerotic plaque stability, impeding thrombogenic response, as well as decrease inflammation and oxidative stress (Liao and Laufs, 2005). Statins play an instrumental role in cardiovascular medicine. Evidence from clinical trials suggests that with statin therapy there are decreased cardiovascular-related deaths (Wright et al., 1994, Schwartz et al., 2001, Shepherd et al., 1995). Atorvastatin (Ato) is a synthetic derivative of mevalonate and pyridine (Matuszewicz et al., 2015). The structure of Ato consists of a pyrrole and heptanoic acid derivative which resembles HMG-CoA. Hydrophobic statins like Ato predominantly undergo metabolism via the cytochrome P-450 3A4 enzyme family (Schachter, 2005).

Cancer is the second leading cause of death in the world, after cardiovascular disease (Ma and Yu, 2006). Due to the significant disease burden and related mortality, the need for better treatment options with reduced side-effects is essential. Several hallmarks contribute to the complexity of tumour growth and progression. These include, withstanding cell death, maintaining proliferative signalling, inducing angiogenesis, enabling replicative immortality, evasion of growth suppressors, and activating invasion and metastasis (Hanahan and Weinberg, 2011). Apoptosis is a type of programmed destruction of the cell that ultimately leads to death (Hengartner, 2000). It is through this process that cells maintain equilibrium between proliferation and death (Schwartzman and Cidlowski, 1993). Survival of cancer cells occurs through their ability to evade apoptosis (Hanahan and Weinberg, 2011). Statins have been shown to exert apoptotic effects in vascular smooth muscle cells (Erl, 2005). The apoptotic effects of Cerivastatin through geranylgeranyl pyrophosphate (GGPP) inhibition have been depicted *in vivo* (Johnson et al., 2004). Furthermore, the apoptotic-inducing effects of

Lovastatin and Simvastatin via the extrinsic pathway were illustrated in prostate cancer cells (Hoque et al., 2008).

Numerous signal transduction pathways have been identified in normal cellular function. Transformation of normal cells to a cancerous state is a result of aberrant signalling. Phosphoinositide 3-kinases (PI3Ks) are a part of a family of lipid kinases that promote Protein Kinase B (Akt) recruitment via phosphorylation of phosphatidylinositol-3, 4, 5-triphosphate (PIP<sub>3</sub>) (Cantley, 2002). Consequently cell survival, proliferation and differentiation are augmented. Cancer development through amplified PI3K/Akt-mediated signalling is well documented. A few targets of this pathway include Bax, Bcl-2, NF-κB, ubiquinone, cell cycle regulators such as p21, and glycogen synthase kinase-3 (GSK-3) (Chang et al., 2003, Luo et al., 2003). An important mechanism of this pathway is apoptotic inhibition; hence novel chemotherapeutic agents that target this cascade may be a promising approach.

The mevalonate pathway is responsible for production of a range of end products that have essential roles in cell function. Included in these products are isoprene units that encompass sterol and nonsterol compounds like dolichol, ubiquinone, cholesterol, GGPP, and farnesyl pyrophosphate (FPP) (Goldstein and Brown, 1990). Isoprenoids are responsible for Ras and Rho prenylation (Kamat and Nelkin, 2005). Prenylation of these GTPase proteins result in reactive oxygen species (ROS) oxysterol production, inhibition of endothelial nitric oxide synthase (eNOS), as well as activation of the PI3K/Akt pathway, which collectively contribute to tumourigenesis (Stryjowska-Gora et al., 2015). Recent evidence indicates that Atorvastatin, Fluvastatin and Simvastatin induce lymphoma cell death via activation of anti-apoptotic molecule, Bcl-2; increased intracellular ROS levels; p38 activation and suppression of Akt and ERK pathways (Qi et al., 2013). However, the exact molecular mechanisms involved in statin-mediated cancer cell death are intricate and need to be explored further.

### **1.1.1 Study Rationale and aims**

*In vitro* investigations have indicated the potential of statins as anti-cancer agents (Agarwal et al., 1999, Aprigliano et al., 2008, Kanugula et al., 2014, Stryjowska-Gora et al., 2015). Considering that the majority of studies are either preclinical or observational clinical studies,

the need arises to investigate statins further. Understanding the underlying mechanisms of statins and how they may exert their effects prior to an *in vivo* or clinical study is essential.

The liver plays a fundamental role in carbohydrate, protein, lipid and xenobiotic metabolism. Atorvastatin is primarily metabolised by the liver. Hepatocellular carcinoma (HCC) is a primary malignancy of the liver. The liver derived HepG2 cells are often used as HCC model as they represent a pure cell line due to the absence of viral infection. It is also known to express HMGCR (Molowa and Cimis, 1989). Atorvastatin was selected for this study as it is the most commonly prescribed and well-tolerated statin.

### **1.1.2 Aim**

The aim of this study was to determine the effect of Ato on cellular proliferation/metabolic activity, oxidative status, and elucidate the mode by which Ato exerts its effects in Hepatocellular Carcinoma, HepG2 cells.

### **1.1.3 Objectives of this study were designed to:**

- Evaluate cytotoxicity (MTT assay) and apoptotic regulators such as caspase (-8, -9, and -3/7) activity, NF- $\kappa$  $\beta$ , I $\kappa$  $\kappa$ - $\beta$ , and p53.
- Measure oxidative stress parameters via evaluation of MDA, nitrite levels, GSH, and CYP3A4 activity.
- Assess the inflammatory status by measuring cytokine levels of TNF- $\alpha$ , IL-6 using ELISA
- Determine the protein expressions of AKT, GSK-3( $\alpha$ / $\beta$ ) using western blotting

### **1.1.4 Hypothesis**

Atorvastatin exerts anti-oxidant, anti-inflammatory, and apoptotic effects via inhibition of the PI3K/Akt pathway in HepG2 cells

## 1.2 LITERATURE REVIEW

### 1.2.1 Statins

Atorvastatin (Ato), trade name Lipitor, is one of the most commonly prescribed drugs in the treatment of heart disease (Puntarulo and Cederbaum, 1998). The differentiating factors of statins lie in their pharmacokinetic properties (Liou and Storz, 2010, Kanugula et al., 2014). Their chemical structures play important roles in water solubility, which influences absorption, metabolism, distribution and excretion. Atorvastatin is a synthetic mevalonate derivative. Its structure (Figure 1.1) is comprised of three main groups, these include two hydrophobic hydroxyl hexahydro naphthalene ring structures and the HMGCoA equivalent (Halliwell and Chirico, 1993). Metabolism of Ato mainly occurs in the liver, by either an acyl glucuronide intermediate or coenzyme-A dependent pathway, where biotransformation of the acid component to a lipophilic lactone occurs. The CYP3A4 enzyme is responsible for further metabolism of Ato and its associated lactone form, whilst CYP2C8 metabolises it to a lesser extent. Hydrolysis of the Ato lactone to its acidic form occurs by paraoxonases and esterases or nonenzymatically (Liu et al., 2002, Dröge, 2002).

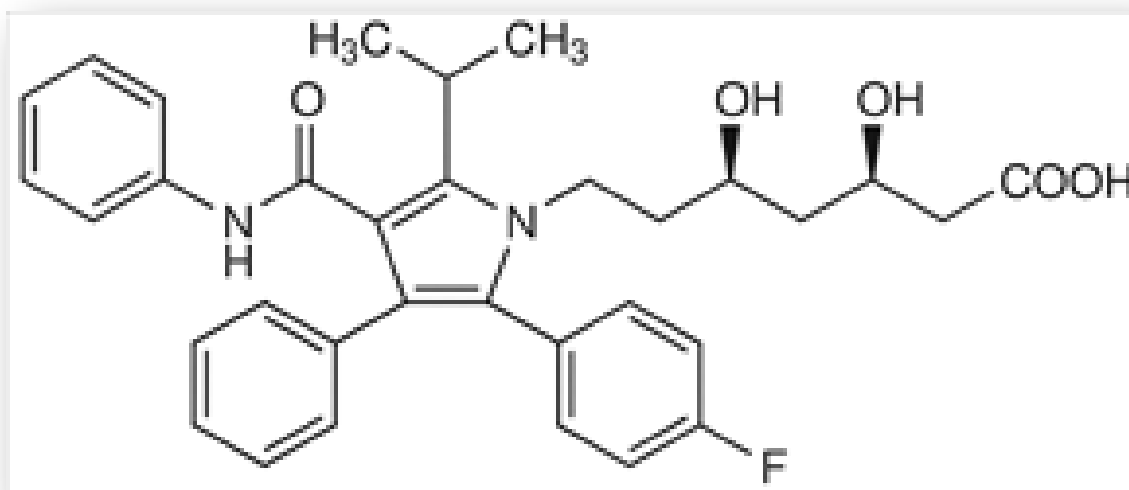


**Figure 1.1:** Chemical structure of Atorvastatin. (Kracun et al., 2009)

### ***1.2.1.1 Mode of action of statins in Coronary Artery Disease***

Cholesterol biosynthesis is regulated by the rate-limiting enzyme- HMG-CoA reductase (HMGCR). The reduction of 3-hydroxy-3-methylglutaryl-coenzyme A (HMG-CoA) to mevalonate is catalysed by this enzyme. Statins mimic the HMG-CoA molecule, thus allowing competitive inhibition of HMGCR. This slows down or decreases the rate at which mevalonate is produced. Statins are used as primary prevention of strokes and heart attacks in cardiovascular disease (Rosa et al., 2014).

Atorvastatin is a synthetic compound that reduces *de novo* cholesterol synthesis and increases the expression of hepatic low density lipoprotein (LDL) receptors (Goldstein and Brown, 1990). As a result, LDL catabolism by hepatocytes is increased, and blood LDL-cholesterol is decreased (Nawrocki et al., 1995). Triglyceride blood levels are also reduced by Ato with a slight increase in high density lipoprotein (HDL)-cholesterol levels.

### ***1.2.1.2 Mechanism of action of statins and cancer***

Mevalonate production serves as a precursor of many sterols. Upon inhibition, various downstream metabolites are also affected (Figure 1.2). Isoprenoid production is an essential component in posttranslational modification of numerous proteins, including Farnesyl Pyrophosphate (FPP) and Geranylgeranyl pyrophosphate (GGPP) (Yeganeh et al., 2014). Ras and Rho protein GTPases are prenylated by isoprenoids. This facilitates their translocation to the cell membrane, which allows intracellular signalling to occur. The potential antioxidant properties of statins involve reactive oxygen species (ROS) inhibition via suppression of NADPH oxidase activity (Chen et al., 2012). The anti-inflammatory properties of statins have been depicted via effects on C-reactive protein (CRP) (Jialal et al., 2001); tumour necrosis factor  $\alpha$  (TNF  $\alpha$ ) (Bruegel et al., 2006); interleukin-6 and -8 (IL-6, IL-8) (Park et al., 2008b); and nuclear factor  $\kappa$ B (NF  $\kappa$ B) (Yeganeh et al., 2014).

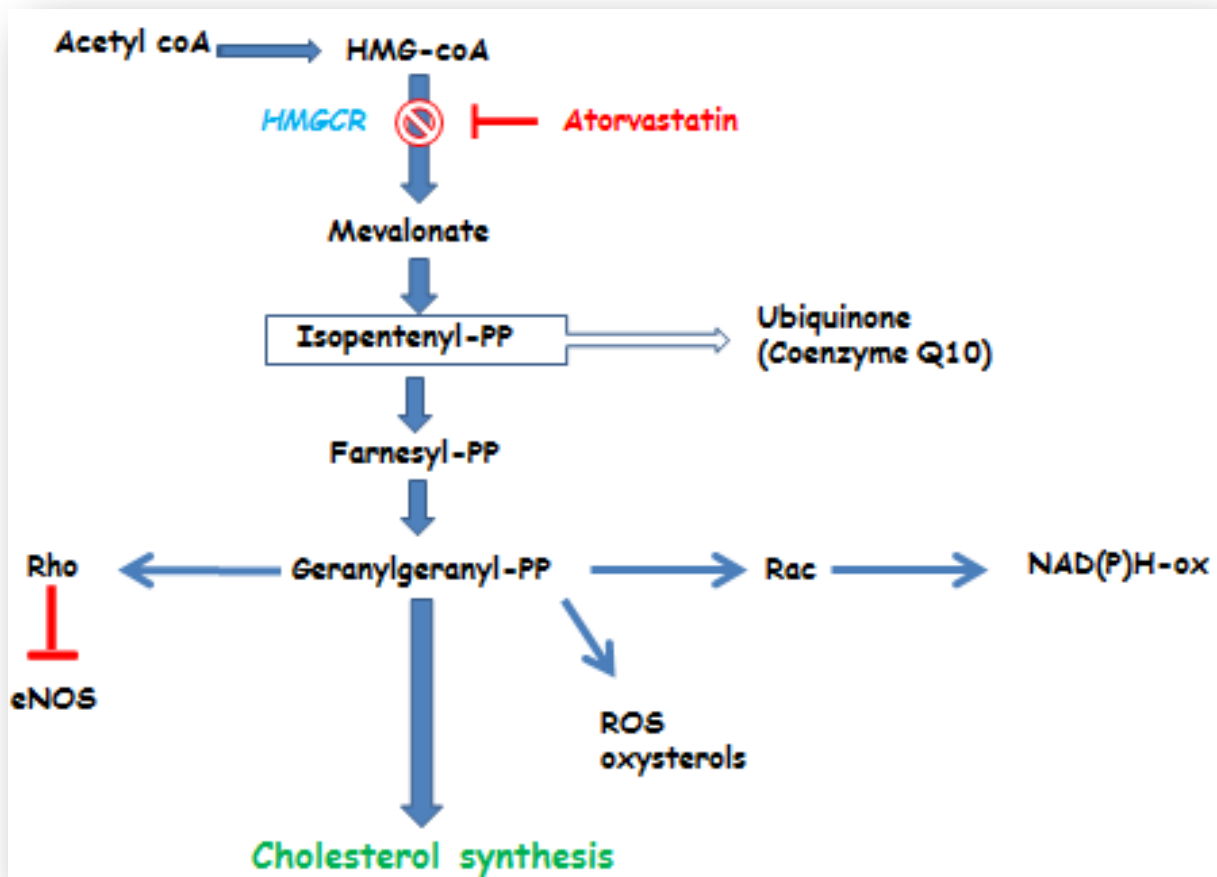


**Figure 1.2:** Mechanism of action of Atorvastatin: inhibits cholesterol synthesis (prepared by author: Docrat, 2016). HMG-CoA: 3-hydroxy-3-methyl-glutaryl-coenzyme A, HMGCR: 3-hydroxy-3-methyl-glutaryl-coenzyme A reductase, PP: Pyrophosphate, ROS: Reactive oxygen species, eNOS: endothelial nitric oxide synthase, NAD(P)H-ox phosphate.

### 1.2.1.3 Epidemiological link between HMG-CoA reductase inhibitors and cancer

In the past 15 years, there has been an exponential increase in the use of statins resulting in their long term safety becoming more apparent. Initially, concerns regarding decrease in serum cholesterol leading to increased rates of cancer were raised. Evidence suggests a possible association between low serum cholesterol and cancer associated mortality among men (Jacobs et al., 1992). Thereafter, concern that statins have intrinsic carcinogenic properties existed. The

adverse outcomes of statin use originated from studies in animal models as well as epidemiological data in humans. The potential carcinogenicity of statins on rodents was reviewed and concluded that lipid-lowering drugs should be avoided unless patients are at high risk of coronary heart disease (Newman and Hulley, 1996). Additionally, human cohort studies supported this observation (Jacobs et al., 1992). The majority of the information relating to the impact of statins on cancer was obtained from observational studies; these results could be distorted by numerous factors. Confounding variables, such as pre-existing cancer, concurrent statin and cardiovascular treatment (e.g.: acetylsalicylic acid), high body mass index (BMI), elderly patients with a sedentary lifestyle, incorrect feeding, frequent dependence on tobacco, and their retrospective nature limited these studies. These factors influence the risk of cancer to a different degree.

Despite the anxiety caused by these studies, other studies showed no significant increase in cancer mortality (Law and Thompson, 1991, Nielsen et al., 2012) Reassurance was provided regarding the risk of cancer from statin use in long-term studies on secondary prevention of coronary artery disease with statins (Pedersen et al., 2000). Several studies have affirmed the safety of statins, demonstrating no increase in cancer incidence with statin usage (Delgado and Leon, 2010, Lakha et al., 2012, Lee et al., 2011, Beg et al., 1993, Cantley, 2002, Mansouri et al., 2013, Wang et al., 1996, Ng et al., 2011, Beg and Baltimore, 1996, Beg and Baldwin, 1993).

#### ***1.2.1.4 Biochemical effects of statins***

Although statins have proved to be therapeutic and preventative agents in cardiovascular disease, recent interests have emerged in their use as anti-tumour agents. The basis of these interests lies in the preclinical evidence of their pro-apoptotic, anti-proliferative and anti-invasive properties. Mevalonate and its downstream products, which are reduced by statins, have critical roles in cellular functions such as cell signalling, membrane integrity, cell cycle progression, and protein synthesis (Chan et al., 2003a). Tumour initiation, growth and metastasis can therefore be controlled in cells treated with statins due to perturbations of these processes.

The anti-proliferative effects of HMG-CoA reductase inhibitors have been shown by tumour cell synchronisation via blocking of the G<sub>1</sub>-S phase in the cell cycle (Keyomarsi et al., 1991). Addition of mevalonate reverses this effect. Lovastatin has been shown to inhibit cell growth



(DeClue et al., 1991). Evidence suggests that HMG-CoA reductase inhibitors exert anti-proliferative effects via cell cycle arrest due to increase mRNA and protein expression in two cyclin-dependant kinase (CDK) inhibitors, p21 and p27 (Denoyelle et al., 2001, Law and Thompson, 1991). Apoptotic induction has been shown in human acute myeloid leukaemia cells treated with lovastatin (Xia et al., 2001). Studies also show that lovastatin increased expression in proapoptotic protein, Bax, and decreased expression in the anti-apoptotic protein, Bcl-2 (Agarwal et al., 1999). Statins also induce apoptosis via activation of caspases-3, -8 and, -9, in human myeloma tumour cells (Cafforio et al., 2005). Atorvastatin has been shown to down-regulate the pro-apoptotic protein, Bim, in endothelial progenitor cells (Urbich et al., 2005). Statins do have cytotoxic potential; however, the exact mechanism by which statins exert their effects is yet to be determined.

## **1.2.2 Liver cancer**

Cancer is one of the leading causes of morbidity and mortality, with an approximated 14 million new cases and 8.2 million cancer-related deaths in 2012 worldwide (Stewart and Wild, 2016). New cases are expected to increase by 70% in the next 2 decades. Liver cancer remains the fifth most common in men and the eighth most common in women across the globe. Hepatocellular Carcinoma (HCC), a type of liver cancer, is the most common. Infections like Hepatitis B or C usually result in HCC. Other risk factors include alcohol consumption, tobacco usage and metabolic toxins like aflatoxin (Emerit, 1994).

### ***1.2.2.1 HepG2 cells***

The liver, being the hub of metabolism, is central to xenobiotic metabolism. The HepG2 cell line is liver derived and its detoxification abilities are attributed to inducible phase I & II enzymes. According to Mersch-Sundermann, HepG2 cells reflect xenobiotic metabolism in the human body to a greater extent in comparison to conventional cell lines that are metabolically incompetent (Mersch-Sundermann et al., 2004). Hence, the use of HepG2 cells for detection of cytotoxicity is of great relevance.

### **1.2.3 Reactive oxygen species (ROS)**

#### ***1.2.3.1 Free Radicals***

Free radicals are molecules containing single or multiple unpaired electrons and can exist independently (Halliwell and Chirico, 1993). Oxygen-derived radicals have both hazardous and beneficial roles in cell functioning. Free radicals include, superoxide ( $O_2^{\cdot-}$ ) and related reactive oxygen species (ROS) as well as nitric oxide ( $NO^{\cdot}$ ). These radicals may be sourced from, but not limited to, the mitochondrial electron transport chain (ETC), NADPH-oxidase, xanthine oxidase, NO synthase, and intracellular xenobiotic mechanisms ( $CYP_{450}$ ) (Chen et al., 2003, Dröge, 2002, Liu et al., 2002). Carcinogenesis may occur as a result of free radicals by various means. These include promoting cell growth by activation of proliferative pathways, preventing apoptosis as well as inducing DNA damage and inhibition of repair mechanisms (Federico et al., 2007).

Cellular maintenance of redox-signalling is essential for growth and proliferation. Upon ROS exposure, redox homeostasis is established to prevent oxidative damage (Dröge, 2002). The concentration of free radicals is determined by the oxidant-antioxidant balance. It is well established that tumourigenesis is promoted by oxidative stress as a result of an imbalance between oxidant-antioxidant systems (Ambrosone, 2000, Emerit, 1994, Klaunig et al., 1998, Storz, 2005). Numerous studies indicate the antioxidant properties of statins (Davignon et al., 2004, Kanugula et al., 2014, Qi et al., 2013).

#### ***1.2.3.2 Antioxidants***

Antioxidants are defined as substances that are able to inhibit oxidation of substrates, at relatively low concentrations (Halliwell and Gutteridge, 2015). These include the enzymes glutathione peroxidase (GPx), superoxide dismutase (SOD), catalase, as well as other compounds that are non-enzymatic like ascorbic acid and glutathione (GSH) (Dröge, 2002).

Glutathione plays an important role in protecting the cell from free radical and peroxide damage. The reduction of hydrogen peroxide ( $H_2O_2$ ) and lipid hydroperoxides to water is catalysed by the GPx enzyme, whilst GSH functions as an electron donor (Ott et al., 2007,

Reuter et al., 2010) Following conversion of GSH to its oxidised form glutathione disulphide (GSSG), glutathione reductase (GR) recycles GSSG back to GSH which prevents depletion (Nakano et al., 2006, Reuter et al., 2010). This reaction is NADPH-dependent (Figure 1.4).

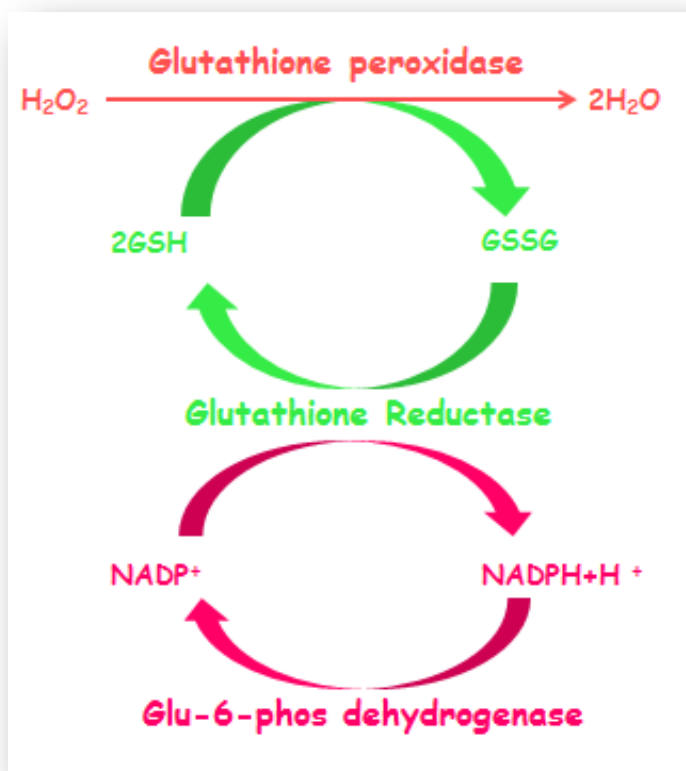


**Figure 1.3:** Antioxidant activity of GSH (prepared by author: Docrat, 2016)

### 1.2.3.3 Cytochrome P450 3A4

Cytochrome P<sub>450</sub> (CYP<sub>450</sub>) enzymes are a superfamily of haem-containing mono-oxygenases that have essential roles in biotransformation and detoxification. They are located within the endoplasmic reticulum in majority of human tissues (Zangar et al., 2004). Exogenous substances e.g., drugs or carcinogens undergo oxidative metabolism by CYPs. The catalytic mechanism of detoxification by CYPs involves phase I reactions where xenobiotics are modified to promote phase II reactions (Westerink and Schoonen, 2007). In the liver, the CYP3A subfamily is most abundant, making up approximately half of the CYP content (Ding

and Kaminsky, 2003, Pan et al., 2010). CYP3A4 activity is known to promote ROS production in viable cells (Zangar et al., 2011).

#### **1.2.4 Apoptosis**

Apoptosis is the physiological process of programmed cell death. This process is crucial in regulating cell numbers during development by eliminating cells that are damaged, redundant or irreparable (Schwartzman and Cidlowski, 1993). This sequential process is characterised by distinct morphological changes that lead to disintegration and destruction of the cell. During apoptosis, two distinct phases are involved in programming cell death. The first phase consists of cytoplasmic and nuclear condensation, resulting in membrane breakage and release of structurally intact organelles. During the second phase, phagocytosis of the apoptotic bodies occurs by neighbouring cells. In contrast to necrosis, apoptosis prevents an inflammatory response via maintenance of organelle integrity which allows for minimal intracellular content leakage (Chen et al., 2012). Disturbances of the apoptotic mechanism are implicated in various pathological conditions, ranging from auto-immune diseases to degenerative disorders and cancer (Adams, 2003, Bours et al., 2000).

Apoptosis is driven by caspases, a group of aspartate-specific cysteinyl proteases. The initiator caspases are responsible for activation of a second group of caspases, the executioners, by proteolytic cleavage (Luzzi and Marletta, 2005). The caspase enzymes have active cysteine sites which function in cleavage of substrates containing aspartate residues. Caspases are maintained as inactive zymogens with three domains: the N-terminus prodomain, a p10 and a p20 domain located in a mature caspase. Cleavage of zymogens between the p20 and prodomain or between the p10 and p20 domains, allows for caspase activation. The morphological changes of cells undergoing apoptosis are a result of the executioner caspases. In mammalian cells, two major apoptotic pathways exist: the intrinsic mitochondrial-mediated pathway and the extrinsic death receptor-mediated pathway (Figure 1.4). Control of these pathways is tightly maintained by a host of regulatory molecules that are highlighted below (Figure 1.5).

#### ***1.2.4.1 The intrinsic pathway of apoptosis***

The intrinsic apoptotic pathway is commonly known as mitochondrial apoptosis due to its dependence on factors released from the mitochondria. Activation of this pathway occurs by various cellular stressors including, deprivation of growth factors, disruption of the cytoskeleton, accumulation of unfolded proteins, insufficient cytokine support, damaged DNA, hypoxia, amongst others (Adams, 2003, Lalier et al., 2007). Mitochondrial membrane permeabilisation is controlled by the Bcl-2 family of proteins (Lalier et al., 2007). This step is a crucial for release of apoptotic proteins from the mitochondria. When mitochondrial membrane integrity is lost, pro-apoptotic proteins including Smac/DIABLO, Endonuclease G, Caspase Activated DNase (CAD) and AIF (Apoptosis-Inducing Factor) are released (Schimmer, 2004). Caspase-9 activation is energy dependent (Zangar et al., 2011) In a resting cell, both caspase-9 and Apaf-1 exist as cytosolic, inactive monomers. When the cell experiences stress, mitochondrial release of cytochrome *c* occurs. Cytochrome *c* binds to Apaf-1, leading to recruitment of pro-caspase 9 and apoptosome formation (Figure 1.5). Initiator caspase 9 is activated and proteolytically cleaves the zymogens of executioner caspases, -3, -6, and -7 (Hengartner, 2000). This is followed by a cascade of events leading to apoptosis.

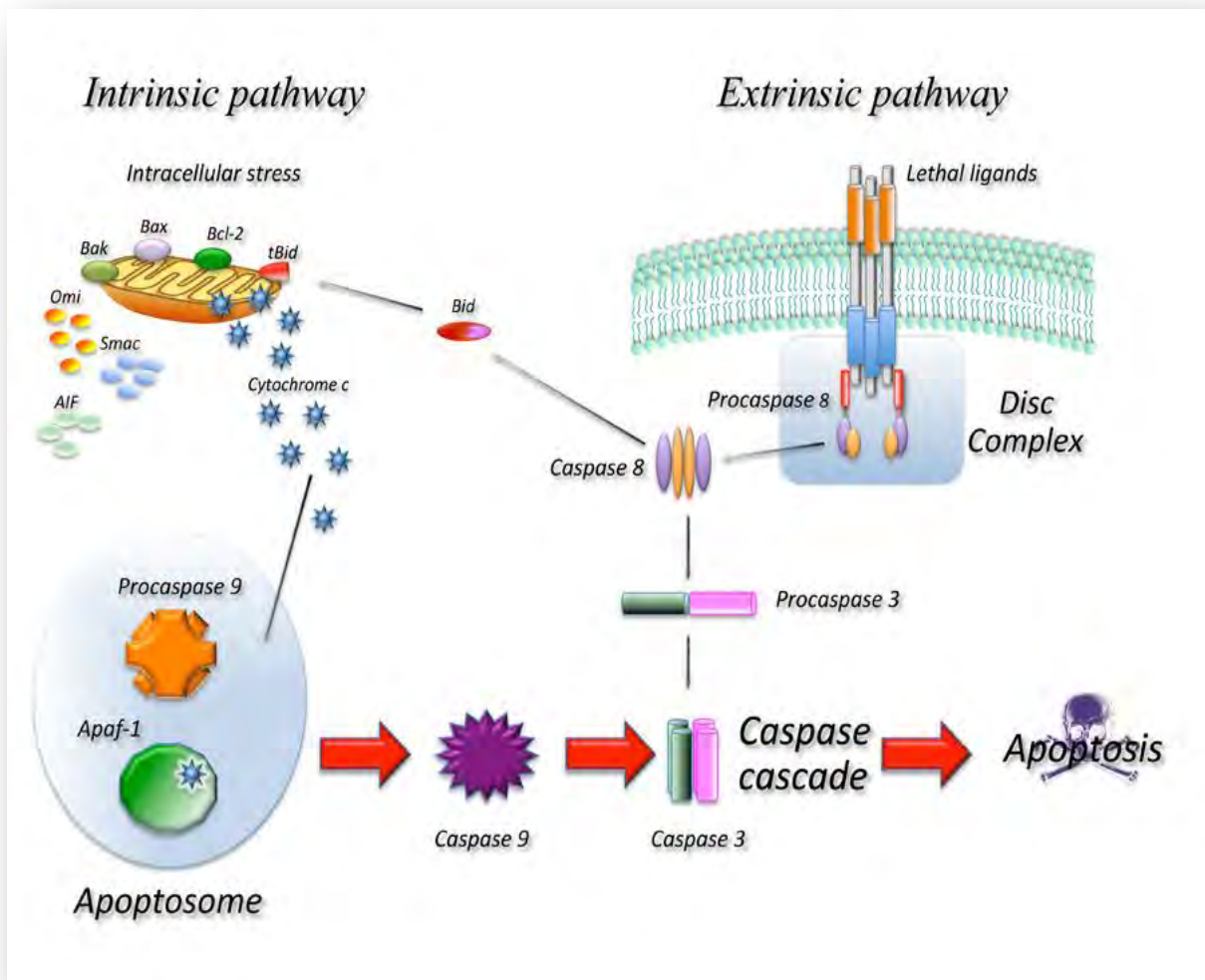


**Figure 1.4:** Schematic representations of the main molecular pathways leading to apoptosis (Favaloro et al., 2012)

#### 1.2.4.2 The extrinsic pathway of apoptosis

The extrinsic apoptotic pathway is triggered by transmembrane death receptor-mediated reactions. The tumour necrosis factor (TNF)- $\alpha$  death receptor family is a well-documented mechanism for activation of the extrinsic pathway. Apoptotic signals are known to be induced by TNF-related apoptosis-inducing ligand (TRAIL)-R1/R2, TNF- $\alpha$  receptor 1 (TNF-R1), Fas (CD95)-R, CAR-1, and DR3, which form part of the TNF- $\alpha$  family (Reed, 1999). The receptors of this family are known as the death domain (DD), which is composed of a cysteine rich extracellular domain and a cytoplasmic DD (Jucker et al., 2002). Death domains function in

signal transmission from the outer surface of the cell to intracellular signalling pathways. Activation of the extrinsic pathway via ligand-receptor binding has been extensively characterised with Fas ligand (Fas-L)/Fas-receptor (Fas-R) and TNF/TNF-R models (Jucker et al., 2002, Lin et al., 1999, Fry, 2001, Rubio-Moscardo et al., 2005). Death receptors cluster at the cell membrane where homologous trimeric ligands bind. Cytoplasmic adaptor proteins and their corresponding DDs are recruited. Fas associated protein and its DD (FADD) is recruited by Fas-L/Fas-R, and TNF-R1 associated protein and its DD (TRADD) with FADD and RIP are recruited by TNF/TNF-R (Krasilnikov et al., 1999, Mistafa and Stenius, 2009). Additionally, FADD contains the death effector domain (DED). The binding of FADD to a homologous DED found on procaspase-8, results in the formation of a death inducing signalling complex (DISC) which catalyses caspase-8 cleavage and activation (Zhou et al., 2000). Apoptosis is then executed by subsequent cleavage and activation of effector procaspase-3/7. Insufficient caspase-8 activation at the DISC, promotes mitochondrial amplification of death signals through the intrinsic pathway (Figure 1.5), mediating full caspase activation (Aprigliano et al., 2008, Minichsdorfer and Hohenegger, 2009).

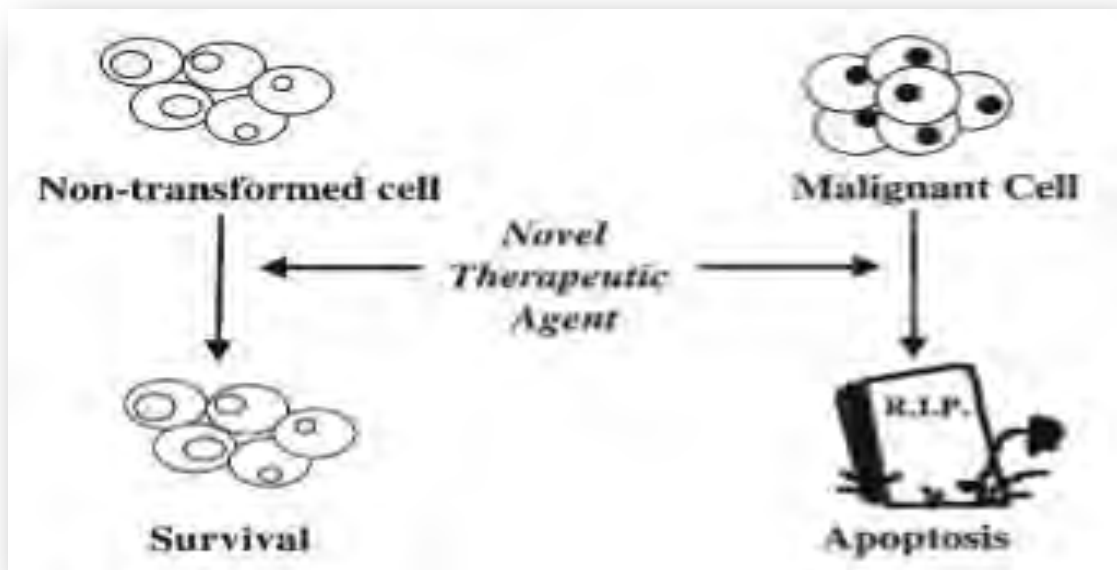


**Figure 1.5:** Induction of apoptosis in malignant cells due to novel chemotherapeutic agents that act in a specific manner (Wong et al., 2002)

### 1.2.5 Necrosis

Necrosis is a type of cell injury that leads to premature cell death by autolysis in living tissue (Proskuryakov et al., 2003). External factors which may result in necrosis include trauma, toxins or injury that causes unregulated digestion of cell components. Usually, the effects of apoptosis are beneficial to the organism whilst necrotic effects are detrimental and could possibly be fatal due to harmful chemicals released. In necrosis, receptor activation leads to loss of integrity in the cellular membrane as well as liberates products of cell death into the extracellular space (Proskuryakov et al., 2003). Due to this, an inflammatory response is initiated in nearby tissue which prevents elimination of dead cells by phagocytosis (Schwartzman and Cidlowski, 1993).

### 1.2.6 Role of PI3K/Akt signalling pathway in apoptosis and cell survival

Protein Kinase B/Akt is a well-recognised cell cycle regulator (Luo et al., 2003). Many disorders, including cancer are associated with aberrant activation of this kinase (Datta et al., 1997, McCubrey et al., 2007). Cytokine-specific receptor binding allows for lipid Phosphatidylinositol 3-Kinase, (PI3K), activation which occurs via two mechanisms. The first involves activation of Ras protein GTPase. PI3K consists of a regulatory (p85) and catalytic (p110) subunit. The second mechanism involves docking of the p85 subunit at the tyrosine residue, which results in p110 recruitment. (Lakha et al., 2012, Mansouri et al., 2013). Phosphatidylinositol (4, 5)-biphosphate (PIP<sub>2</sub>) is phosphorylated by PI3K to form phosphatidylinositol (3, 4, 5)-triphosphate PIP<sub>3</sub> (Cole, 1986b, Cole, 1986a). Phosphatidylinositol dependent protein kinase 1 (PDK1) is activated by PIP<sub>3</sub> and results in Akt recruitment to the lipid-rich plasma membrane. Nuclear translocation of Akt is essential for cell proliferation and anti-apoptosis (Chen et al., 2003). Signalling initiated by PI3K is primarily mediated by Akt and alteration to downstream substrates in this pathway may cause oncogenic transformation. Examples of PI3K substrates include IKK-beta, nuclear factor- κB (NF- κB), inhibitor of apoptosis proteins (IAPs), Bax, Bcl-2, p21, and phosphorylated glycogen synthase kinase-3-α/β (pGSK-3-α/β) (Figure 1.6). These substrates play important roles in inhibition of apoptosis and cell cycle progression (Ng et al., 2011, Cantley, 2002). PI3K activity is associated with numerous human tumours, including melanomas, lung cancer, breast cancer and leukaemias (Nielsen et al., 2012, Park et al., 2008b, Bruegel et al., 2006).



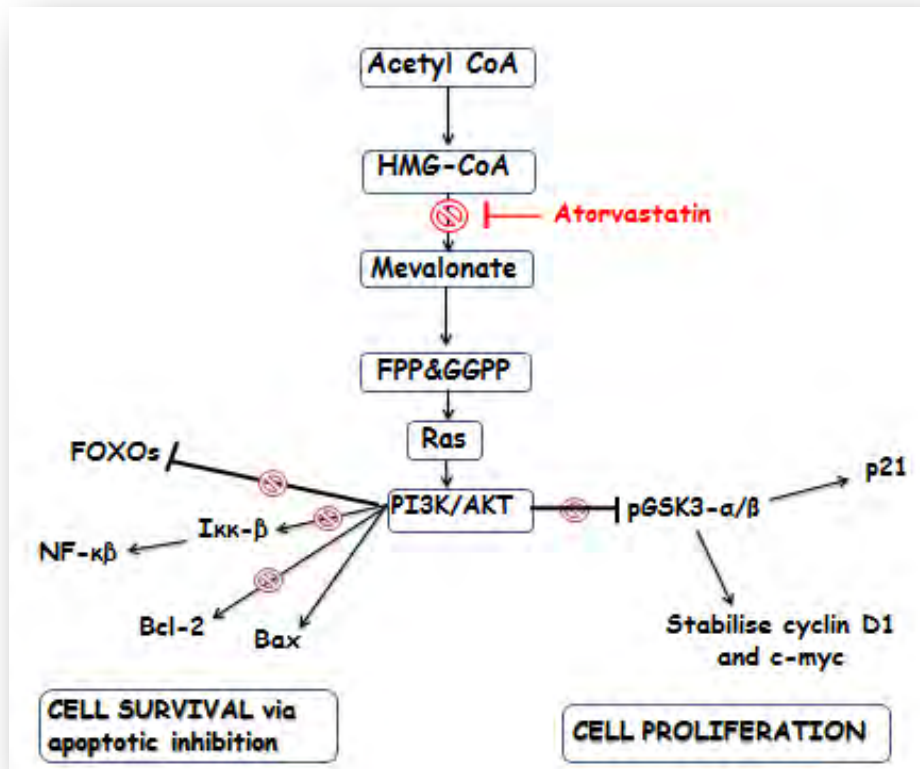


**Figure 1.6:** Inhibitory effect of statins on mevalonate and its downstream effects on PI3K/AKT signalling pathway (prepared by author: Docrat, 2016)

### 1.2.7 Forkhead Box (FOXOs), c-Myc and the cell cycle

A requirement for higher organism development is increased complexity. This is evident from the regulatory role played by the Forkhead box (FoxO) family. Thus far, four isoforms of FoxO have been identified in mammalian cells (FoxO1, FoxO3a, FoxO4 and FoxO6) (Cole, 1986b). A conserved evolutionary feature of FoxOs, despite their diversification, is their function as downstream effectors of PI3K/Akt (Escot et al., 1986). At the molecular level, Akt directly represses FoxO through phosphorylation, promoting its export from the nucleus, reduced transactivation activity and proteosomal degradation (Little et al., 1983, Cole, 1986b, Amati et al., 1998, Freytag, 1988). Deregulation of these kinases and PKB have been frequently observed in proliferative disorders and may contribute to tumourigenesis (Kulinsky, 2007, Dennis et al., 2002). Numerous regulators of the cell cycle are controlled by FoxO, resulting in its important

role in regulating cell cycle senescence. Inhibition of PI3K in primary mouse embryo fibroblasts using chemical inhibitors can induce cell cycle arrest through FoxO-induced p27<sup>Kip1</sup> expression, similar to that of cellular senescence (Howe, 2007). Further evidence of FoxOs role in cellular senescence is provided by an *in vivo* study that demonstrates repression of the PI3K/Akt signalling pathway with subsequent FoxO induction (Coussens and Werb, 2002). It can be assumed that cancer cells have repressed levels of FoxO3a as studies show that re-introduction of FoxO3a results in tumour cell death (Suganuma et al., 1999). One of the key pathways involved in activation of the cell cycle is the Wnt pathway. Cancer cell entry into the cell cycle is regulated by the Wnt pathway via activation of c-Myc, cyclin D and p53 (Sun et al., 2010, Kanugula et al., 2014, Xie et al., 2014, Wassmann et al., 2002). Studies suggest convergence of the PI3K/Akt/mTOR and Wnt pathways in regulation and progression of the cell cycle through the G<sub>0</sub>/S phase in cancer cells (Wang et al., 2008).

The c-Myc gene is activated in human cancers via various mechanisms. C-Myc, a member of the Myc family of proteins, is known for its ability to regulate proliferation and apoptosis in normal cells. Through various mechanisms, deregulation of Myc-proteins occurs, resulting in one-third of human cancers. Normal c-Myc gene expression is under immaculate control. Formation of lymphoid malignancies are promoted by juxtaposing translocations of the c-Myc proto-oncogene (Cole, 1986b). Up-regulation of the c-Myc gene occurs in various cancers including lung and breast carcinomas (Little et al., 1983, Escot et al., 1986). Initial studies implicated c-Myc in the G<sub>0</sub>/G<sub>1</sub> phase of the cell cycle (Freytag, 1988). Further insight was provided on the function of c-Myc upon CDK inhibitors, CDKs and cyclins emergence (Figure 1.7) (Amati et al., 1998). C-Myc and cyclin-D<sub>1</sub> function in S-phase entry of the cell cycle (Figure 1.7). Cyclins are up-regulated when c-Myc is activated (Cole, 1986b). Therefore, c-Myc plays a vital role in cell cycle progression.

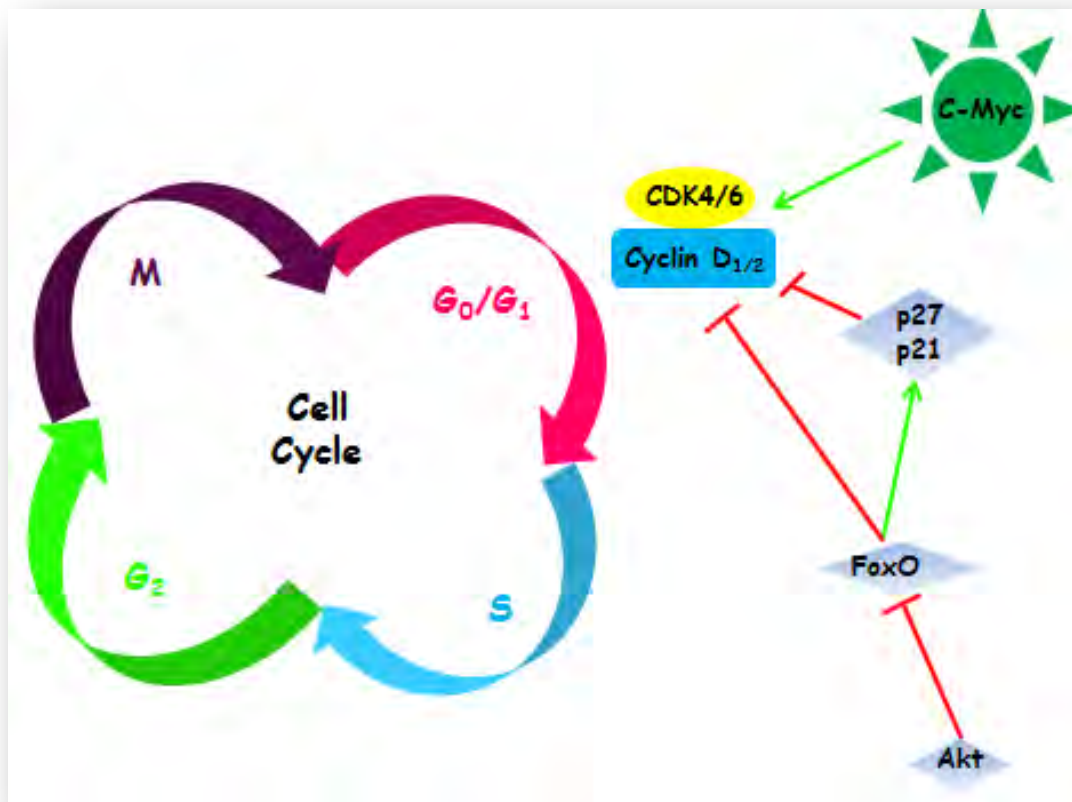


Figure 1.7: Cell cycle regulation (prepared by author: Docrat, 2016)

### 1.2.8 PI3K/Akt and cell cycle progression

P21<sup>Cip1</sup> is a potent cyclin-dependent kinase inhibitor (CKI). Binding of p21<sup>Cip1</sup> to Cdk4/cyclin D and Cdk6/cyclin D complexes, induces kinase activity from early G<sub>1</sub>-until the middle of S-phase. This inhibitory process is prevented by PI3K/Akt via p21 phosphorylation (Sherr and Roberts, 1999). Cyclin D1, a key player in progression of the cell cycle, is strongly activated by the PI3K/Akt pathway. Numerous proteins are phosphorylated and degraded by active/phosphorylated GSK-3( $\alpha/\beta$ ) which inhibits the activity of their downstream targets cyclin D; c-Myc and glycogen synthase (Cantley, 2002, Woodgett, 1994). GSK-3( $\alpha/\beta$ ) activation regulates the protein levels of cyclin D<sub>1</sub> which allows for its stabilisation. Apoptotic regulation by GSK-3( $\alpha/\beta$ ) is controversial; however studies have shown that GSK-3( $\alpha/\beta$ ) overexpression can result in apoptosis (Kotliarova et al., 2008).

### ***1.2.8.1 PI3K/Akt and NF- $\kappa$ B***

The direct downstream effector of PI3K, Protein Kinase B/AKT plays a pivotal role in growth, survival and proliferation of cells via regulation of numerous downstream signals. Among these signals, the most commonly mentioned target is the nuclear factor- $\kappa$ B (NF- $\kappa$ B) pathway. Binding of inhibitor of  $\kappa$ B (I $\kappa$ B) to NF- $\kappa$ B causes localisation to the cytosol where it cannot regulate transcription. In the absence of I $\kappa$ B, NF- $\kappa$ B is localised to the nucleus where transcription is induced. Initially, NF- $\kappa$ B was associated as a promoter of apoptosis. Agents like TNF- $\alpha$ , that induce apoptosis, also induce NF- $\kappa$ B (Beg and Baldwin, 1993, Beg et al., 1993), however, inhibition of NF- $\kappa$ B has been shown to potentiate apoptosis (Beg and Baltimore, 1996, Wang et al., 1996). This is indicative NF- $\kappa$ B being an antiapoptotic molecule. Inhibitor of  $\kappa$ B kinase (IKK) degrades the active form, I $\kappa$ B via catalytic IKK- $\beta$  and IKK- $\gamma$ . Akt induces degradation of I $\kappa$ B, the inhibitor of NF- $\kappa$ B by phosphorylation and IKK activation, causing apoptotic inhibition (Romashkova and Makarov, 1999). The PI3K/Akt-regulated NF- $\kappa$ B activation, via IKK- $\beta$  dependent mechanism is now well recognised (Shao et al., 2001, Sun et al., 2010) Tumour proliferation can be stopped via apoptosis or increasing sensitivity of these cells to anti-tumour agents by blocking NF- $\kappa$ B (Escarcega et al., 2007).

### ***1.2.8.2 PI3K/Akt and p53 crosstalk***

Integration of stress signals and survival pathways lead to cellular commitment to apoptosis. Apoptotic cell death is regulated via involvement of two proteins, p53 and Akt (Gottlieb et al., 2002). The serine/threonine protein kinase B/Akt has an essential role in aversion of cell death (Lo and Cruz, 1995, Zhao et al., 2016). Various substrates regulated by Akt have been implicated in the inhibition of apoptosis and survival promotion (Lo and Cruz, 1995, Zhao et al., 2016). Cellular stressors, such as damaged DNA, hypoxia and deregulation of oncogene expression, activate the tumour suppressor protein, p53. (Townsend and Tew, 2003, Berkholz et al., 2008, Qi et al., 2013). This transcription factor is central to regulating apoptosis. (Townsend and Tew, 2003, Crescencio et al., 2009, Sánchez et al., 2008). The cell death mechanism elicited by p53 may include direct transcriptional transactivation of various pro-apoptotic genes or transactivation-independent mechanisms. Akt and p53 are major, yet opposing components of cellular survival signalling pathways. The ultimate decision- death or survival may be attributed to a cross-talk between these two proteins. Studies have shown decreased expression of Akt in cells undergoing p53-dependent apoptosis (Sánchez et al., 2008, Velho et al., 2006). The ability

of Akt to directly impinge on the p53 pathway, quenching its apoptotic activity, is an attractive possibility. The Murine double minute 2, (Mdm2), onco-protein is an important physiological p53 regulator. It is a negative regulator of p53 and functions via p53 ubiquitinylation and induces rapid proteosomal degradation (Nakahara et al., 1994, Pierno et al., 1999, Qi et al., 2013). Upon phosphorylation by Akt, Mdm2 efficiently translocates to the nucleus, where it binds to and degrades p53. Inspection of human Mdm2's amino acid sequence, revealed two consensus sites, 166 and 186, phosphorylated by Akt (Park et al., 2008a). Thus, p53 function is inhibited via Akt-mediated Mdm2 phosphorylation, attenuating the apoptotic effects of p53 and cellular survival. Furthermore, p53 exerts positive effects on the tumour suppressor gene, phosphatase and tensin homologue (PTEN) promoter. PTEN is responsible for inhibition of the PI3K/Akt pathway via PIP<sub>3</sub> dephosphorylation (Chan et al., 2003b).

### **1.2.9 Inflammatory status and cytokines**

The inflammatory response functions to protect against foreign bodies and pathogens. Its induction occurs via immune cells such as macrophages. These cells are activated and recruited and in turn regulate expression of cell adhesion proteins, chemokines and pro-inflammatory cytokines such as, TNF- $\alpha$ , IL-6, and IL-1 (Kulinsky, 2007). Studies suggest that the inflammatory response is closely associated with cancer; these include prostate, breast and lung carcinoma (Howe, 2007, Lin et al., 2001b, Dennis et al., 2002). TNF-  $\alpha$  overexpression leads to increased tumour size (Suganuma et al., 1999). Data suggests that inhibition of PI3K signalling results in decreased pro-inflammatory cytokine production (Xie et al., 2014). These findings suggest the PI3K/Akt pathway has a potential therapeutic target for cancer and inflammatory disorders.

## CHAPTER 2

### 2.1 Materials and methods

#### 2.1.1 *Materials*

Atorvastatin (20mg, Aspavor, Pharmacia) was purchased from a local pharmacy (Dischem, Westwood). HepG2 cells were purchased from Highveld Biologicals (Johannesburg, SA). Tissue culture consumables were purchased from Lonza (Biowhittaker, Switzerland), and ATP and Caspase-Glo<sup>®</sup> -3/7, -8, and -9 assays, were purchased from Promega (Madison, USA). Western blot reagents were purchased from Bio-Rad (Hercules, CA, USA) and primary antibodies were purchased from Cell Signalling Technology, (Massachusetts, USA). Unless otherwise stated, the remaining consumables were purchased from Merck, (Darmstadt, Germany).

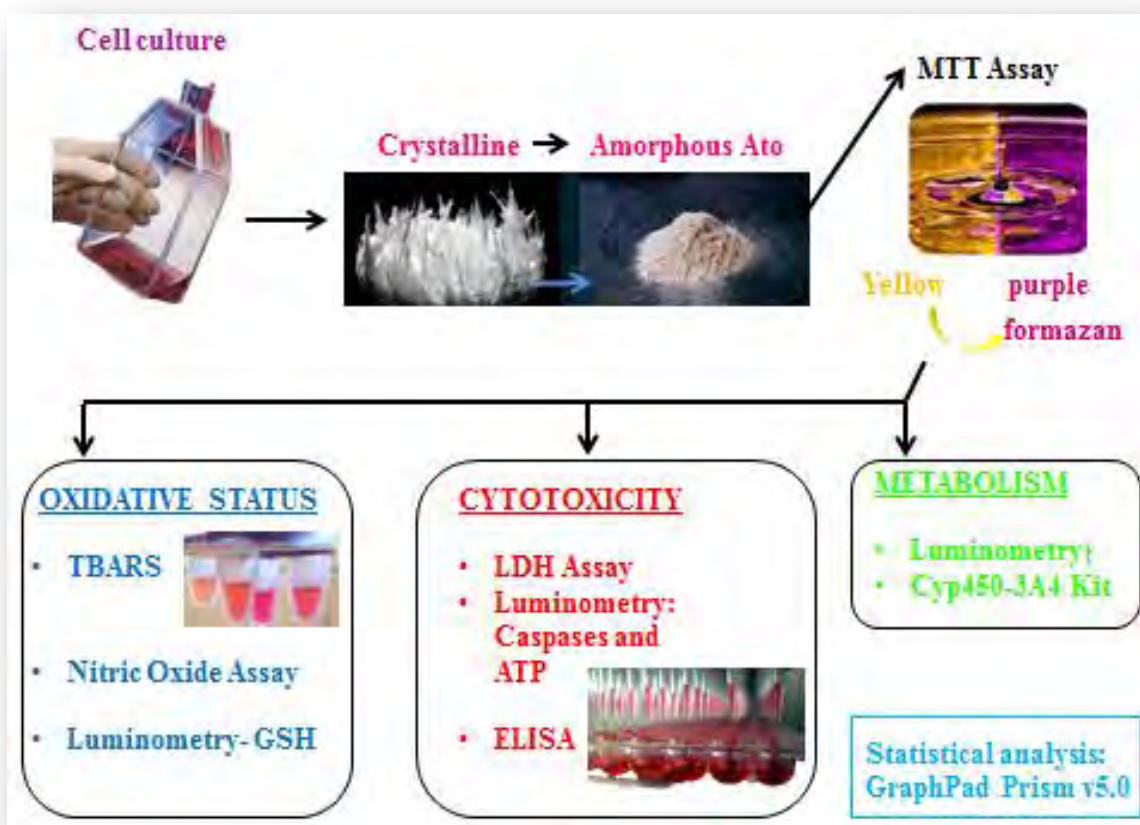


**Figure 2.1:** A summary of methodology used in all experiments in the study (prepared by author: Docrat, 2016)

## 2.2 Cell culture and maintenance

The main site for drug metabolism is the liver. The adherent, epithelial, HepG2 cells are a derivative of liver hepatocellular carcinoma from a 15year old Caucasian male. The general use of HepG2 cells involves assessment of bioactivation or metabolism of xenobiotics. Their morphology resembles the parenchymal cells of the liver, and they retain the majority of normal liver cell functions. Cells were maintained in 75cm<sup>3</sup> culture flasks (37°C, 5% CO<sub>2</sub>) (Figure 2.1). Complete culture media (CCM) [Eagle’s minimum essential medium (EMEM) supplemented with 1% L-glutamine, 1% penstrepfungizone, and 10% Foetal calf serum (FCS)], was provided for cell growth. Media was replenished every second day. Cells were sub-cultured at 90-100% confluency, rinsed thrice with 0.1M phosphate buffer saline (PBS) (5ml, 0.1M), and followed

by detachment using trypsin-EDTA (Lonza Biowhittaker) (2ml, 10-15min, 37 ° C). Cells were monitored by the use of an inverted light microscope (Olympus IXSI; 20x magnification), when rounded, CCM was added in the ratio 2:1 to inactivate the trypsin. Agitation of flask allowed for detachment.

The Trypan blue dye exclusion method is based on the principle that healthy cells possess intact cellular membranes, preventing dye entry whereas damaged/dead cells allow for staining to occur (Figure 2.2). The number of viable cells in suspension was determined using this method. All experiments were conducted in triplicate.

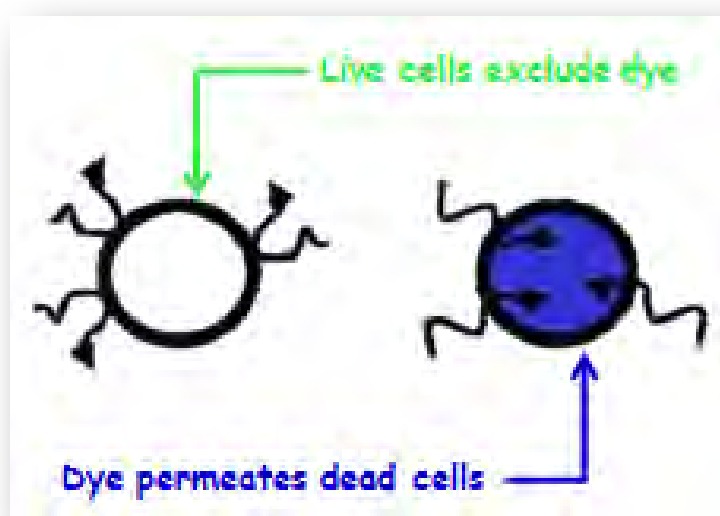


**Figure 2.2:** Trypan Blue dye exclusion method (prepared by author: Docrat, 2016)

### 2.3 Atorvastatin preparation

The crystalline structure of Ato diminishes its solubility. The solubility of Ato was enhanced by altering its chemical structure to a more soluble amorphous form (Figure 2.3). The following steps were followed:

- a) Crushed Ato tablets (300mg) were completely dissolved in a non-hydroxlic solvent (1, 4-Dioxane) (50ml, 45-50°C, 20min) until a clear solution was obtained.
- b) To precipitate the Ato calcium, the dissolved Ato was added (drop-wise) to a non-polar anti-solvent (N-heptane) (200ml, 25-30 °C, 20min).



- c) Contents were stirred on a heat block (25-30 °C) using a magnetic stirrer (2hours).
- d) Thereafter, the solvent was removed via filtration, and dried in an oven overnight (45-50 °C) yielding amorphous Ato.

This process yielded 85% of initial mass used. The Ato produced was dissolved in deionised water [1000µg/ml] and freeze-dried (VirTis 2.0). Thereafter, the freeze dried product was weighed, dissolved in dH<sub>2</sub>O, and filter sterilised [0.22 µM filter (Millipore)] to make up a stock treatment [5000µg/ml]. For each assay, treatment was freshly prepared to prevent degradation and inefficiency.



**Figure 2.3:** Preparation of Atorvastatin from crystalline to amorphous form (PACE- Physician's Academy for Cardiovascular Education, 2016)

## 2.4 Cell proliferation and metabolic activity

### 2.4.1 MTT assay

Cellular proliferation in HepG2 cells treated with Atorvastatin was assessed using the colorimetric methylthiazol tetrazolium dye reduction, [3, (4, 5-dimethylthiazol-2-yl)-2, 5-diphenyl tetrazolium bromide] (MTT) assay. The principle of this assay is dependent on the ability of metabolically active/viable cells to convert the yellow water-soluble MTT salt to its purple insoluble formazan product (Figure 2.4). This reaction is dependent on the activity of dehydrogenase enzymes and the redox potential of the cell. Dimethyl sulfoxide (DMSO) was used to dissolve the insoluble MTT crystals and a spectrophotometer (Bio-tek µQuant) was used

to measure absorbance values. The intensity of the formazan product is directly proportional to cellular viability and metabolic activity.

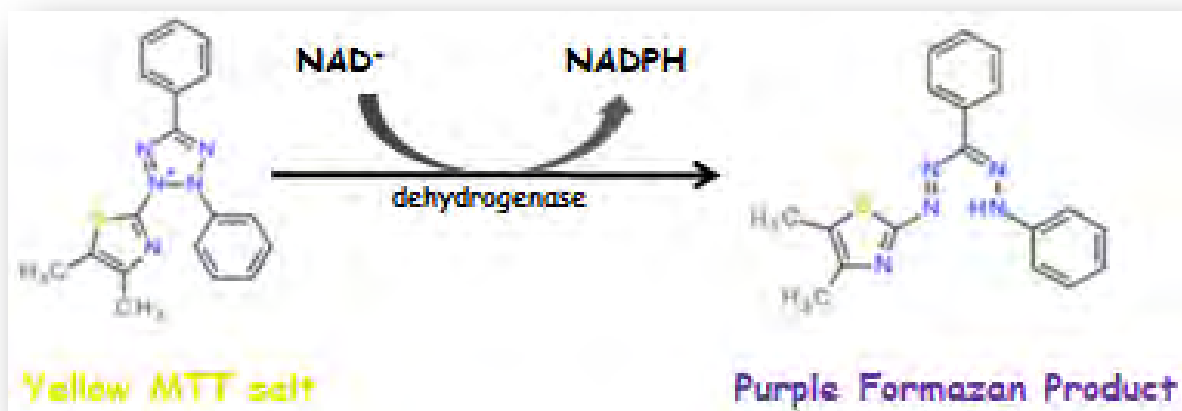


**Figure 2.4:** Principle of MTT assay (prepared by author: Docrat, 2016)

HepG2 cells were seeded (10 000cells/well) in a 96well-microtitre plate, and incubated with a range of Ato concentrations (200, 400, 600, 800, 1000, 1200µg/ml) in triplicate for 48h. Untreated control cells were incubated with CCM only. Thereafter, cells were incubated for 4h with the MTT substrate (5mg/ml in 0.1M PBS, 37°C, 5% CO<sub>2</sub>). Following aspiration of supernatants, DMSO was added to all wells (100µl/well) and incubated for 1h. Optical densities (OD) were measured at 570nm with a reference of 690nm using a spectrophotometer (Bio-Tek µQuant). Data is represented as percentage cell viability (Figure 2.5), from which the IC<sub>50</sub> (50% inhibitory concentration) was obtained.

$$\% \text{ cell viability} = \frac{\text{average OD treated cells}}{\text{average OD control cells}} \times 100$$

**Figure 2.5:** Formula used to calculate cell viability as a percentage (prepared by author: Docrat, 2016)

#### **2.4.2 Treatment for subsequent assays**

An IC<sub>50</sub> was extrapolated from the dose response curve and used to treat all subsequent assays. All treatments for assays subsequent to the MTT were conducted in 6-well plates. HepG2 cells were seeded (350 000cells/well) and allowed to grow to approximately 60% confluency. For each assay, untreated control and Ato-treated cells (IC<sub>50</sub> value-678.8µg/ml) were prepared as three biological replicates, and incubated for 48h (37°C, 5% CO<sub>2</sub>). CCM and treatments were replenished after 24h. Following incubation, the supernatants were aspirated and stored at -80°C. To ensure removal of any residual media, the cell sheet was rinsed with 0.1M PBS.

#### **2.4.3 The ATP quantification assay**

Intracellular levels of ATP were determined using the CellTiter-Glo® kit (Promega, United States, Madison, USA). The principle of the ATP quantification assay is based on bioluminescence. In the luciferase reaction, the presence of magnesium ions (Mg<sup>2+</sup>) and ATP facilitates the conversion of luciferin to oxyluciferin (Figure 2.6). As a result, energy is released in the form of light which is proportional to the intracellular ATP concentration.

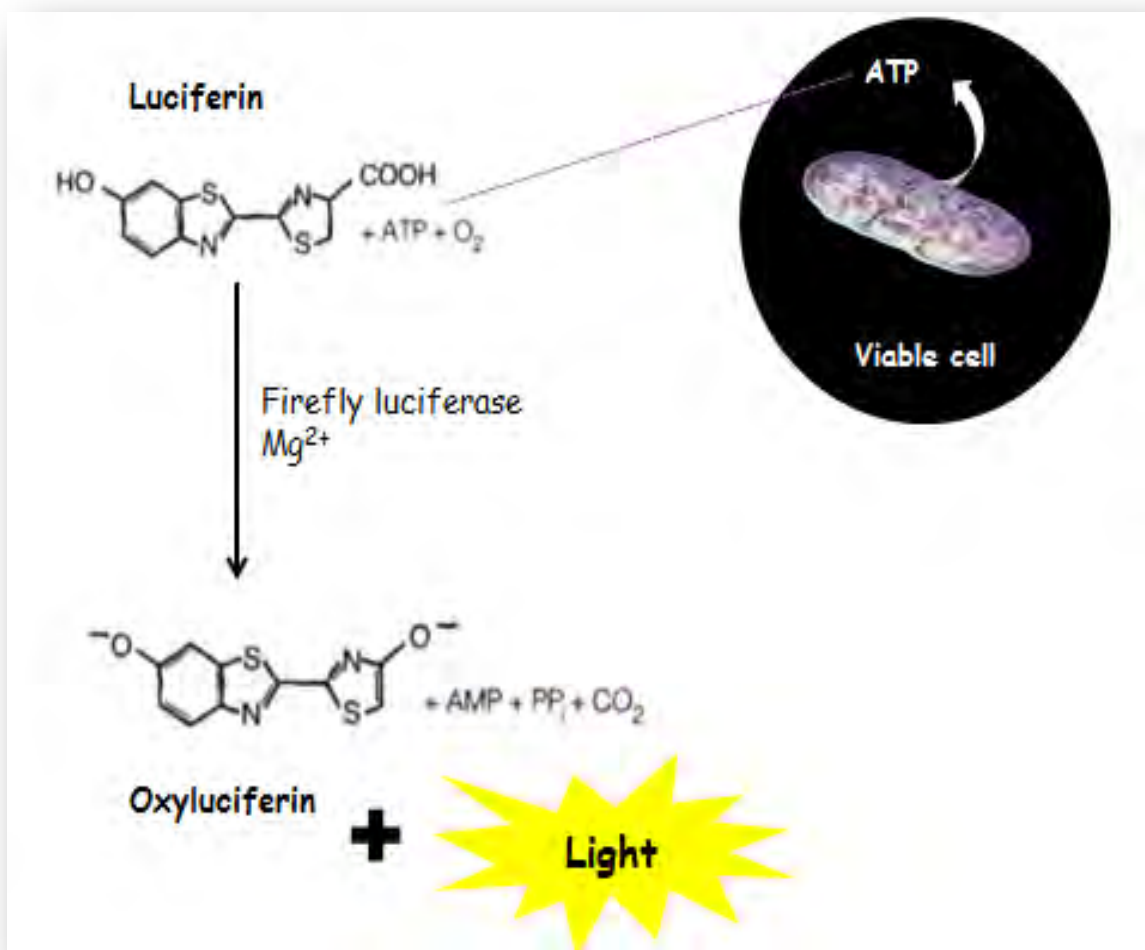


**Figure 2.6:** Luciferase reaction where mono-oxygenation of luciferase occurs (prepared by author: Docrat, 2016)

Cells were seeded in triplicate (20 000cells/well) into a microtiter luminometer plate. Following addition of 50µl CellTitre Glo™ reagent (Promega, Madison, USA) to each well, the plate was incubated in the dark at room temperature (RT) for 30min. This facilitated cell lysis and the luciferase-based reaction (Figure 2.5). The luminescent signal produced was read using a Modulus™ microplate luminometer (Turner Biosystems, USA). The ATP concentrations obtained were expressed in Relative Light Units (RLU).

## 2.5 Oxidative status

### 2.5.1 The thiobarbituric acid reactive substance assay

Malondialdehyde (MDA) remains one of the most common biomarkers of lipid peroxidation (Ott et al., 2007). The thiobarbituric acid (TBA) reactive substance (TBARS) assay measures levels of MDA formed by lipid peroxidising systems. The procedure involves the condensation between TBA molecules and an MDA molecule (2:1), which yields a pink chromogen (Figure 2.7).

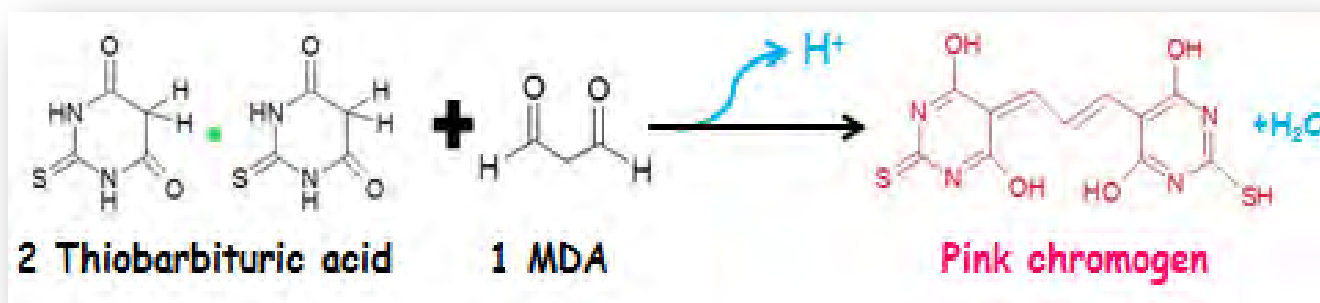


**Figure 2.7:** Principle of TBARS assay (prepared by author: Docrat, 2016)

Following the 48h treatment, supernatants (200 $\mu$ l) were added to pre-labelled glass test tubes containing 200 $\mu$ l 2% phosphoric acid (H<sub>3</sub>PO<sub>4</sub>). A blank was used as a negative control to eliminate background absorbance. To each tube, 7% H<sub>3</sub>PO<sub>4</sub> (200 $\mu$ l), TBA/Butylated hydroxytoluene (BHT) (400 $\mu$ l), and HCl (1M) was added. HCl (3mM, 400 $\mu$ l) was added to the blank. A positive control, containing MDA (1 $\mu$ l) was prepared. Samples were vortexed and placed in a water bath (100°C, 15min) and then allowed to cool (RT). After cooling, butanol was added (1500 $\mu$ l), vortexed and allowed to separate into two distinct phases. Thereafter, the upper butanol layer (100 $\mu$ l) was aliquoted in triplicate into a 96-well microtiter plate which was read on a spectrophotometer (Bio-Tek  $\mu$ Quant) at absorbance 532nm with a reference wavelength 600nm.

### 2.5.2 The Griess assay

To determine the levels of nitric oxide (NO) metabolites produced, the standard protocol was used as described by (Reuter et al., 2010). The principle involves detection of nitrite ( $\text{NO}_2^-$ ) present in solution via a diazotization reaction (Figure 2.8).

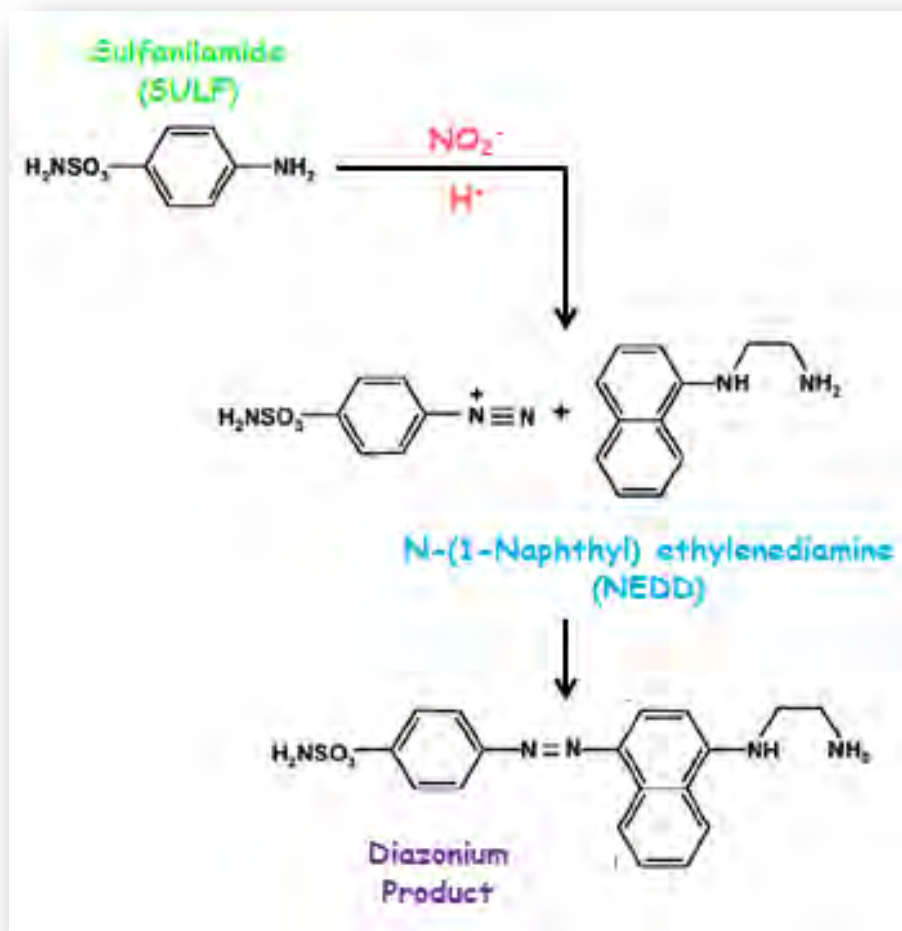


**Figure 2.8:** Principle of Griess reaction (prepared by author: Docrat, 2016)

Following preparation of standards with known concentrations (0-200 $\mu\text{M}$ ) using stock sodium nitrate (200  $\mu\text{M}$ ), samples were pipetted into a 96-well microtiter plate (50 $\mu\text{l}$ , duplicate). Vanadium (III) Chloride ( $\text{VCl}_3$ ) (8mg/ml, 50 $\mu\text{l}$ ), 2% Sulfanilamide (SULF) (25 $\mu\text{l}$ ), and Naphthylethylenediamine dihydrochloride (NEDD) (0.1% in 5% HCl, 50 $\mu\text{l}$ ) were added to each well respectively. The plate was incubated in the dark (30min, 37 $^\circ\text{C}$ ), and absorbance was determined on a spectrophotometer (Bio-Tek  $\mu\text{Quant}$ ), 540nm with reference wavelength

690nm. Data is represented as concentration ( $\mu\text{M}$ ), determined by extrapolation from the standard curve.

### 2.5.3 GSH-Glo™ Glutathione assay

Cellular glutathione levels are an indication of endogenous antioxidant capacity. In the presence of GSH, Glutathione- S- transferase (GST) catalyzes the conversion of a luciferin derivative to luciferin (Figure 2.9). The amount of glutathione present in the sample is directly proportional to the signal produced.

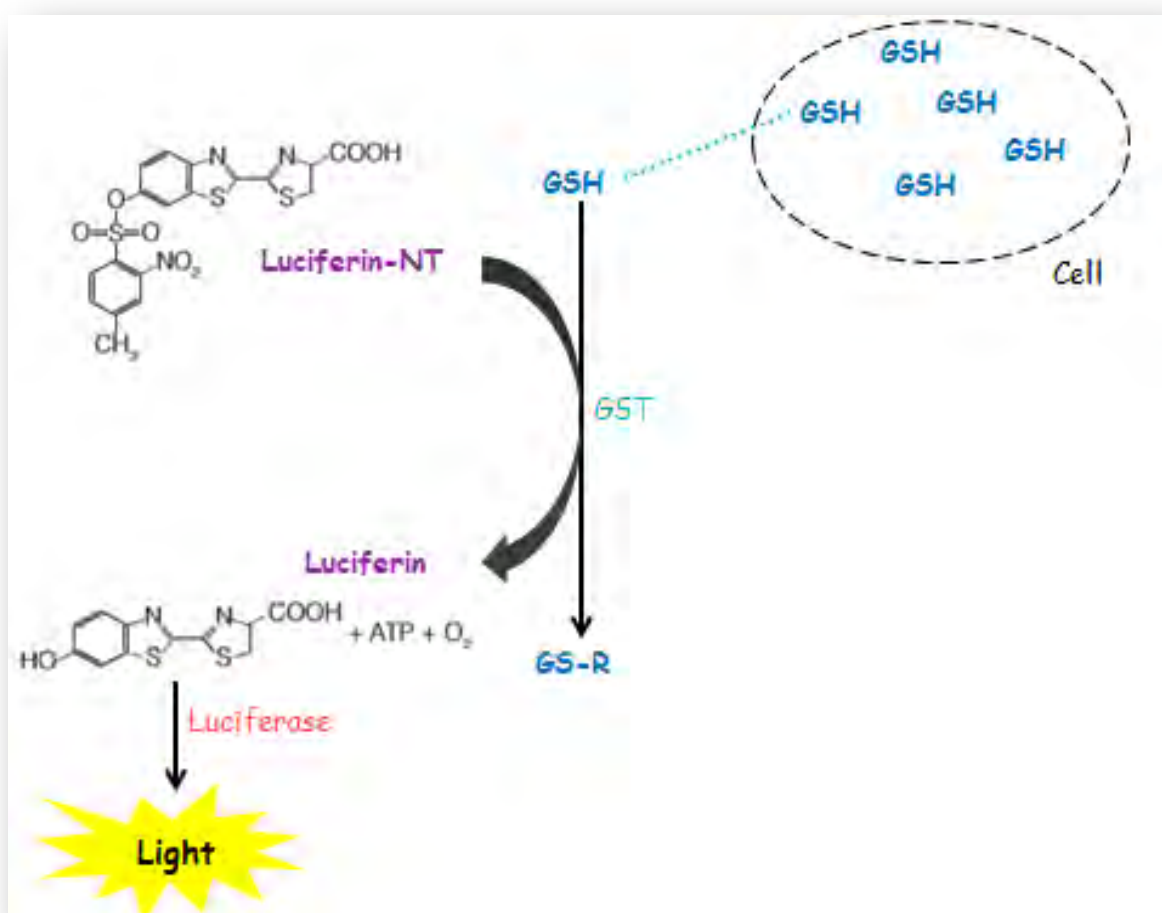


**Figure 2.9:** Overview of GSH-Glo™ Glutathione Assay principle (prepared by author: Docrat, 2016).

Cellular GSH levels were analysed using the GSH-Glo™ Glutathione Assay kit as per manufacturer's instructions (Promega, Madison, USA). Following treatment, cells were seeded in a white luminometer plate (20,000cells/well, triplicate in 0.1M PBS). Standards of known concentration (0-50µM) were prepared and pipetted in triplicate; from this a standard curve was generated. To each well GSH-Glo™ Reagent (50µl) was added followed by a brief agitation (30sec). The plate was incubated in the dark (RT, 30min). Thereafter, Luciferin Detection Reagent (100µl) was added followed by a second incubation in the dark (RT, 15min). The Modulus™ plate reader (Turner Biosystems, Sunnyvale, CA) was used to detect luminometric emission. Data is represented as concentration (µM), determined by extrapolation from the standard curve (Appendix 2).

#### **2.5.4 Cytochrome-P<sub>450</sub> 3A4 assay kit**

The effect of Ato on CYP3A4 activity in HepG2 cells was determined using the P450-Glo™ assay (Promega). CYP3A4 being a member of the cytochrome P450 family of proteins, has an essential role in oxidative metabolism of endogenous compounds and xenobiotics in the liver (Nakano et al., 2006). The principle of the P450-Glo™ 3A4 assay is based on a luminescent method for detection of CYP3A4 activity. Luminogenic CYP3A4 substrate is converted to luciferin by the CYP3A4 enzyme (Figure 2.10). The luciferase reaction produces a luminescent signal, which is directly proportional to CYP3A4 activity. Dexamethasone (Sigma, Aldrich, USA) was used as a positive control, as it's known to induce CYP3A4 (Nakano et al., 2006). The reconstituted luciferin detection reagent was prepared as per manufacturer's instructions. HepG2 cells were treated (48h) with Ato and dexamethasone (50µM in CCM) respectively. Cells were then seeded into a 96-well luminometer plate (50µl, 20,000cells/well, triplicate). Following incubation (in dark, RT, 4hours) with the luciferin-PFBE substrate (50µl/well), the luciferin detection reagent (50µl) was added and incubated (in dark, RT, 30min). The luminescence was detected with a Modulus™ microplate luminometer (Turner Biosystems, Sunnyvale, USA) and data expressed in relative light units (RLU).



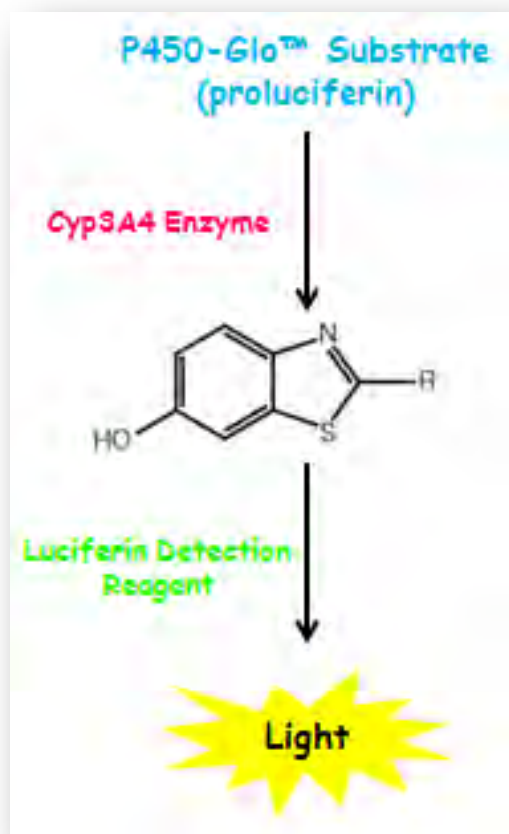


**Figure 2.10:** Reaction involved in the P450-Glo™ assay (prepared by author: Docrat, 2016)

## 2.6 Cellular Death

### 2.6.1 The lactate dehydrogenase assay

Cell death/membrane damage was measured using the Lactate dehydrogenase (LDH) cytotoxicity detection kit (Roche, Germany). When cellular membrane integrity is compromised or lost, LDH, an otherwise stable cytosolic enzyme, is released into the extracellular space. This assay is colorimetric, and quantifies the level of LDH present in the supernatant of treated cells. This principle of this assay is based on a two-step enzymatic process. LDH acts as a catalyst in the conversion of lactate to pyruvate, which promotes reduction of  $\text{NAD}^+$  to  $\text{NADH}/\text{H}^+$  (Figure 2.11). The newly formed  $\text{NADH}/\text{H}^+$  is used by a diaphorase to catalyze the reduction of a tetrazolium salt to a pigmented formazan product.

Briefly, 100µl supernatant was aliquoted in triplicate into a 96-well microtiter plate. Substrate mixture (100µl) consisting of a diaphorase/NAD<sup>+</sup> catalyst and a sodium lactate/INT dye solution was added to each sample and incubated for 25min (RT). The optical density (OD) of the formazan product was read on a spectrophotometer (Bio-Tek µQuant) at 500nm. Data is represented as mean OD.

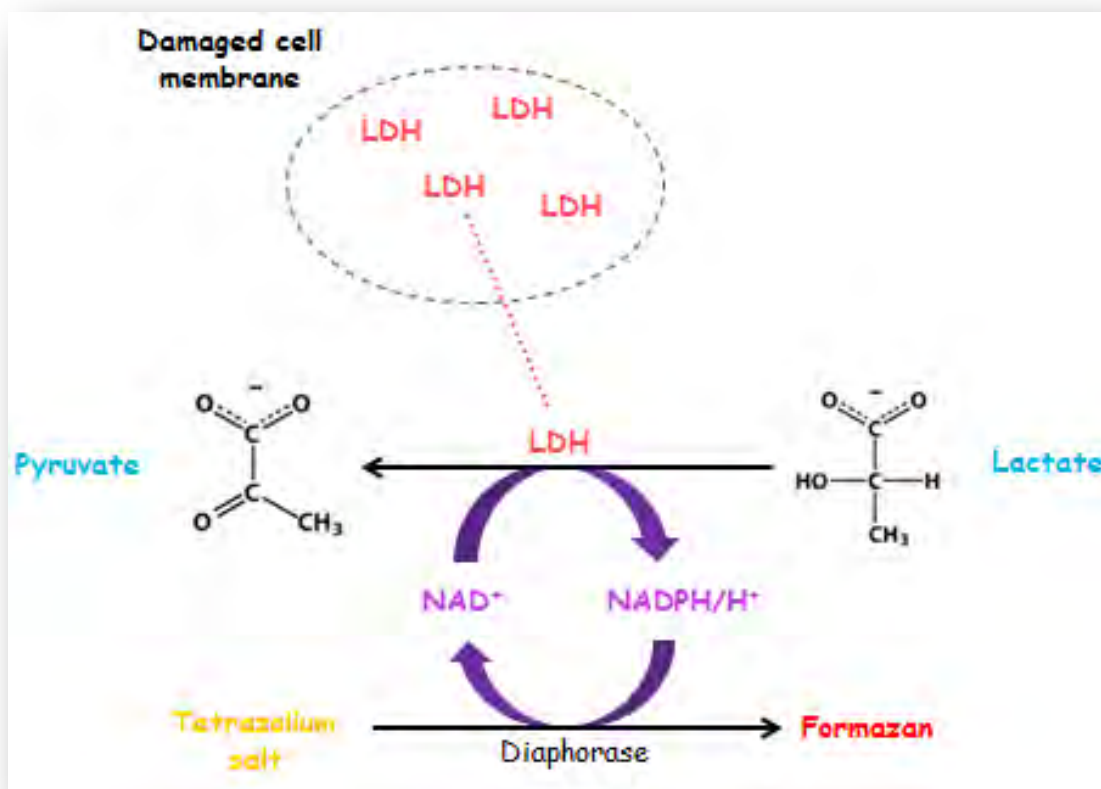


**Figure 2.11:** Principle of LDH cytotoxicity assay (prepared by author: Docrat, 2016).

### 2.6.2 Analysis of caspase activity

Caspase activity was detected using the Caspase Glo® 3/7, Caspase Glo® 8, and Caspase Glo® 9 Assay kits (Promega, Madison, USA). These assays have a homogenous and luminescent nature. Each assay kit contains their respective luminogenic substrates in buffer systems that have been optimised for caspase, cell lysis and luciferase activity. A luminescent signal is generated as a result of the luciferase reaction (Figure 2.12).

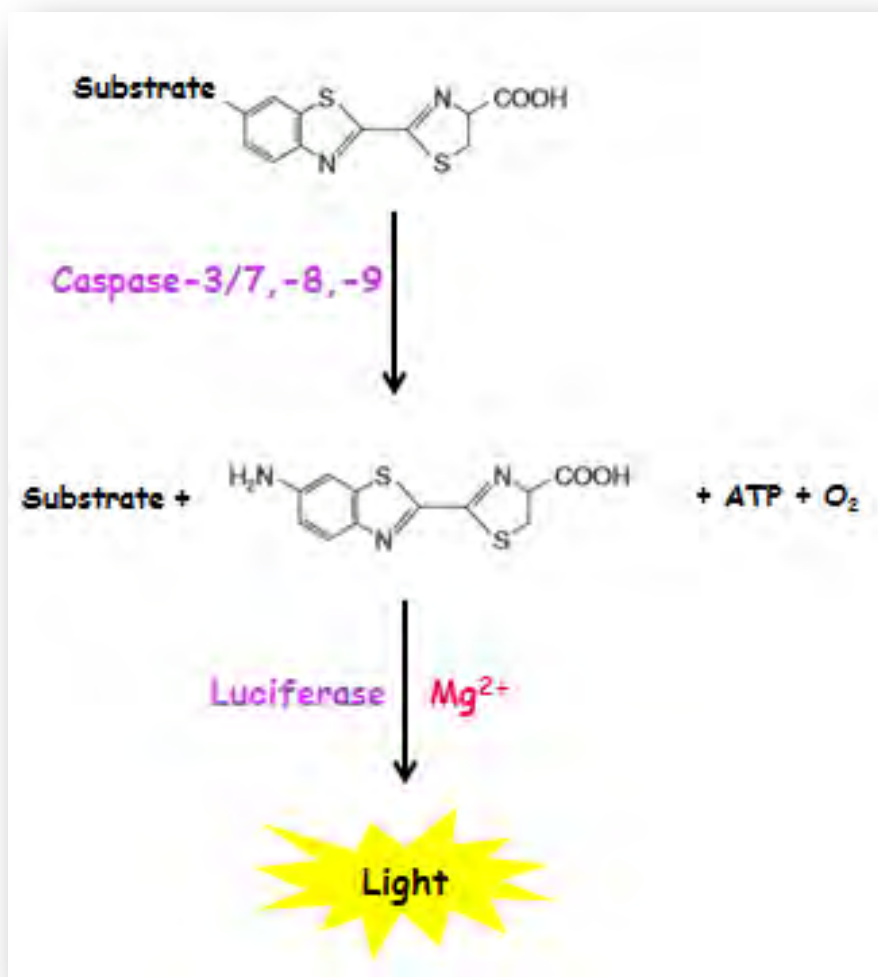


**Figure 2.12:** Overview of the caspase activity assay (prepared by author: Docrat, 2016)

Following the 48h treatment, cells were seeded in triplicate in a 96-well luminometer plate (20,000cells/well). The Caspase Glo® reagents (caspases -8, -9, and -3/7) were prepared according to manufacturer's instructions (Promega) and were added to each sample (20µl). Following incubation in the dark (RT, 30min), the plate was read with a Modulus™ microplate luminometer (Turner Biosystems, Sunnyvale, USA) and data expressed in relative light units (RLU).

### 2.6.3 Enzyme-linked immunosorbent assay (ELISA)

The cytokine activity of Interleukin-6 (IL-6) and Tumour necrosis factor-alpha (TNF- $\alpha$ ) were measured using the Human IL-6 and Human TNF- $\alpha$  ELISA kits (BD OptEIA™, USA). As per manufacturer's instructions, a 96-well plate was coated (overnight) with IL-6 and TNF- $\alpha$  monoclonal antibodies (capture antibody diluted in coating buffer). Following 3 washes (1 $\times$  detergent solution with ProClin™-150); ELISA Assay diluent (0.09% sodium azide, 12ml buffered protein base) was added to each well as a blocking agent (RT, 1hour). Standards were prepared (Figure 2.13) and added along with samples to appropriate wells (100 $\mu$ l), followed by a 2hour incubation (RT). Following 5 washes, working detector (Streptavidin-horseradish peroxidase and Biotinylated anti-human monoclonal antibody) was added to each well and incubated in the dark (100 $\mu$ l, RT, 1hour). Thereafter, wells were washed seven times and TMB (3, 3', 5, 5'-tetramethylbenzidine) One-Step Substrate Reagent was added. The plate was incubated in the dark (RT, 30min). Stop solution (1M phosphoric acid) was added (50 $\mu$ l/well). The absorbance was measured with a microplate reader (Bio-Tek  $\mu$ Quant, United States) at 450nm with a reference wavelength of 570nm. Cytokine concentrations were determined by extrapolation from the standard curve (Appendix 3).

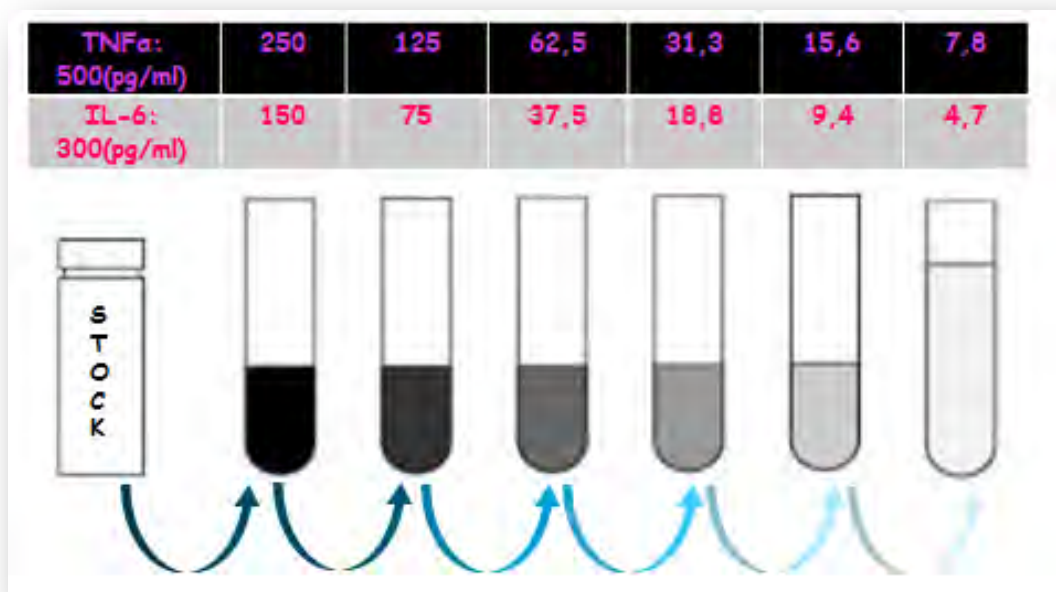


**Figure 2.13:** Serial dilutions for preparation of standards (prepared by author: Docrat, 2016).

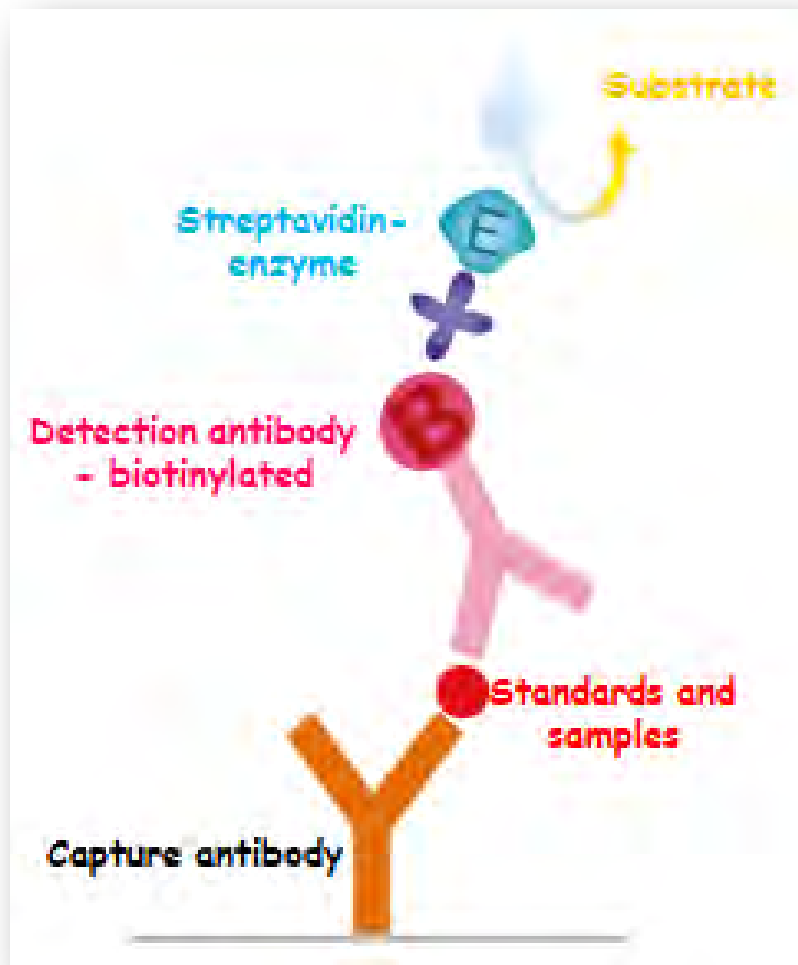


**Figure 2.14:** ELISA Assay principle outlining configuration (prepared by author: Docrat, 2016)

## 2.7 Western Blotting

### 2.7.1 Protein extraction, quantification and standardisation

HepG2 cells were treated as described in section 2.4.2 for protein isolation. Cytobuster™ reagent (Novagen®, SA), supplemented with phosphatase and protease inhibitors (Roche, SA) was added to the cells (100µl/well) and placed on ice (30min). Cells were harvested via mechanical scraping and centrifuged (10 000xg; 4°C, 10min). Supernatants were transferred to previously labelled 1.5ml microcentrifuge tubes and placed on ice.

The bicinchoninic acid (BCA) assay was used to quantify the crude protein extract. This colorimetric assay is based on a two-step reaction (Figure 2.15). The first step involves reduction of  $\text{Cu}^{2+}$  ions to  $\text{Cu}^+$  by the peptide bonds in protein. The quantity of reduced  $\text{Cu}^{2+}$  is directly proportional to the amount of protein present in solution. The second step occurs when two BCA molecules chelate with a  $\text{Cu}^+$  ion, resulting in an intense purple colour that absorbs light at 562nm.

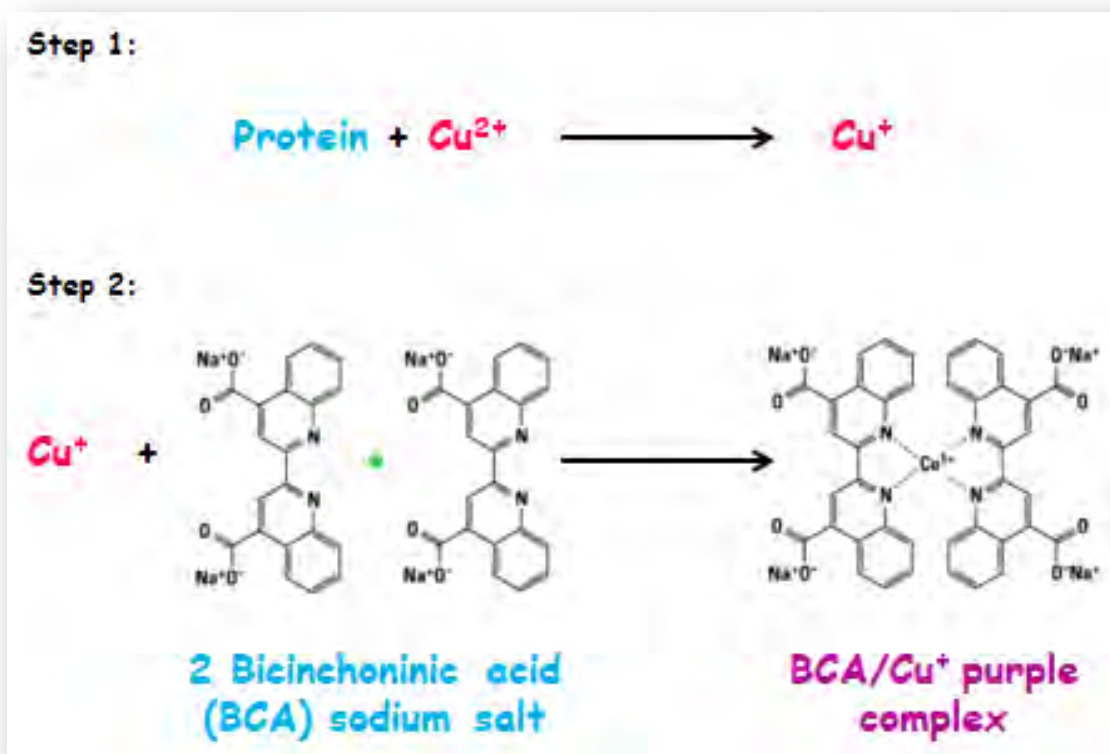


**Figure 2.15:** Principle of BCA Assay (prepared by author: Docrat, 2016)

Serial dilutions (0.2, 0.4, 0.6, 0.8 and 1.0mg/ml) were prepared from a bovine serum albumin (BSA) stock (1mg/ml in  $\text{dH}_2\text{O}$ ). From this a standard curve was constructed. Samples and BSA standards were transferred to a 96-well plate (25 $\mu\text{l}$ ). Thereafter, the BCA working solution (200 $\mu\text{l}$ ; 198 $\mu\text{l}$  BCA and 4 $\mu\text{l}$   $\text{CuSO}_4$ ) was added to each well and incubated (30min, 37 $^\circ\text{C}$ ). A spectrophotometer (BioTek  $\mu\text{Quant}$ ) was used to read the absorbance at 562nm. The protein concentrations were determined by extrapolation from the standard curve (Appendix 4), and standardised to 0.64mg/ml.

### **2.7.2 SDS-PAGE**

The separation of proteins, dependent on their size, is accomplished with sodium dodecyl sulphate-polyacrylamide gel electrophoresis (SDS-PAGE). Sample preparation involved denaturation of proteins with Laemmli buffer [dH<sub>2</sub>O, 10% SDS, β-mercaptoethanol, 0.5M Tris-HCl (pH 6.8), glycerol, 1% bromophenol blue, (1:1)]. The tertiary structure of protein is maintained by disulphide bridges which are reduced by β-mercaptoethanol, whereas the anionic detergent SDS strongly binds to and denatures the protein. This produces protein with a uniform, negative charge that facilitates movement toward the positive electrode through the gel (Wilson, 2010).

The molecular sieving properties of the gel allow the SDS-protein complexes to migrate through the resolving gel (Ding and Kaminsky, 2003). Polyacrylamide gels were prepared following set up of the Mini-PROTEAN 3 SDS-PAGE apparatus (Bio-Rad, USA) according to manufacturer's instructions. The 7.5% resolving gel [1.5M Tris-HCl (pH 8.8), 10% SDS, 30% bis/acrylamide, dH<sub>2</sub>O, 10% APS, TEMED] was added between the glass plates, followed by a 4% stacking gel [0.5M Tris-HCl (pH 6.8), 10% SDS, 30% bis/acrylamide, dH<sub>2</sub>O, 10% APS, TEMED]. The molecular weight marker (for identification of migrated proteins) and samples (35μl) were loaded into appropriate wells, followed by electrophoresis (150V, 1hour). Transfer buffer (192mM glycine, 25mM Tris, 20% methanol, pH 8.3) was used for equilibration of gels (RT, 10min).

### **2.7.3 Protein transfer**

The transfer of proteins to a nitrocellulose membrane from a SDS-PAGE was done using electrophoresis [Trans-Blot® Turbo Transfer system (Bio-Rad)]. This allowed for the membrane to be probed for the antibody of interest. The procedure involved pre-soaking of nitrocellulose fibre pads in transfer buffer. This was followed by the assembly of a gel-sandwich (Figure 2.16) (fibre pad, nitrocellulose membrane, equilibrated gel, and a second fibre pad) which was placed into the cassette (400mA, 45min).

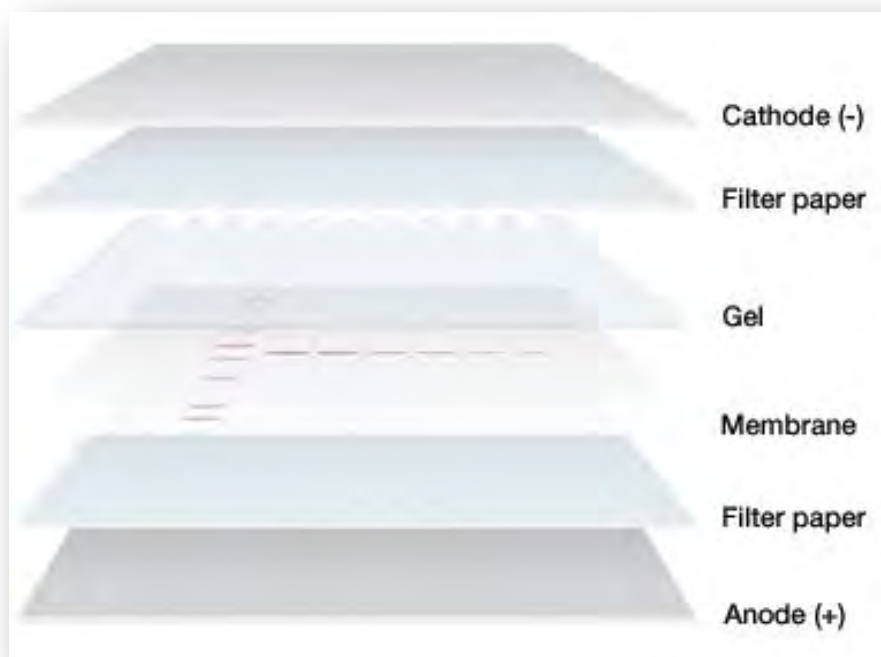


**Figure 2.16:** Gel sandwich assembly (Bio-Rad laboratories, inc., 2016)

#### **2.7.4 Immuno-Blotting**

Proteins express antigenic epitopes, which allow specific reactions to occur between target proteins and the primary antibody. Membranes were blocked (RT, 2hours) with 5% BSA in TTBS [Tris-buffered saline (TBS) consisting of 0.5% Tween20] to prevent nonspecific binding. The membranes were incubated with following primary antibodies (1:1 000 in 5% BSA) overnight (4°C): NF- $\kappa$ B (9936T), I $\kappa$ B- $\beta$  (2370), pAKT (4060), AKT (9272), pGSK-3( $\alpha/\beta$ ) (8566), p53 (2527). Membranes were then washed with TTBS (5 times, 10min), followed by addition of horseradish peroxidase (HRP) conjugated secondary antibody [goat-anti rabbit IgG (H0913), 1:10 000 in 5% BSA] (RT, 1hour). This was followed by a final wash of membranes with TTBS (5 times, 10min). Chemiluminescent detection [Clarity western ECL substrate (BioRad)] facilitated visualisation of protein bands on the membrane on the Chemidoc™ imaging system (Bio-Rad).



### **2.7.5 Quantification of band density using Chemiluminescence**

The immunoblots were used to detect the proteins by using the enhanced chemiluminescence substrates (reagent A and B in 1:1 dilution). Following exposure, densitometric analysis was carried out on the Image Lab™ software (Bio-Rad) and measured as relative band density (RBD).

### **2.7.6 Membrane re-probing**

Membranes were quenched with hydrogen peroxide (H<sub>2</sub>O<sub>2</sub>) (30min, 37°C) to allow for probing with house-keeping protein  $\beta$ -actin. Following quenching, membranes were washed (3times, 10min) and thereafter blocked (5% BSA, 2hours). Membranes were then probed using HRP-conjugated anti- $\beta$ -actin (CS1615, Sigma). Results are normalised as RBD of proteins of interest divided by RBD of  $\beta$ -actin.

## **2.8 Statistical Analysis**

Data analysis was performed using the GraphPad prism V5.0 software (GraphPad Software Inc., La Jolla, USA). Statistical comparisons between results were made using either the one-way analysis of variance (ANOVA) followed by a Bonferroni test for multiple group comparison (data is presented as 95% CI) or the unpaired t-test with Welch correction (mean  $\pm$  standard deviation). Results were considered statistically significant at a  $p$ -value  $< 0.05$ .

## CHAPTER THREE

### RESULTS

#### 3.1 Cell proliferation and metabolic activity

##### 3.1.1 Cell Viability

The effect of Ato on cell proliferation was measured by assessing the metabolic activity in HepG2 cells using the MTT assay. Following a 48h incubation period with serial dilutions of Ato (0-1200 $\mu$ g/ml), a dose-dependent decline in cell viability was observed. An  $IC_{50}$  (50% inhibitory concentration) value was obtained at 678.8 $\mu$ g/ml, and used in all subsequent assays (48hr incubation).

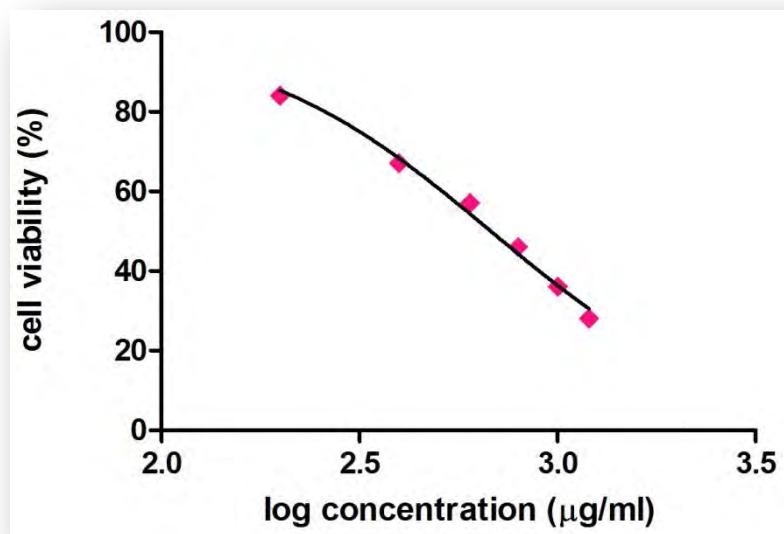


**Figure 3.1:** A dose-dependent decline in HepG2 cell viability following Ato treatment (48hr).

### 3.1.2 Intracellular ATP levels

The level of cellular ATP was determined (luminometric assay). In comparison to the control (2,  $6 \times 10^6$  RLU  $\pm 8 \times 10^4$  RLU), Ato significantly reduced ATP levels (5,  $1 \times 10^5$  RLU  $\pm 1, 3 \times 10^4$  RLU;  $p=0.005$ ) (Figure 3.2).

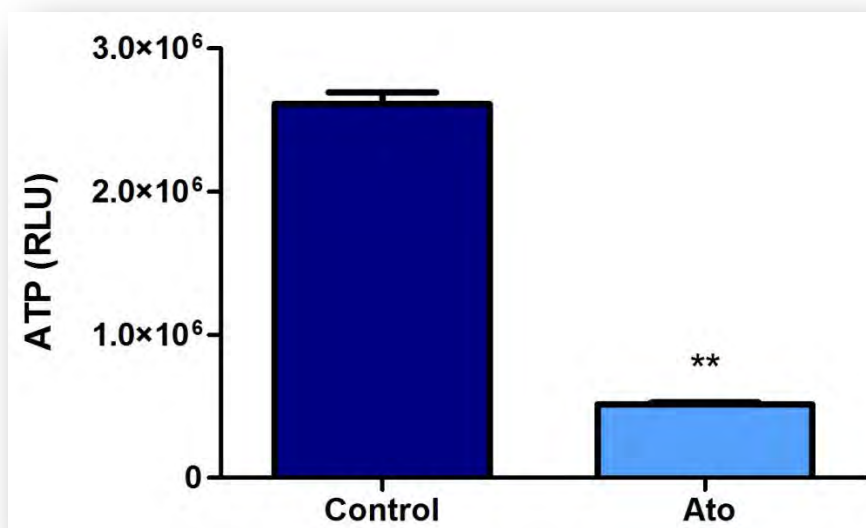


**Figure 3.2:** Level of intracellular ATP was significantly reduced in Ato-treated cells when compared to control cells (\*\* $p \leq 0.005$ ). RLU: relative light units

## 3.2 Oxidative status

The effects of Ato induced oxidative stress in HepG2 cells was determined by measuring lipid peroxidation, levels of nitrites, glutathione (GSH), and CYP3A4 activity.

### 3.2.1 Lipid Peroxidation

The level of MDA, a lipid peroxidation biomarker, was assessed with the TBARS assay. MDA levels were significantly reduced following Ato exposure compared to the control ( $1.7 \times 10^{-1} \mu\text{M} \pm 3.7 \times 10^{-3} \mu\text{M}$  vs.  $2.6 \times 10^{-1} \mu\text{M} \pm 1.6 \times 10^{-2} \mu\text{M}$ ;  $p=0.0097$ ) (Figure 3.3).

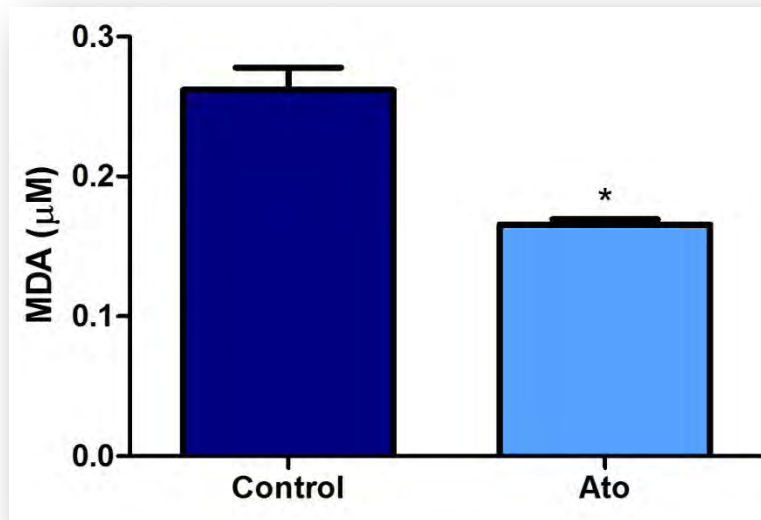


**Figure 3.3:** Level of malondialdehyde in Ato-treated cells is significantly reduced ( $*p \leq 0.05$ ).

### 3.2.2 Level of nitrates and nitrites

Nitrite and nitrate levels were measured using the Griess assay. The nitrite/nitrate levels were significantly increased by Ato as compared to the control ( $14.98 \mu\text{M} \pm 1 \times 10^{-5} \mu\text{M}$  vs.  $12.6 \mu\text{M} \pm 1.3 \times 10^{-1} \mu\text{M}$ ;  $p=0.001$ ) (Figure 3.4)

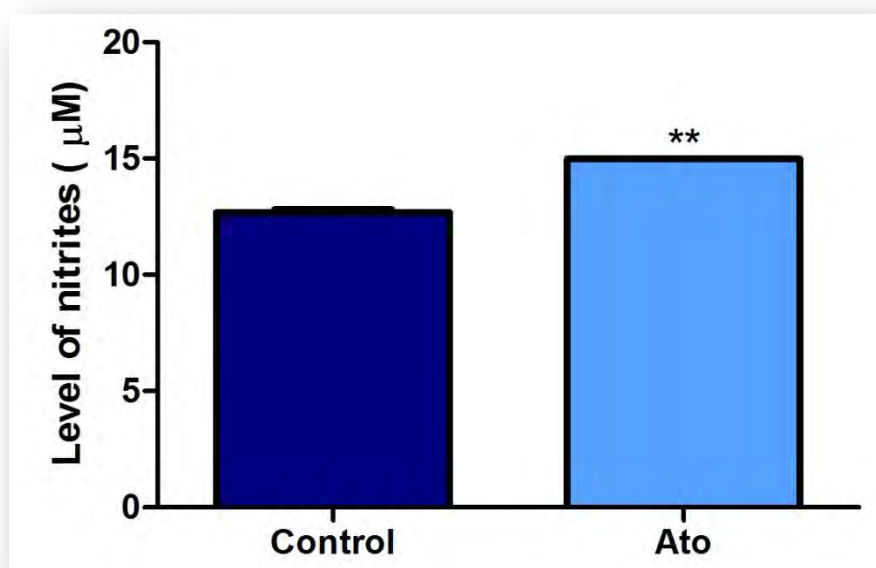


**Figure 3.4:** Extracellular nitrite and nitrate levels were increased in cells exposed to Ato (\*\* $p \leq 0.005$ ).

### 3.2.3 *Glutathione concentration*

The intracellular concentration of GSH was determined using the GSH-Glo™ Glutathione assay. GSH concentrations in HepG2 cells were significantly decreased by Ato treatment as compared to the control ( $1.24 \mu\text{M} \pm 5.2 \times 10^{-3} \mu\text{M}$  vs.  $3.14 \mu\text{M} \pm 5.6 \times 10^{-2} \mu\text{M}$ ;  $p=0.0003$ ) (Figure 3.5).

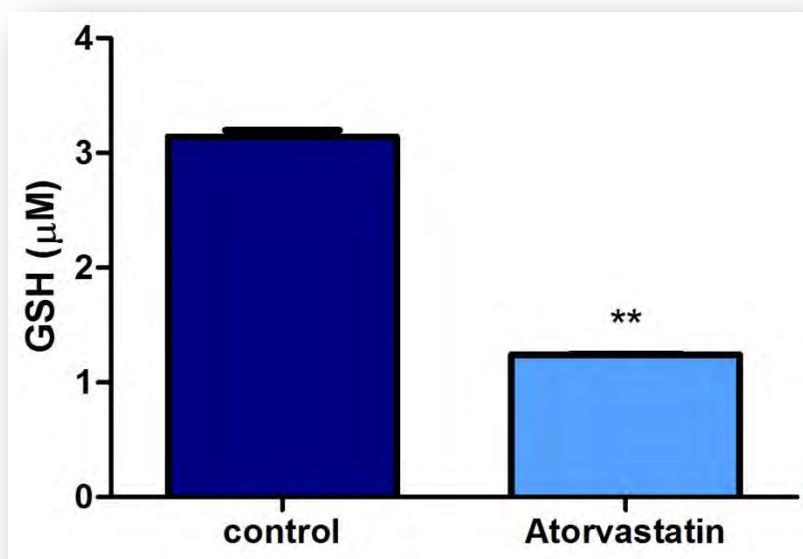


**Figure 3.5:** Glutathione concentrations significantly decreased in HepG2 cells after exposure to Ato (\*\* $p \leq 0.005$ )

### 3.2.4 Cytochrome P450 3A4 Activity

Induction of CYP3A4 enzyme activity was measured using luminometry. Dexamethasone (dex; positive control) and Ato treated cells significantly increased CYP3A4 activity in comparison to the control ( $p=0.0079$ ; control vs. Dex: 95% CI,  $-6.2 \times 10^2$  RLU to  $-1.3 \times 10^2$  RLU; control vs. Ato:  $-5.5 \times 10^2$  RLU to  $-5.7 \times 10^1$  RLU) (Figure 3.6).

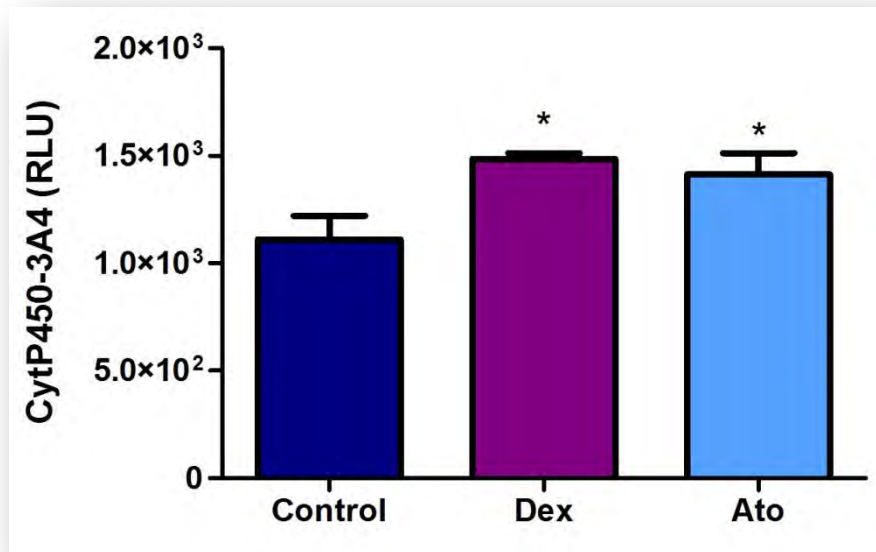


**Figure 3.6:** CYP3A4 activity in HepG2 cells was significantly induced by Ato in comparison to the control ( $*p \leq 0.05$ ). RLU: relative light units. Dex: Dexamethasone

### 3.3 Cellular Death

#### 3.3.1 Extracellular LDH level

The level of extracellular LDH was measured as a marker of compromised cell membrane integrity. Ato treated cells had increased LDH levels in comparison to untreated cells ( $1.27 \text{ units} \pm 1.3 \times 10^{-2} \text{ units}$  vs.  $7.1 \times 10^{-1} \text{ units} \pm 5.5 \times 10^{-3} \text{ units}$ ;  $p=0.0002$ ) as depicted (Figure 3.7)

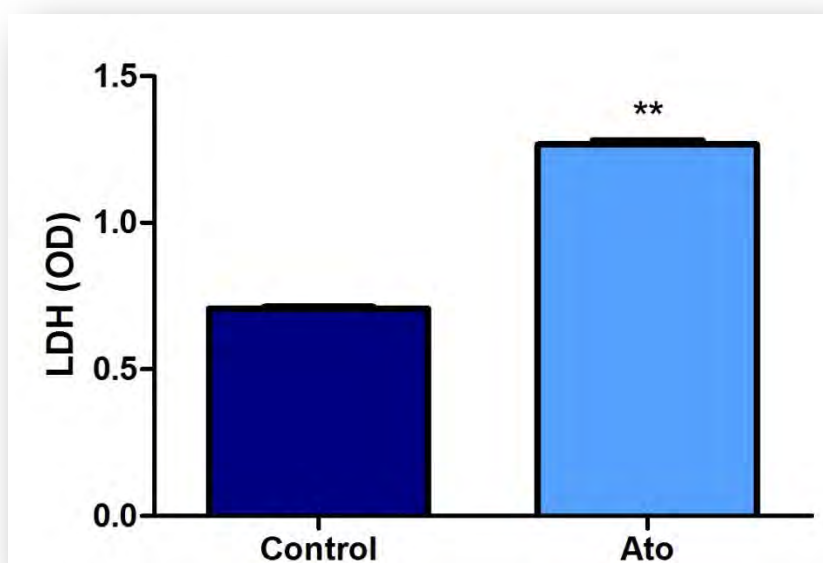


**Figure 3.7:** Level of extracellular LDH in ato treated cells (\*\* $p \leq 0.005$ ). OD: Optical density.

### 3.3.2 Analysis of caspases

Apoptotic cell death was evaluated by quantifying caspase activity using the Caspase-Glo® assays. Atorvastatin significantly increased the activities of caspase-3/7 ( $4.8 \times 10^5$  RLU  $\pm$   $1.3 \times 10^4$  RLU vs. control:  $1.7 \times 10^5$  RLU  $\pm$   $2.5 \times 10^4$  RLU;  $p=0.0003$ ) and -9 ( $2.6 \times 10^5$  RLU  $\pm$   $2.6 \times 10^3$  RLU vs. control:  $2.3 \times 10^5$  RLU  $\pm$   $1.4 \times 10^3$  RLU;  $p < 0.0001$ ) in comparison to the control. However, caspase-8 activity was significantly decreased by Ato compared to untreated cells ( $7.6 \times 10^4$  RLU  $\pm$   $1.5 \times 10^3$  RLU vs. control:  $1.8 \times 10^5$  RLU  $\pm$   $2.3 \times 10^4$  RLU;  $p=0.0025$ ) (Figure 3.8).



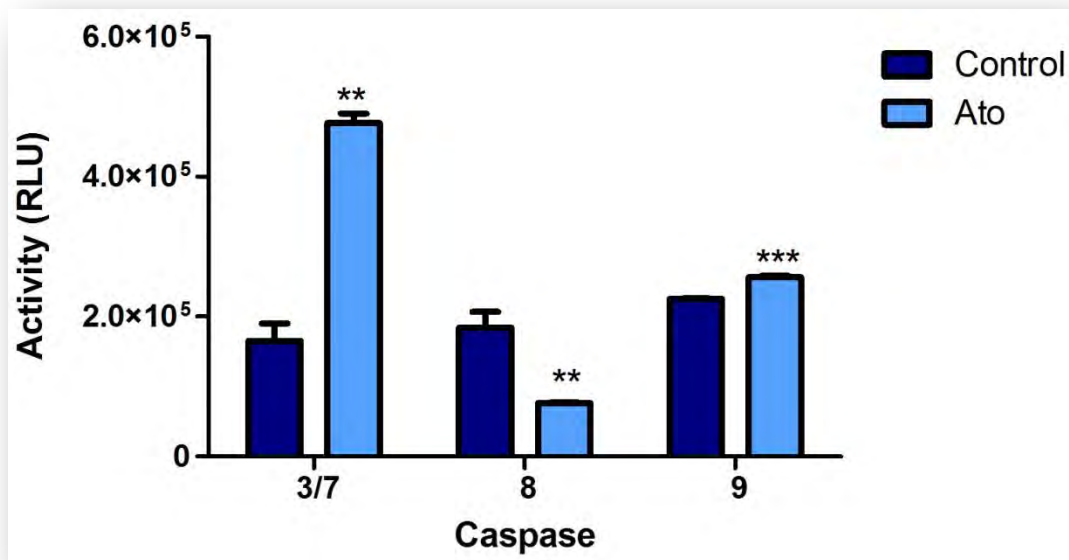


**Figure 3.8:** Caspase- 3/7 (\*\* $p \leq 0.005$ ), and -9 activities were significantly increased (\*\* $p \leq 0.0001$ ), and caspase-8 activity was significantly decreased in Ato treated cells (\*\* $p \leq 0.005$ ). RLU: relative light units.

### 3.3.3 Cytokine analysis

Next, the caspase-8 change was investigated as to its relation to the cytokine concentration of TNF- $\alpha$ , as well as the effect of Ato on IL-6. A significant decrease was seen in TNF- $\alpha$  following ato treatment as compared to the control ( $14.69 \pm 1.57$  pg/ml vs. control:  $18.11 \pm 1.57$  pg/ml;  $p = 0.0105$ ) (Figure 3.9 A). However, the IL-6 concentration was increased in treated cells ( $337.5 \pm 3.93$  pg/ml vs. control:  $286.4 \pm 6.20$  pg/ml;  $p = 0.0012$ ) (Figure 3.9 B).

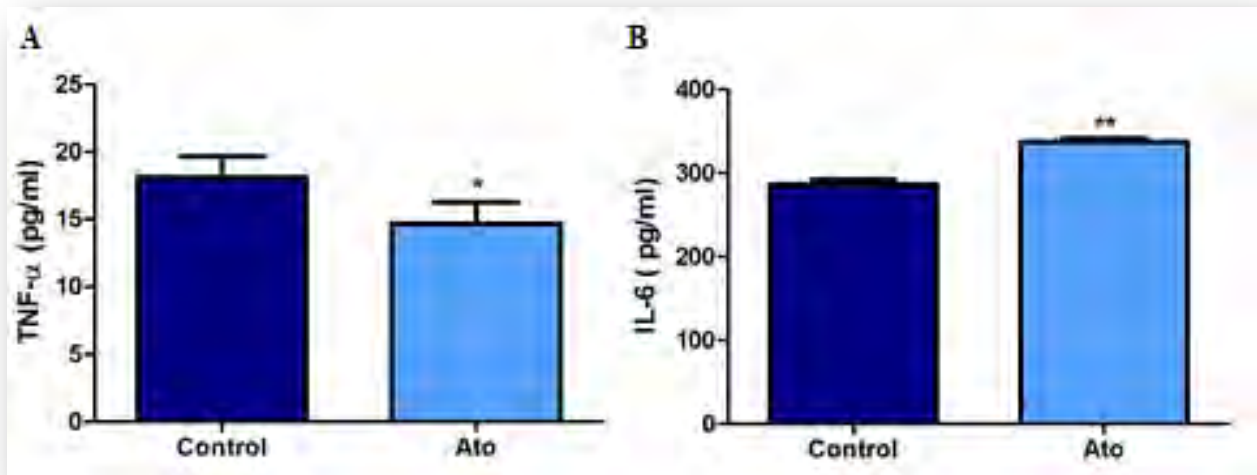


**Figure 3.9:** Mean cytokine concentration of (A) TNF- $\alpha$  was significantly decreased (\* $p \leq 0.05$ ), however IL-6 was elevated significantly (B) (\*\* $p \leq 0.01$ ).

### 3.4 Western Blotting

Due to the increased caspase -3/7 and -9 activity, protein expression of molecules involved in signalling pathway that promotes cell survival and growth was investigated. Western blot analysis confirmed significant decreases in both pAKT ( $0.41 \times 10^{-1}$  RBD  $\pm$   $6.7 \times 10^{-2}$  RBD vs. control:  $8.3 \times 10^{-1}$  RBD  $\pm$   $5.2 \times 10^{-2}$  RBD;  $p=0.0035$ ) (Figure 3.10 A) and AKT ( $5.1 \times 10^{-1}$  RBD  $\pm$   $1.2 \times 10^{-2}$  RBD vs. control:  $1.5$  RBD  $\pm$   $1.6 \times 10^{-1}$  RBD;  $p=0.0077$ ) in response to Ato treatment as compared to the control (Figure 3.10 B). This confirms that Ato inhibits the Protein kinase B signalling pathway in HepG2 cells.

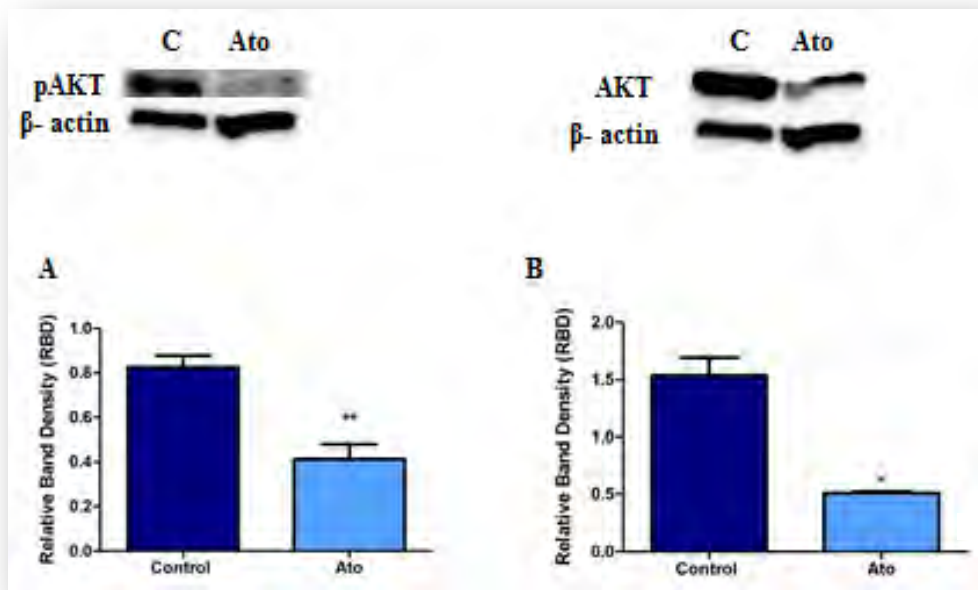


**Figure 3.10:** Protein expression of (A) pAKT (\*\* $p \leq 0.005$ ), and (B) AKT ( $*p \leq 0.05$ ) in HepG2 cells was significantly decreased following ato exposure. RBD: Relative band density

Next, we investigated protein expression of the downstream targets of AKT. Significant increases in pGSK3-( $\alpha/\beta$ ) ( $2.1 \times 10^{-1}$  RBD  $\pm 3.3 \times 10^{-2}$  RBD vs. control:  $1.3 \times 10^{-1}$  RBD  $\pm 2.0 \times 10^{-2}$  RBD;  $p=0.0338$ ) (Figure 3.11 A) and p53 ( $5.8 \times 10^{-1}$  RBD  $\pm 6.4 \times 10^{-2}$  RBD vs. control:  $2.0 \times 10^{-1}$  RBD  $\pm 4.4 \times 10^{-2}$  RBD;  $p=0.0032$ ) were seen in treated cells in comparison to the control (Figure 3.11 B).

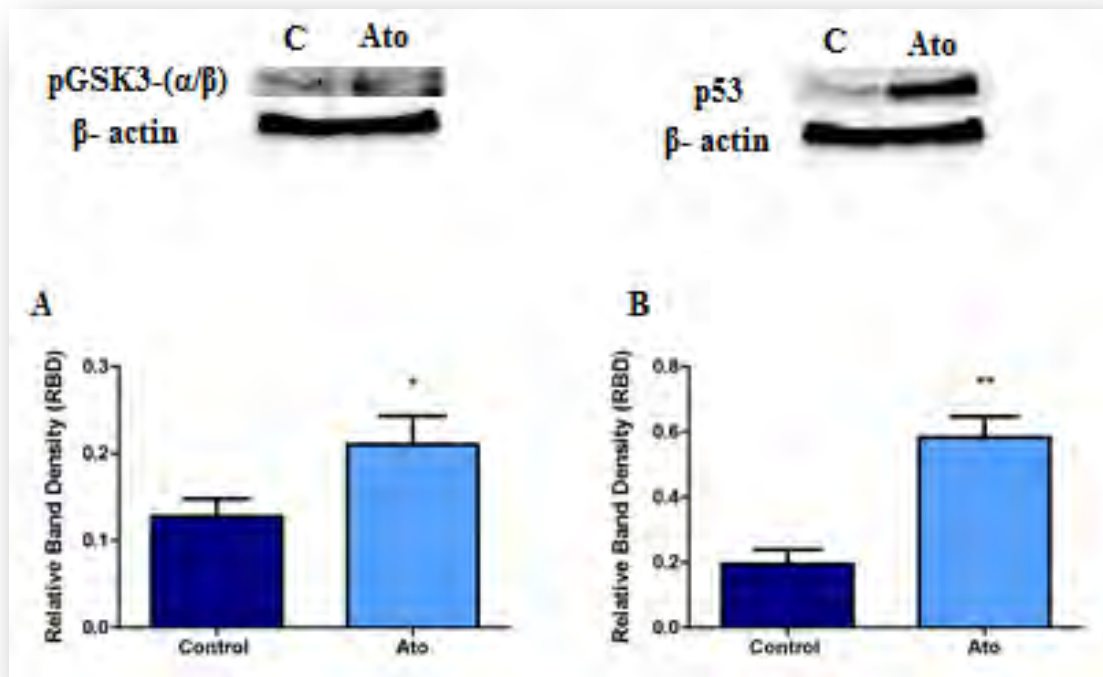


**Figure 3.11:** Protein expression of (A) pGSK3-(α/β) (\* $p \leq 0.05$ ) and (B) p53 (\*\* $p \leq 0.005$ ) was significantly increased by Atorvastatin. RBD: Relative band density

Anti-apoptotic targets of AKT: NF-κB, and IKK-β, were analysed for protein expression. Atorvastatin exposure led to significant decreases in both NF-κB ( $8.7 \times 10^{-1}$  RBD  $\pm$   $1.3 \times 10^{-1}$  RBD vs. control:  $1.4$  RBD  $\pm$   $1.2 \times 10^{-1}$  RBD;  $p=0.013$ ) (Figure 3.12 A) and IKK-β ( $3.8 \times 10^{-2}$  RBD  $\pm$   $8.3 \times 10^{-3}$  RBD vs. control:  $3.2 \times 10^{-1}$  RBD  $\pm$   $4.6 \times 10^{-2}$  RBD;  $p=0.0094$ ) expression in HepG2 cells as compared to the control (Figure 3.12 B).

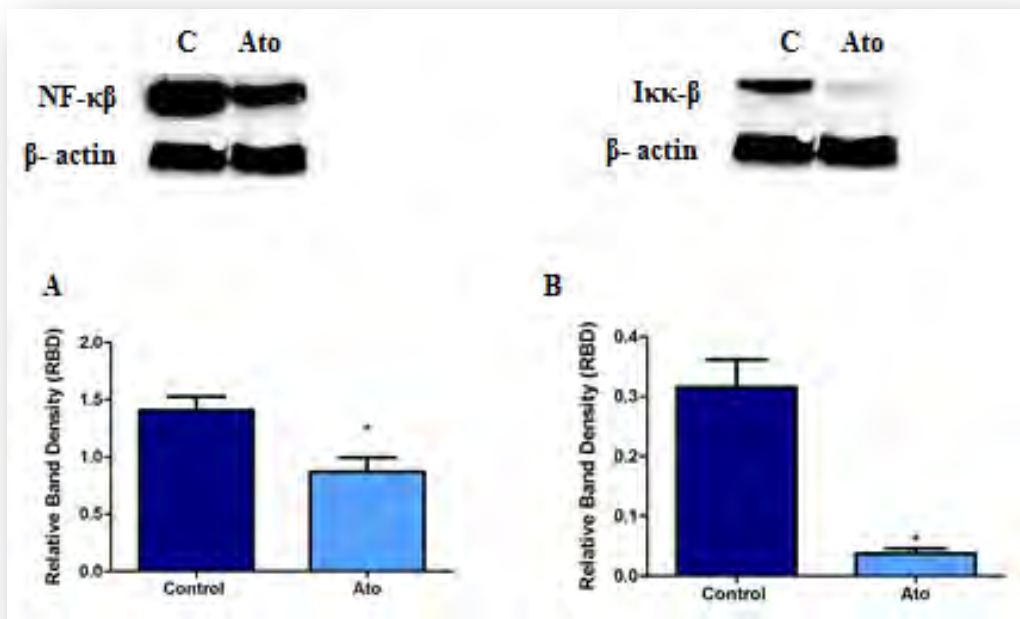


**Figure 3.12:** Protein expression of (A) NF-κB ( $*p \leq 0.05$ ) and (B) IKK-β ( $*p \leq 0.05$ ) in treated cells. RBD: Relative band density

## CHAPTER FOUR

### DISCUSSION

Statins are the most commonly prescribed drugs for treatment of cardiovascular disease (Watcharasi et al., 2002). Atorvastatin is the most frequently prescribed statin as it is well-tolerated and has a lower therapeutic dose in comparison to lovastatin, simvastatin and cerivastatin. Clinical trials have demonstrated the high benefit-risk ratio of atorvastatin (van Weeren et al., 1998). Recent studies suggest that statin use results in increased survival rates of cancer patients (Nielsen et al., 2012).

Tumourigenesis is a result of aberrant cellular growth accompanied by low apoptotic rates (Luzzi and Marletta, 2005). The process of apoptosis is either aberrant or inhibited in cancer cells (Schuler and Green, 2001). Cancerous cells are able to evade the apoptotic cascade, resulting in their uncontrolled growth (Hanahan and Weinberg, 2000). The effect of statins on cancer cells have been studied from as early as the 1990's (Agarwal et al., 1999). However, the molecular mechanism involved in their apoptotic effects remains a major focus of investigation.

In this study, we evaluated the effects of Ato on hepatocellular carcinoma (HepG2) cells. The MTT results depicted decreased dose-dependent cell viability (Figure 3.1) and reduced metabolic activity (Figure 3.2) by Ato in HepG2 cells. The enzyme HMGCR is responsible for the conversion of HMG-CoA to mevalonate. The compromised metabolic function may be a result of statin-induced HMGCR inhibition (Stancu and Sima, 2001); acetyl-coA accumulates in the mitochondria and is converted to citrate which is pumped to the cytosol (Oh et al., 2012). The conversion of dissolved MTT salts to its insoluble formazan product occurs via dehydrogenase enzymes (Slater et al., 1963). This may result in diminished reducing equivalents, hence, decreased conversion of MTT and production of intracellular ATP. Tumour cells promote ATP production by mitochondrial oxidative phosphorylation, which may be shifted to glycolysis for additional ATP production (Kim et al., 2008). Inhibition of HMGCR by statins limits not only cholesterol synthesis, but other vital isoprenoid intermediary metabolites, such as electron transport chain proteins like ubiquinone. The observed decrease in ATP levels (Figure 3.2) may be a result of impaired glucose uptake and reduced mt function due to the decreased ubiquinone level in HepG2 cells.

Numerous studies suggest that cancer cells experience increased oxidative stress associated with oncogenic transformation, changes in metabolic activity, and elevated levels of ROS, which promotes tumour progression and development (Behrend et al., 2003, Hileman et al., 2001, Kang and Hamasaki, 2003, Toyokuni et al., 1995). During cholesterol metabolism, Ras and Rac activation by geranylgeranylpyrophosphate (GGPP) stimulates NADPH oxidase, which is responsible for ROS production (Behrend et al., 2003, Wang et al., 2008, Wassmann et al., 2002, Yeganeh et al., 2014). Malondialdehyde was used as a measure of oxidative stress. The significant decrease in MDA (Figure 3.3) indicates decreased lipid peroxidation. The decreased ROS production may be a consequence of HMGCR inhibition. Furthermore, metabolically active mitochondria produce ROS via oxidative phosphorylation (Liou and Storz, 2010). The observed decrease in ATP concentration indicates impaired activity of mt ETC, correlating with diminished ROS production. Additionally, growth factors and cytokines such as TNF- $\alpha$  are known to stimulate ROS production (Lo and Cruz, 1995). The decreased level of TNF- $\alpha$  (Figure 3.9 A) is in agreement with the lower levels of ROS in treated cells.

The elevated levels of ROS in tumour cells, result in their acquisition of a concomitant robust antioxidant capacity, which leads to cancer cell growth (Zhao et al., 2016). Overproduction of GSH is well documented in various cancers (Townsend and Tew, 2003). During GSH production, NADPH is essential for the enzymatic function of glutathione reductase which converts GSSG to GSH (Berkholz et al., 2008). The decreased GSH concentration (Figure 3.5) is most likely a result of its NADPH-dependent mechanism, and correlates with diminished ROS levels.

Atorvastatin is metabolised by the CYP3A4 enzyme during first pass metabolism (Park et al., 2008a). During the catalytic cycle, one-electron transfer reactions take place which lead to the continuous formation of ROS (Puntarulo and Cederbaum, 1998). Interestingly, Ato decreased ROS levels despite the significant increase in CYP3A4 activity (Figure 3.6). The increase in CYP3A4 activity may be attributed to biotransformation of Ato.

In contrast to this study, other studies indicate that cancer cell death occurs via enhanced oxidative stress (Crescencio et al., 2009, Sánchez et al., 2008, Qi et al., 2013). The ROS-mediated cell death in these studies may be due to the presence of calcium in Ato. Studies which support the central role of calcium depicted altered calcium homeostasis following statin treatment (Nakahara et al., 1994, Pierno et al., 1999, Sirvent et al., 2005). Furthermore, statins have been shown to induce Ca<sup>2+</sup>-dependent mt permeability transition (Velho et al., 2006). In

this study, the amorphous form of Ato has a lower calcium level which corresponds to the lower level of ROS production.

The prenylation of Rho GTPases result in inhibition of endothelial NOS (eNOS) (Strykowska-Gora et al., 2015). Oxidation of L-Arginine to L-citrulline is catalysed by the NOS enzyme to generate NO (Luzzi and Marletta, 2005). Zhou et al., (2016) showed that high levels of NO inhibit the metastatic cascade in HCC (Zhou et al., 2016). Atorvastatin and simvastatin have been shown to decrease Rho prenylation in vascular smooth muscle cells (Blanco-Colio et al., 2002). This study indicates significantly increased NO metabolite production (Figure 3.4), which may be attributed to the ability of Ato to decrease Rho prenylation. This result is in agreement with Kanugula et al., (2014) where statins were shown to induce cell death by increased NO and diminished ROS (Kanugula et al., 2014). Taken together, these results provide evidence of the anti-proliferative and antioxidant effects of Ato in HepG2 cells, which are mediated by decreased ROS and increased NO production.

Cellular membranes are lipid in nature, allowing cholesterol-mediated lipid interactions to occur (Eggeling et al., 2009). The observed increase in LDH (Figure 3.7) may be due to the lipophilic nature of Ato. As a result, membrane damage and LDH leakage occurred. Cytokine-receptor binding promotes lipid PI3K activation at the cell membrane (Cantley, 2002). Activation of the Ras protein GTPase promotes PI3K activation of Akt to the lipid-rich membrane. Aberrant PI3K activity has been associated with various cancers (Chang et al., 2003, Fry, 2001, Jucker et al., 2002, Krasilnikov et al., 1999, 2010, Lin et al., 1999, Lin et al., 2001a). The decreased protein expression of both the active, phosphorylated form of AKT (pAKT) and total AKT (Figure 3.10) validates the LDH result. Atorvastatin inhibition of HMGCR prevents Ras-mediated PI3K activation which may lead to AKT inhibition. Our results are in agreement with a study that showed Ato-inhibition of Protein kinase B signalling in pancreatic cancer cells (Mistafa and Stenius, 2009).

Caspases are intracellular proteases that initiate apoptosis. Akt is known to phosphorylate pro-apoptotic members, resulting in caspase inhibition (Zhou et al., 2000). Our study indicates that Ato increased caspase -9 and -3/7 activity (Figure 3.8) which correlates with the decreased protein expression of Akt. The observed decrease in the extrinsic caspase-8 (Figure 3.8) indicates that Ato induces mitochondrial-mediated apoptosis. This result is in agreement with Aprigliano et al., where Ato was shown to induce apoptosis via the caspase-9-dependent pathway in hepatic stellate cells (Aprigliano et al., 2008). The decrease in TNF-  $\alpha$  cytokine



levels (Figure 3.9 A) by Ato may prevent ligand receptor binding at the cell membrane. This could explain why the extrinsic pathway was not activated as caspase-8 activity is mediated by this binding. However, it has been shown that with longer incubation periods, statins may induce caspase-8 activation (Minichsdorfer and Hohenegger, 2009).

Glycogen synthase kinase-3, a downstream target of Akt, plays an integral role in cell proliferation and apoptosis (Jope and Johnson, 2004). Apoptosis is promoted by GSK-3 via activation of tumour suppressor protein, p53, as well as inactivation of cell survival promoters like cyclin D<sub>1</sub> by phosphorylation (Watcharasit et al., 2002). Protein kinase B/Akt activation leads to GSK-3 inhibition (van Weeren et al., 1998). The observed upregulation of pGSK-3( $\alpha/\beta$ ) (active form) (Figure 3.11 A) correlates to the decreased Akt expression in treated cells. One of the mechanisms involved in apoptotic inhibition by Akt involves enhancement of Mdm2, which promotes p53 degradation (Gottlieb et al., 2002). The noted increase in p53 protein expression (Figure 3.11 B) may be attributed to inhibition of Mdm2. These results agree with a study showing pre-treatment with statins attenuates activity of cytostatic drugs, resulting in Akt inhibition and p53 stabilisation in HepG2, A549 and H1299 cells (Roudier et al., 2006). Schuler et al., (1999) showed that p53 potentiates apoptosis via cytochrome-c release (Schuler and Green, 2001). Together, the increased p53 expression as well as caspase-9 and -3/7 activity confirm mitochondrial-mediated cell death. Furthermore, the increased p53 expression may promote the tumour suppressor gene PTEN, resulting in the noted downregulation in Akt. Our results are in agreement with a study that shows modulation of PTEN expression with a concomitant decrease in Akt following treatment with (Miraglia et al., 2012) .

The anti-apoptotic and anti-inflammatory protein NF- $\kappa$ B, and its active form, IKK- $\beta$ , are downstream Akt substrates (Shao et al., 2001, Sun et al., 2010). Protein expression of NF- $\kappa$ B and IKK- $\beta$  (Figure 3.12) was significantly downregulated by Ato. This correlates with the decreased Akt expression. Although TNF- $\alpha$  plays a role in caspase activity, it is known to induce proinflammatory NF- $\kappa$ B (Beg and Baldwin, 1993, Beg and Baltimore, 1996). Additionally, the decreased NF- $\kappa$ B and IKK- $\beta$  expression may be a result of the decreased TNF- $\alpha$  cytokine level (Figure 3.9 A), thus indicating the anti-inflammatory effect of Ato. This result is consistent with a study by Rashidian et al., (2016), that showed the anti-inflammatory effect of Ato via decreased TNF- $\alpha$  levels and concomitant NF- $\kappa$ B inhibition (Rashidian et al., 2016).

Protein Kinase B is known to phosphorylate and inhibit FoxO (Kim et al., 2008). Evidence suggests the relation between IL-6 cytokine activity and STAT-3 mediated import of FoxO to

the nucleus, where its accumulation coincides with increased inhibitor or kappa-B kinase (IKK) and p27 expression. (Oh et al., 2012). Atorvastatin increased IL-6 activity (Figure 3.9 B) which validates the decreased IKK- $\beta$  expression; this may be a result of activation of IKK (inhibitor or kappa-B kinase) by FoxO. Evidence suggests that repressed PI3K/Akt activity leads to concomitant FoxO induction (Coussens and Werb, 2002). The Wnt pathway controls cell cycle entry C-myc activation via activation of c-Myc, cyclin D and p53 (Kanugula et al., 2014, Sun et al., 2010, Wassmann et al., 2002, Xie et al., 2014). Progression of the cell cycle through the G<sub>0</sub>/S phase may result through convergence of the PI3K/Akt/mTOR and Wnt pathways (Zhang et al., 2011). The decreased Akt (Figure 3.10) may have led to increased FoxO-mediated p53 (Figure 3.11 B) through p21 and p27 activation.

Previous studies have implicated the potential use of statins as anticancer agents (Chan et al., 2003a, Crescencio et al., 2009, Malenda et al., 2012). Simultaneously, it is well known that the PI3K/Akt signalling pathway is a major molecular target for chemotherapy (Chang et al., 2003). Collectively, the data suggests that Ato induces HepG2 cell death, as well as provides underlying mechanisms involved in the decreased oxidative stress and inhibition of the PI3K/Akt pathway.

## CHAPTER FIVE

### 5.1 Limitations of study

The use of one cell line, the molecular mechanism depicted by this study could be looked at in other cancerous cell types.

The results obtained from this *in vitro* study may differ from an *in vivo* study. This could be attributed to the cells being isolated. An *in vivo* study will allow for a truer result as it would look at the effect of Atorvastatin in a whole system.

### 5.2 CONCLUSION

The present study showed that Ato possessed potent apoptotic potential through its ability to reduce cholesterol and isoprenoid levels. This study has shown that Ato regulates HepG2 cell growth and proliferation by exerting antioxidant effects, which include decreased ROS and increased NO metabolite production. The mitochondrial mediated apoptotic pathway was activated via direct inhibition of the PI3K/Akt signalling pathway. Furthermore, Ato induced anti-inflammatory effects in HepG2 cells via inhibition of the NF- $\kappa$ B pathway.

This study provides evidence of the potential usage of Atorvastatin in chemotherapy. However, further studies are required in other cancerous cell lines to ensure consistency of Ato's effects. Atorvastatin-induced cell death via its involvement in the Pi3k/Akt/mTOR/Wnt pathways creates an avenue for further research. Prior to the use of statins in cancer treatment, it is essential to investigate the drug *in vivo*, as well as perform randomised clinical trials. It may also be interesting to determine the effect of statins in combined therapy, if they are found to be inefficient as monotherapy. It can be concluded that Ato shows potential as a therapeutic intervention in cancer.

## REFERENCES

- ADAMS, J. M. 2003. Ways of dying: multiple pathways to apoptosis. *Genes Dev*, 17, 2481-95.
- AGARWAL, B., BHENDWAL, S., HALMOS, B., MOSS, S. F., RAMEY, W. G. & HOLT, P. R. 1999. Lovastatin augments apoptosis induced by chemotherapeutic agents in colon cancer cells. *Clin Cancer Res*, 5, 2223-9.
- AMATI, B., ALEVIZOPOULOS, K. & VLACH, J. 1998. Myc and the cell cycle. *Front Biosci*, 3, d250-68.
- AMBROSONE, C. B. 2000. Oxidants and antioxidants in breast cancer. *Antioxidants & redox signaling*, 2, 903-917.
- APRIGLIANO, I., DUDAS, J., RAMADORI, G. & SAILE, B. 2008. Atorvastatin induces apoptosis by a caspase-9-dependent pathway: an in vitro study on activated rat hepatic stellate cells. *Liver International*, 28, 546-557.
- BEG, A. A. & BALDWIN, A. S., JR. 1993. The I kappa B proteins: multifunctional regulators of Rel/NF-kappa B transcription factors. *Genes Dev*, 7, 2064-70.
- BEG, A. A. & BALTIMORE, D. 1996. An essential role for NF-kappaB in preventing TNF-alpha-induced cell death. *Science*, 274, 782-4.
- BEG, A. A., FINCO, T. S., NANTERMET, P. V. & BALDWIN, A. S., JR. 1993. Tumor necrosis factor and interleukin-1 lead to phosphorylation and loss of I kappa B alpha: a mechanism for NF-kappa B activation. *Mol Cell Biol*, 13, 3301-10.
- BEHREND, L., HENDERSON, G. & ZWACKA, R. M. 2003. Reactive oxygen species in oncogenic transformation. *Biochemical Society Transactions*, 31, 1441-1444.
- BERKHOLZ, D. S., FABER, H. R., SAVVIDES, S. N. & KARPLUS, P. A. 2008. Catalytic cycle of human glutathione reductase near 1 Å resolution. *J Mol Biol*, 382, 371-84.
- BLANCO-COLIO, L. M., VILLA, A., ORTEGO, M., HERNÁNDEZ-PRESA, M. A., PASCUAL, A., PLAZA, J. J. & EGIDO, J. 2002. 3-Hydroxy-3-methyl-glutaryl coenzyme A reductase inhibitors, atorvastatin and simvastatin, induce apoptosis of vascular smooth muscle cells by downregulation of Bcl-2 expression and Rho A prenylation. *Atherosclerosis*, 161, 17-26.
- BOURS, V., BENTIREN-ALJ, M., HELLIN, A. C., VIATOUR, P., ROBE, P., DELHALLE, S., BENOIT, V. & MERVILLE, M. P. 2000. Nuclear factor-kappa B, cancer, and apoptosis. *Biochem Pharmacol*, 60, 1085-9.
- BRUEGEL, M., TEUPSER, D., HAFFNER, I., MUELLER, M. & THIERY, J. 2006. Statins reduce macrophage inflammatory protein-1alpha expression in human activated monocytes. *Clin Exp Pharmacol Physiol*, 33, 1144-9.
- CAFFORIO, P., DAMMACCO, F., GERNONE, A. & SILVESTRIS, F. 2005. Statins activate the mitochondrial pathway of apoptosis in human lymphoblasts and myeloma cells. *Carcinogenesis*, 26, 883-91.
- CANTLEY, L. C. 2002. The phosphoinositide 3-kinase pathway. *Science*, 296, 1655-7.
- CHAN, K. K., OZA, A. M. & SIU, L. L. 2003a. The statins as anticancer agents. *Clin Cancer Res*, 9, 10-9.
- CHAN, K. K. W., OZA, A. M. & SIU, L. L. 2003b. The Statins as Anticancer Agents. *Clinical Cancer Research*, 9, 10-19.
- CHANG, F., LEE, J., NAVOLANIC, P., STEELMAN, L., SHELTON, J., BLALOCK, W., FRANKLIN, R. & MCCUBREY, J. 2003. Involvement of PI3K/Akt pathway in cell cycle progression, apoptosis, and neoplastic transformation: a target for cancer chemotherapy. *Leukemia*, 17, 590-603.
- CHEN, J., LIU, B., YUAN, J., YANG, J., ZHANG, J., AN, Y., TIE, L., PAN, Y. & LI, X. 2012. Atorvastatin reduces vascular endothelial growth factor (VEGF) expression in human non-small cell lung carcinomas (NSCLCs) via inhibition of reactive oxygen species (ROS) production. *Mol Oncol*, 6, 62-72.

- CHEN, Q., VAZQUEZ, E. J., MOGHADDAS, S., HOPPEL, C. L. & LESNEFSKY, E. J. 2003. Production of reactive oxygen species by mitochondria central role of complex III. *Journal of Biological Chemistry*, 278, 36027-36031.
- COLE, M. D. 1986a. Activation of the c-myc oncogene. *Basic Life Sci*, 38, 399-406.
- COLE, M. D. 1986b. The myc oncogene: its role in transformation and differentiation. *Annu Rev Genet*, 20, 361-84.
- COUSSENS, L. M. & WERB, Z. 2002. Inflammation and cancer. *Nature*, 420, 860-7.
- CRESCENCIO, M. E., RODRÍGUEZ, E., PÁEZ, A., MASSO, F. A., MONTAÑO, L. F. & LÓPEZ-MARURE, R. 2009. Statins inhibit the proliferation and induce cell death of human papilloma virus positive and negative cervical cancer cells. *International journal of biomedical science: IJBS*, 5, 411.
- DATTA, S. R., DUDEK, H., TAO, X., MASTERS, S., FU, H., GOTOH, Y. & GREENBERG, M. E. 1997. Akt phosphorylation of BAD couples survival signals to the cell-intrinsic death machinery. *Cell*, 91, 231-41.
- DAVIGNON, J., JACOB, R. F. & MASON, R. P. 2004. The antioxidant effects of statins. *Coronary Artery Disease*, 15, 251-258.
- DECLUE, J. E., VASS, W. C., PAPAGEORGE, A. G., LOWY, D. R. & WILLUMSEN, B. M. 1991. Inhibition of cell growth by lovastatin is independent of ras function. *Cancer Res*, 51, 712-7.
- DELGADO, M. D. & LEON, J. 2010. Myc roles in hematopoiesis and leukemia. *Genes Cancer*, 1, 605-16.
- DENNIS, L. K., LYNCH, C. F. & TORNER, J. C. 2002. Epidemiologic association between prostatitis and prostate cancer. *Urology*, 60, 78-83.
- DENOYELLE, C., VASSE, M., KORNER, M., MISHAL, Z., GANNE, F., VANNIER, J. P., SORIA, J. & SORIA, C. 2001. Cerivastatin, an inhibitor of HMG-CoA reductase, inhibits the signaling pathways involved in the invasiveness and metastatic properties of highly invasive breast cancer cell lines: an in vitro study. *Carcinogenesis*, 22, 1139-48.
- DING, X. & KAMINSKY, L. S. 2003. HUMAN EXTRAHEPATIC CYTOCHROMES P450: Function in Xenobiotic Metabolism and Tissue-Selective Chemical Toxicity in the Respiratory and Gastrointestinal Tracts\*. *Annual review of pharmacology and toxicology*, 43, 149-173.
- DRÖGE, W. 2002. Free radicals in the physiological control of cell function. *Physiological reviews*, 82, 47-95.
- EGGELING, C., RINGEMANN, C., MEDDA, R., SCHWARZMANN, G., SANDHOFF, K., POLYAKOVA, S., BELOV, V. N., HEIN, B., VON MIDDENDORFF, C. & SCHÖNLE, A. 2009. Direct observation of the nanoscale dynamics of membrane lipids in a living cell. *Nature*, 457, 1159-1162.
- EMERIT, I. 1994. Reactive oxygen species, chromosome mutation, and cancer: possible role of clastogenic factors in carcinogenesis. *Free Radical Biology and Medicine*, 16, 99-109.
- ERL, W. 2005. Statin-induced vascular smooth muscle cell apoptosis: a possible role in the prevention of restenosis? *Current Drug Targets-Cardiovascular & Hematological Disorders*, 5, 135-144.
- ESCARCEGA, R. O., FUENTES-ALEXANDRO, S., GARCIA-CARRASCO, M., GATICA, A. & ZAMORA, A. 2007. The transcription factor nuclear factor-kappa B and cancer. *Clin Oncol (R Coll Radiol)*, 19, 154-61.
- ESCOT, C., THEILLET, C., LIDERAU, R., SPYRATOS, F., CHAMPEME, M. H., GEST, J. & CALLAHAN, R. 1986. Genetic alteration of the c-myc protooncogene (MYC) in human primary breast carcinomas. *Proc Natl Acad Sci U S A*, 83, 4834-8.
- FAVALORO, B., ALLOCATI, N., GRAZIANO, V., DI ILIO, C. & DE LAURENZI, V. 2012. Role of apoptosis in disease. *Aging (Albany NY)*, 4, 330-49.
- FEDERICO, A., MORGILLO, F., TUCCILLO, C., CIARDIELLO, F. & LOGUERCIIO, C. 2007. Chronic inflammation and oxidative stress in human carcinogenesis. *International Journal of Cancer*, 121, 2381-2386.

- FREYTAG, S. O. 1988. Enforced expression of the c-myc oncogene inhibits cell differentiation by precluding entry into a distinct predifferentiation state in G0/G1. *Mol Cell Biol*, 8, 1614-24.
- FRY, M. J. 2001. Phosphoinositide 3-kinase signalling in breast cancer: how big a role might it play? *Breast Cancer Research*, 3, 1.
- GOLDSTEIN, J. L. & BROWN, M. S. 1990. Regulation of the mevalonate pathway. *Nature*, 343, 425.
- GOTTLIEB, T. M., LEAL, J. F., SEGER, R., TAYA, Y. & OREN, M. 2002. Cross-talk between Akt, p53 and Mdm2: possible implications for the regulation of apoptosis. *Oncogene*, 21, 1299-303.
- HALLIWELL, B. & CHIRICO, S. 1993. Lipid peroxidation: its mechanism, measurement, and significance. *The American journal of clinical nutrition*, 57, 715S-724S.
- HALLIWELL, B. & GUTTERIDGE, J. M. 2015. *Free radicals in biology and medicine*, Oxford University Press, USA.
- HANAHAH, D. & WEINBERG, R. A. 2000. The hallmarks of cancer. *cell*, 100, 57-70.
- HANAHAH, D. & WEINBERG, R. A. 2011. Hallmarks of cancer: the next generation. *cell*, 144, 646-674.
- HENGARTNER, M. O. 2000. The biochemistry of apoptosis. *Nature*, 407, 770-776.
- HILEMAN, E. A., ACHANTA, G. & HUANG, P. 2001. Superoxide dismutase: an emerging target for cancer therapeutics. *Expert Opinion on Therapeutic Targets*, 5, 697-710.
- HOQUE, A., CHEN, H. & XU, X.-C. 2008. Statin induces apoptosis and cell growth arrest in prostate cancer cells. *Cancer Epidemiology Biomarkers & Prevention*, 17, 88-94.
- HOWE, L. R. 2007. Inflammation and breast cancer. Cyclooxygenase/prostaglandin signaling and breast cancer. *Breast Cancer Res*, 9, 210.
- JACOBS, D., BLACKBURN, H., HIGGINS, M., REED, D., ISO, H., MCMILLAN, G., NEATON, J., NELSON, J., POTTER, J., RIFKIND, B. & ET AL. 1992. Report of the Conference on Low Blood Cholesterol: Mortality Associations. *Circulation*, 86, 1046-60.
- JIALAL, I., STEIN, D., BALIS, D., GRUNDY, S. M., ADAMS-HUET, B. & DEVARAJ, S. 2001. Effect of hydroxymethyl glutaryl coenzyme a reductase inhibitor therapy on high sensitive C-reactive protein levels. *Circulation*, 103, 1933-5.
- JOHNSON, T. E., ZHANG, X., BLEICHER, K. B., DYSART, G., LOUGHLIN, A. F., SCHAEFER, W. H. & UMBENHAUER, D. R. 2004. Statins induce apoptosis in rat and human myotube cultures by inhibiting protein geranylgeranylation but not ubiquinone. *Toxicology and applied pharmacology*, 200, 237-250.
- JOPE, R. S. & JOHNSON, G. V. 2004. The glamour and gloom of glycogen synthase kinase-3. *Trends in biochemical sciences*, 29, 95-102.
- JUCKER, M., SUDEL, K., HORN, S., SICKEL, M., WEGNER, W., FIEDLER, W. & FELDMAN, R. 2002. Expression of a mutated form of the p85a regulatory subunit of phosphatidylinositol 3-kinase in a Hodgkin's lymphoma-derived cell line (CO). *Leukemia*, 16, 894-901.
- KAMAT, A. M. & NELKIN, G. M. 2005. Atorvastatin: a potential chemopreventive agent in bladder cancer. *Urology*, 66, 1209-1212.
- KANG, D. & HAMASAKI, N. 2003. Mitochondrial oxidative stress and mitochondrial DNA. *Clinical chemistry and laboratory medicine*, 41, 1281-1288.
- KANUGULA, A. K., GOLLAVILLI, P. N., VASAMSETTI, S. B., KARNEWAR, S., GOPOJU, R., UMMANNI, R. & KOTAMRAJU, S. 2014. Statin-induced inhibition of breast cancer proliferation and invasion involves attenuation of iron transport: intermediacy of nitric oxide and antioxidant defence mechanisms. *FEBS Journal*, 281, 3719-3738.
- KEYOMARSI, K., SANDOVAL, L., BAND, V. & PARDEE, A. B. 1991. Synchronization of tumor and normal cells from G1 to multiple cell cycles by lovastatin. *Cancer Res*, 51, 3602-9.

- KIM, D. H., KIM, J. Y., YU, B. P. & CHUNG, H. Y. 2008. The activation of NF- $\kappa$ B through Akt-induced FOXO1 phosphorylation during aging and its modulation by calorie restriction. *Biogerontology*, 9, 33-47.
- KLAUNIG, J. E., XU, Y., ISENBERG, J. S., BACHOWSKI, S., KOLAJA, K. L., JIANG, J., STEVENSON, D. E. & WALBORG JR, E. F. 1998. The role of oxidative stress in chemical carcinogenesis. *Environmental Health Perspectives*, 106, 289.
- KOTLIAROVA, S., PASTORINO, S., KOVELL, L. C., KOTLIAROV, Y., SONG, H., ZHANG, W., BAILEY, R., MARIC, D., ZENKLUSEN, J. C., LEE, J. & FINE, H. A. 2008. Glycogen synthase kinase-3 inhibition induces glioma cell death through c-MYC, nuclear factor-kappaB, and glucose regulation. *Cancer Res*, 68, 6643-51.
- KRACUN, M., KOCIJAN, A., BASTARDA, A., GRAHEK, R., PLAVEC, J. & KOCJAN, D. 2009. Isolation and structure determination of oxidative degradation products of atorvastatin. *J Pharm Biomed Anal*, 50, 729-36.
- KRASILNIKOV, M., ADLER, V., FUCHS, S. Y., DONG, Z., HAIMOVITZ-FRIEDMAN, A., HERLYN, M. & RONAI, Z. E. 1999. Contribution of phosphatidylinositol 3-kinase to radiation resistance in human melanoma cells. *Molecular carcinogenesis*, 24, 64-69.
- KULINSKY, V. I. 2007. Biochemical aspects of inflammation. *Biochemistry (Mosc)*, 72, 595-607.
- LAKHA, F., THEODORATOU, E., FARRINGTON, S. M., TENESA, A., CETNARSKYJ, R., DIN, F. V., PORTEOUS, M. E., DUNLOP, M. G. & CAMPBELL, H. 2012. Statin use and association with colorectal cancer survival and risk: case control study with prescription data linkage. *BMC Cancer*, 12, 487.
- LALIER, L., CARTRON, P. F., JUIN, P., NEDELKINA, S., MANON, S., BECHINGER, B. & VALLETTE, F. M. 2007. Bax activation and mitochondrial insertion during apoptosis. *Apoptosis*, 12, 887-96.
- LAW, M. R. & THOMPSON, S. G. 1991. Low serum cholesterol and the risk of cancer: an analysis of the published prospective studies. *Cancer Causes Control*, 2, 253-61.
- LEE, J. E., BABA, Y., NG, K., GIOVANNUCCI, E., FUCHS, C. S., OGINO, S. & CHAN, A. T. 2011. Statin use and colorectal cancer risk according to molecular subtypes in two large prospective cohort studies. *Cancer Prev Res (Phila)*, 4, 1808-15.
- LIAO, J. K. & LAUFS, U. 2005. Pleiotropic effects of statins. *Annual review of pharmacology and toxicology*, 45, 89.
- LIN, J., ADAM, R. M., SANTIESTEVEAN, E. & FREEMAN, M. R. 1999. The phosphatidylinositol 3'-kinase pathway is a dominant growth factor-activated cell survival pathway in LNCaP human prostate carcinoma cells. *Cancer Research*, 59, 2891-2897.
- LIN, X., BÖHLE, A., DOHRMANN, P., LEUSCHNER, I., SCHULZ, A., KREMER, B. & FÄNDRICH, F. 2001a. Overexpression of phosphatidylinositol 3-kinase in human lung cancer. *Langenbeck's Archives of Surgery*, 386, 293-301.
- LIN, X., BOHLE, A. S., DOHRMANN, P., LEUSCHNER, I., SCHULZ, A., KREMER, B. & FÄNDRICH, F. 2001b. Overexpression of phosphatidylinositol 3-kinase in human lung cancer. *Langenbecks Arch Surg*, 386, 293-301.
- LIU, G.-Y. & STORZ, P. 2010. Reactive oxygen species in cancer. *Free radical research*, 44, 479-496.
- LITTLE, C. D., NAU, M. M., CARNEY, D. N., GAZDAR, A. F. & MINNA, J. D. 1983. Amplification and expression of the c-myc oncogene in human lung cancer cell lines. *Nature*, 306, 194-6.
- LIU, Y., FISKUM, G. & SCHUBERT, D. 2002. Generation of reactive oxygen species by the mitochondrial electron transport chain. *Journal of neurochemistry*, 80, 780-787.
- LO, Y. Y. & CRUZ, T. F. 1995. Involvement of reactive oxygen species in cytokine and growth factor induction of c-fos expression in chondrocytes. *Journal of Biological Chemistry*, 270, 11727-11730.

- LUO, J., MANNING, B. D. & CANTLEY, L. C. 2003. Targeting the PI3K-Akt pathway in human cancer: rationale and promise. *Cancer Cell*, 4, 257-62.
- LUZZI, S. D. & MARLETTA, M. A. 2005. L-arginine analogs as alternate substrates for nitric oxide synthase. *Bioorganic & medicinal chemistry letters*, 15, 3934-3941.
- MA, X. & YU, H. 2006. Global burden of cancer. *Yale J Biol Med*, 79, 85-94.
- MALEND A., SKROBANSKA, A., ISSAT, T., WINIARSKA, M., BIL, J., OLESZCZAK, B., SINSKI, M., FIRCUK, M., BUJNICKI, J. M., CHLEBOWSKA, J., STARUCH, A. D., GLODKOWSKA-MROWKA, E., KUNIKOWSKA, J., KROLICKI, L., SZABLEWSKI, L., GACIONG, Z., KOZIAK, K., JAKOBISIAK, M., GOLAB, J. & NOWIS, D. A. 2012. Statins impair glucose uptake in tumor cells. *Neoplasia*, 14, 311-23.
- MANSOURI, D., MCMILLAN, D. C., ROXBURGH, C. S., CRIGHTON, E. M. & HORGAN, P. G. 2013. The impact of aspirin, statins and ACE-inhibitors on the presentation of colorectal neoplasia in a colorectal cancer screening programme. *Br J Cancer*, 109, 249-56.
- MATUSEWICZ, L., MEISSNER, J., TOPORKIEWICZ, M. & SIKORSKI, A. F. 2015. The effect of statins on cancer cells—review. *Tumor Biology*, 36, 4889-4904.
- MCCUBREY, J. A., STEELMAN, L. S., CHAPPELL, W. H., ABRAMS, S. L., WONG, E. W., CHANG, F., LEHMANN, B., TERRIAN, D. M., MILELLA, M., TAFURI, A., STIVALA, F., LIBRA, M., BASECKE, J., EVANGELISTI, C., MARTELLI, A. M. & FRANKLIN, R. A. 2007. Roles of the Raf/MEK/ERK pathway in cell growth, malignant transformation and drug resistance. *Biochim Biophys Acta*, 1773, 1263-84.
- MERSCH-SUNDERMANN, V., KNASMULLER, S., WU, X. J., DARROUDI, F. & KASSIE, F. 2004. Use of a human-derived liver cell line for the detection of cytoprotective, antigenotoxic and cogenotoxic agents. *Toxicology*, 198, 329-40.
- MINICHSDORFER, C. & HOHENEGGER, M. 2009. Autocrine amplification loop in statin-induced apoptosis of human melanoma cells. *British journal of pharmacology*, 157, 1278-1290.
- MIRAGLIA, E., HOGBERG, J. & STENIUS, U. 2012. Statins exhibit anticancer effects through modifications of the pAkt signaling pathway. *International journal of oncology*, 40, 867.
- MISTAFA, O. & STENIUS, U. 2009. Statins inhibit Akt/PKB signaling via P2X7 receptor in pancreatic cancer cells. *Biochemical pharmacology*, 78, 1115-1126.
- MOLOWA, D. T. & CIMIS, G. M. 1989. Co-ordinate regulation of low-density-lipoprotein receptor and 3-hydroxy-3-methylglutaryl-CoA reductase and synthase gene expression in HepG2 cells. *Biochemical Journal*, 260, 731-736.
- NAKAHARA, K., YADA, T., KURIYAMA, M. & OSAME, M. 1994. Cytosolic Ca<sup>2+</sup> increase and cell damage in L6 rat myoblasts by HMG-CoA reductase inhibitors. *Biochemical and biophysical research communications*, 202, 1579-1585.
- NAKANO, H., NAKAJIMA, A., SAKON-KOMAZAWA, S., PIAO, J., XUE, X. & OKUMURA, K. 2006. Reactive oxygen species mediate crosstalk between NF-κB and JNK. *Cell Death & Differentiation*, 13, 730-737.
- NAWROCKI, J. W., WEISS, S. R., DAVIDSON, M. H., SPRECHER, D. L., SCHWARTZ, S. L., LUPIEN, P. J., JONES, P. H., HABER, H. E. & BLACK, D. M. 1995. Reduction of LDL cholesterol by 25% to 60% in patients with primary hypercholesterolemia by atorvastatin, a new HMG-CoA reductase inhibitor. *Arterioscler Thromb Vasc Biol*, 15, 678-82.
- NEWMAN, T. B. & HULLEY, S. B. 1996. Carcinogenicity of lipid-lowering drugs. *JAMA*, 275, 55-60.
- NG, K., OGINO, S., MEYERHARDT, J. A., CHAN, J. A., CHAN, A. T., NIEDZWIECKI, D., HOLLIS, D., SALTZ, L. B., MAYER, R. J., BENSON, A. B., 3RD, SCHAEFER, P. L., WHITCOM, R., HANTEL, A., GOLDBERG, R. M., BERTAGNOLLI, M. M., VENOOK, A. P. & FUCHS, C. S. 2011. Relationship between statin use and colon



- cancer recurrence and survival: results from CALGB 89803. *J Natl Cancer Inst*, 103, 1540-51.
- NIELSEN, S. F., NORDESTGAARD, B. G. & BOJESSEN, S. E. 2012. Statin use and reduced cancer-related mortality. *N Engl J Med*, 367, 1792-802.
- OH, H.-M., YU, C.-R., DAMBUZA, I., MARRERO, B. & EGWUAGU, C. E. 2012. STAT3 protein interacts with Class O Forkhead transcription factors in the cytoplasm and regulates nuclear/cytoplasmic localization of FoxO1 and FoxO3a proteins in CD4+ T cells. *Journal of Biological Chemistry*, 287, 30436-30443.
- OTT, M., GOGVADZE, V., ORRENIUS, S. & ZHIVOTOVSKY, B. 2007. Mitochondria, oxidative stress and cell death. *Apoptosis*, 12, 913-922.
- PAN, Y., ABD-RASHID, B. A., ISMAIL, Z., ISMAIL, R., MAK, J. W., POOK, P. C., ER, H. M. & ONG, C. E. 2010. In vitro modulatory effects on three major human cytochrome P450 enzymes by multiple active constituents and extracts of *Centella asiatica*. *Journal of ethnopharmacology*, 130, 275-283.
- PARK, J. E., KIM, K. B., BAE, S. K., MOON, B. S., LIU, K. H. & SHIN, J. G. 2008a. Contribution of cytochrome P450 3A4 and 3A5 to the metabolism of atorvastatin. *Xenobiotica*, 38, 1240-51.
- PARK, K. W., HWANG, K. K., CHO, H. J., HUR, J., YANG, H. M., YOON, C. H., KANG, H. J., OH, B. H., PARK, Y. B. & KIM, H. S. 2008b. Simvastatin enhances endothelial differentiation of peripheral blood mononuclear cells in hypercholesterolemic patients and induces pro-angiogenic cytokine IL-8 secretion from monocytes. *Clin Chim Acta*, 388, 156-66.
- PEDERSEN, T. R., WILHELMSEN, L., FAERGEMAN, O., STRANDBERG, T. E., THORGEIRSSON, G., TROEDSSON, L., KRISTIANSON, J., BERG, K., COOK, T. J., HAGHFELT, T., KJEKSHUS, J., MIETTINEN, T., OLSSON, A. G., PYORALA, K. & WEDEL, H. 2000. Follow-up study of patients randomized in the Scandinavian simvastatin survival study (4S) of cholesterol lowering. *Am J Cardiol*, 86, 257-62.
- PIERNO, S., DE LUCA, A., LIANTONIO, A., CAMERINO, C. & CAMERINO, D. C. 1999. Effects of HMG-CoA reductase inhibitors on excitation-contraction coupling of rat skeletal muscle. *European journal of pharmacology*, 364, 43-48.
- PROSKURYAKOV, S. Y., KONOPLYANNIKOV, A. G. & GABAI, V. L. 2003. Necrosis: a specific form of programmed cell death? *Exp Cell Res*, 283, 1-16.
- PUNTARULO, S. & CEDERBAUM, A. I. 1998. Production of reactive oxygen species by microsomes enriched in specific human cytochrome P450 enzymes. *Free Radical Biology and Medicine*, 24, 1324-1330.
- QI, X. F., ZHENG, L., LEE, K. J., KIM, D. H., KIM, C. S., CAI, D. Q., WU, Z., QIN, J. W., YU, Y. H. & KIM, S. K. 2013. HMG-CoA reductase inhibitors induce apoptosis of lymphoma cells by promoting ROS generation and regulating Akt, Erk and p38 signals via suppression of mevalonate pathway. *Cell Death Dis*, 4, e518.
- RASHIDIAN, A., MUHAMMADNEJAD, A., DEHPOUR, A.-R., MEHR, S. E., AKHAVAN, M. M., SHIRKOOHI, R., CHAMANARA, M., MOUSAVI, S.-E. & REZAYAT, S.-M. 2016. Atorvastatin attenuates TNBS-induced rat colitis: the involvement of the TLR4/NF-kB signaling pathway. *Inflammopharmacology*, 24, 109-118.
- REED, J. C. 1999. Dysregulation of apoptosis in cancer. *J Clin Oncol*, 17, 2941-53.
- REUTER, S., GUPTA, S. C., CHATURVEDI, M. M. & AGGARWAL, B. B. 2010. Oxidative stress, inflammation, and cancer: how are they linked? *Free Radical Biology and Medicine*, 49, 1603-1616.
- ROMASHKOVA, J. A. & MAKAROV, S. S. 1999. NF-kappaB is a target of AKT in anti-apoptotic PDGF signalling. *Nature*, 401, 86-90.
- ROSA, G. M., CARBONE, F., PARODI, A., MASSIMELLI, E. A., BRUNELLI, C., MACH, F., VUILLEUMIER, N. & MONTECUCCO, F. 2014. Update on the efficacy of statin treatment in acute coronary syndromes. *Eur J Clin Invest*, 44, 501-15.

- ROUDIER, E., MISTAFA, O. & STENIUS, U. 2006. Statins induce mammalian target of rapamycin (mTOR)-mediated inhibition of Akt signaling and sensitize p53-deficient cells to cytostatic drugs. *Molecular cancer therapeutics*, 5, 2706-2715.
- RUBIO-MOSCARDO, F., BLESÁ, D., MESTRE, C., SIEBERT, R., BALASAS, T., BENITO, A., ROSENWALD, A., CLIMENT, J., MARTINEZ, J. I., SCHILHABEL, M., KARRAN, E. L., GESK, S., ESTELLER, M., DELEEUEW, R., STAUDT, L. M., FERNANDEZ-LUNA, J. L., PINKEL, D., DYER, M. J. S. & MARTINEZ-CLIMENT, J. A. 2005. Characterization of 8p21.3 chromosomal deletions in B-cell lymphoma: TRAIL-R1 and TRAIL-R2 as candidate dosage-dependent tumor suppressor genes. *Blood*, 106, 3214-3222.
- SÁNCHEZ, C. A., RODRÍGUEZ, E., VARELA, E., ZAPATA, E., PÁEZ, A., MASSÓ, F. A., MONTAÑO, L. F. & LÓPEZ-MARURE, R. 2008. Statin-induced inhibition of MCF-7 breast cancer cell proliferation is related to cell cycle arrest and apoptotic and necrotic cell death mediated by an enhanced oxidative stress. *Cancer investigation*, 26, 698-707.
- SCHACHTER, M. 2005. Chemical, pharmacokinetic and pharmacodynamic properties of statins: an update. *Fundamental & clinical pharmacology*, 19, 117-125.
- SCHIMMER, A. D. 2004. Inhibitor of apoptosis proteins: translating basic knowledge into clinical practice. *Cancer Res*, 64, 7183-90.
- SCHULER, M. & GREEN, D. 2001. Mechanisms of p53-dependent apoptosis. *Biochemical Society Transactions*, 29, 684-688.
- SCHWARTZ, G. G., OLSSON, A. G., EZEKOWITZ, M. D., GANZ, P., OLIVER, M. F., WATERS, D., ZEIHNER, A., CHAITMAN, B. R., LESLIE, S. & STERN, T. 2001. Effects of atorvastatin on early recurrent ischemic events in acute coronary syndromes: the MIRACL study: a randomized controlled trial. *Jama*, 285, 1711-1718.
- SCHWARTZMAN, R. A. & CIDLOWSKI, J. A. 1993. Apoptosis: the biochemistry and molecular biology of programmed cell death. *Endocr Rev*, 14, 133-51.
- SHAO, R., TSAI, E. M., WEI, K., VON LINDERN, R., CHEN, Y. H., MAKINO, K. & HUNG, M. C. 2001. E1A inhibition of radiation-induced NF-kappaB activity through suppression of IKK activity and IkappaB degradation, independent of Akt activation. *Cancer Res*, 61, 7413-6.
- SHEPHERD, J., COBBE, S. M., FORD, I., ISLES, C. G., LORIMER, A. R., MACFARLANE, P. W., MCKILLOP, J. H. & PACKARD, C. J. 1995. Prevention of coronary heart disease with pravastatin in men with hypercholesterolemia. *New England Journal of Medicine*, 333, 1301-1308.
- SHERR, C. J. & ROBERTS, J. M. 1999. CDK inhibitors: positive and negative regulators of G1-phase progression. *Genes Dev*, 13, 1501-12.
- SIRVENT, P., MERCIER, J., VASSORT, G. & LACAMPAGNE, A. 2005. Simvastatin triggers mitochondria-induced Ca<sup>2+</sup> signaling alteration in skeletal muscle. *Biochemical and biophysical research communications*, 329, 1067-1075.
- SLATER, T., SAWYER, B. & STRÄULI, U. 1963. Studies on succinate-tetrazolium reductase systems: III. Points of coupling of four different tetrazolium salts III. Points of coupling of four different tetrazolium salts. *Biochimica et biophysica acta*, 77, 383-393.
- STANCU, C. & SIMA, A. 2001. Statins: mechanism of action and effects. *Journal of cellular and molecular medicine*, 5, 378-387.
- STEWART, B. & WILD, C. P. 2016. World cancer report 2014. *World*.
- STORZ, P. 2005. Reactive oxygen species in tumor progression. *Front Biosci*, 10, 1881-1896.
- STRANDBERG, T. E., FEELY, J. & SIGURDSSON, E. L. 2004. Twelve-week, multicenter, randomized, open-label comparison of the effects of rosuvastatin 10 mg/d and atorvastatin 10 mg/d in high-risk adults: a DISCOVERY study. *Clinical Therapeutics*, 26, 1821-1833.
- STRYJKOWSKA-GORA, A., KARCZMAREK-BOROWSKA, B., GORA, T. & KRAWCZAK, K. 2015. Statins and cancers. *Contemp Oncol (Pozn)*, 19, 167-75.

- SUGANUMA, M., OKABE, S., MARINO, M. W., SAKAI, A., SUEOKA, E. & FUJIKI, H. 1999. Essential role of tumor necrosis factor alpha (TNF-alpha) in tumor promotion as revealed by TNF-alpha-deficient mice. *Cancer Res*, 59, 4516-8.
- SUN, Z. J., CHEN, G., HU, X., ZHANG, W., LIU, Y., ZHU, L. X., ZHOU, Q. & ZHAO, Y. F. 2010. Activation of PI3K/Akt/IKK-alpha/NF-kappaB signaling pathway is required for the apoptosis-evasion in human salivary adenoid cystic carcinoma: its inhibition by quercetin. *Apoptosis*, 15, 850-63.
- TOWNSEND, D. M. & TEW, K. D. 2003. The role of glutathione-S-transferase in anti-cancer drug resistance. *Oncogene*, 22, 7369-75.
- TOYOKUNI, S., OKAMOTO, K., YODOI, J. & HIAI, H. 1995. Persistent oxidative stress in cancer. *FEBS Letters*, 358, 1-3.
- URBICH, C., KNAU, A., FICHTLSCHERER, S., WALTER, D. H., BRUHL, T., POTENTE, M., HOFMANN, W. K., DE VOS, S., ZEIHNER, A. M. & DIMMELER, S. 2005. FOXO-dependent expression of the proapoptotic protein Bim: pivotal role for apoptosis signaling in endothelial progenitor cells. *FASEB J*, 19, 974-6.
- VAN WEEREN, P. C., DE BRUYN, K. M., DE VRIES-SMITS, A. M., VAN LINT, J. & BOUDEWIJN, M. T. 1998. Essential role for protein kinase B (PKB) in insulin-induced glycogen synthase kinase 3 inactivation characterization of dominant-negative mutant of PKB. *Journal of Biological Chemistry*, 273, 13150-13156.
- VELHO, J. A., OKANOBO, H., DEGASPERI, G. R., MATSUMOTO, M. Y., ALBERICI, L. C., COSSO, R. G., OLIVEIRA, H. C. & VERCESI, A. E. 2006. Statins induce calcium-dependent mitochondrial permeability transition. *Toxicology*, 219, 124-132.
- WANG, C. Y., LIU, P. Y. & LIAO, J. K. 2008. Pleiotropic effects of statin therapy: molecular mechanisms and clinical results. *Trends Mol Med*, 14, 37-44.
- WANG, C. Y., MAYO, M. W. & BALDWIN, A. S., JR. 1996. TNF- and cancer therapy-induced apoptosis: potentiation by inhibition of NF-kappaB. *Science*, 274, 784-7.
- WASSMANN, S., LAUFS, U., MULLER, K., KONKOL, C., AHLBORY, K., BAUMER, A. T., LINZ, W., BOHM, M. & NICKENIG, G. 2002. Cellular antioxidant effects of atorvastatin in vitro and in vivo. *Arterioscler Thromb Vasc Biol*, 22, 300-5.
- WATCHARASIT, P., BIJUR, G. N., ZMIJEWSKI, J. W., SONG, L., ZMIJEWSKA, A., CHEN, X., JOHNSON, G. V. & JOPE, R. S. 2002. Direct, activating interaction between glycogen synthase kinase-3 $\beta$  and p53 after DNA damage. *Proceedings of the National Academy of Sciences*, 99, 7951-7955.
- WESTERINK, W. M. & SCHOONEN, W. G. 2007. Cytochrome P450 enzyme levels in HepG2 cells and cryopreserved primary human hepatocytes and their induction in HepG2 cells. *Toxicology in Vitro*, 21, 1581-1591.
- WILSON, K., AND WALKER, J. 2010. *Principles and Techniques of Biochemistry and Molecular Biology*, Cambridge, Cambridge University Press.
- WONG, W. W., DIMITROULAKOS, J., MINDEN, M. D. & PENN, L. Z. 2002. HMG-CoA reductase inhibitors and the malignant cell: the statin family of drugs as triggers of tumor-specific apoptosis. *Leukemia*, 16, 508-19.
- WOODGETT, J. R. 1994. Regulation and functions of the glycogen synthase kinase-3 subfamily. *Semin Cancer Biol*, 5, 269-75.
- WRIGHT, R., FLAPAN, A., MCMURRAY, J., SLATTERY, J., WHITE, H. & SPAULDING, C. 1994. Randomised trial of cholesterol lowering in 4444 patients with coronary heart disease: the Scandinavian Simvastatin Survival Study (4S). *Lancet*, 344, 1383-1389.
- XIA, Z., TAN, M. M., WONG, W. W., DIMITROULAKOS, J., MINDEN, M. D. & PENN, L. Z. 2001. Blocking protein geranylgeranylation is essential for lovastatin-induced apoptosis of human acute myeloid leukemia cells. *Leukemia*, 15, 1398-407.
- XIE, S., CHEN, M., YAN, B., HE, X., CHEN, X. & LI, D. 2014. Identification of a role for the PI3K/AKT/mTOR signaling pathway in innate immune cells. *PLoS One*, 9, e94496.
- YEGANEH, B., WIECHEC, E., ANDE, S. R., SHARMA, P., MOGHADAM, A. R., POST, M., FREED, D. H., HASHEMI, M., SHOJAEI, S., ZEKI, A. A. & GHAVAMI, S. 2014.

- Targeting the mevalonate cascade as a new therapeutic approach in heart disease, cancer and pulmonary disease. *Pharmacol Ther*, 143, 87-110.
- ZANGAR, R. C., BOLLINGER, N., WEBER, T. J., TAN, R. M., MARKILLIE, L. M. & KARIN, N. J. 2011. Reactive oxygen species alter autocrine and paracrine signaling. *Free Radical Biology and Medicine*, 51, 2041-2047.
- ZANGAR, R. C., DAVYDOV, D. R. & VERMA, S. 2004. Mechanisms that regulate production of reactive oxygen species by cytochrome P450. *Toxicology and applied pharmacology*, 199, 316-331.
- ZHANG, X., TANG, N., HADDEN, T. J. & RISHI, A. K. 2011. Akt, FoxO and regulation of apoptosis. *Biochimica et Biophysica Acta (BBA)-Molecular Cell Research*, 1813, 1978-1986.
- ZHAO, M., LIU, Q., GONG, Y., XU, X., ZHANG, C., LIU, X., ZHANG, C., GUO, H., ZHANG, X., GONG, Y. & SHAO, C. 2016. GSH-dependent antioxidant defense contributes to the acclimation of colon cancer cells to acidic microenvironment. *Cell Cycle*, 15, 1125-33.
- ZHOU, H., LI, X.-M., MEINKOTH, J. & PITTMAN, R. N. 2000. Akt regulates cell survival and apoptosis at a postmitochondrial level. *The Journal of cell biology*, 151, 483-494.
- ZHOU, L., ZHANG, H. & WU, J. 2016. Effects of nitric oxide on the biological behavior of HepG2 human hepatocellular carcinoma cells. *Experimental and therapeutic medicine*, 11, 1875-1880.

## APPENDIX 1

### MTT RAW DATA

<b>CONCENTRATION (<math>\mu\text{g/ml}</math>)</b>	<b>LOG CONCENTRATION</b>	<b>AVERAGE OPTICAL DENSITY</b>	<b>CELL VIABILITY (%)</b>
<b>0</b>	0.00	0.74	100
<b>200</b>	2.30	0.63	84
<b>400</b>	2.60	0.50	67
<b>600</b>	2.78	0.42	57
<b>800</b>	2.90	0.34	46
<b>1000</b>	3.00	0.27	36
<b>1200</b>	3.08	0.21	28

## APPENDIX 2

### GSH standards

<b>Standard</b>	<b>Average optical density</b>
<b>0</b>	521313
<b>3.125</b>	1169990
<b>6.25</b>	2310695
<b>12.5</b>	4002510
<b>25</b>	5613455
<b>50</b>	6614740

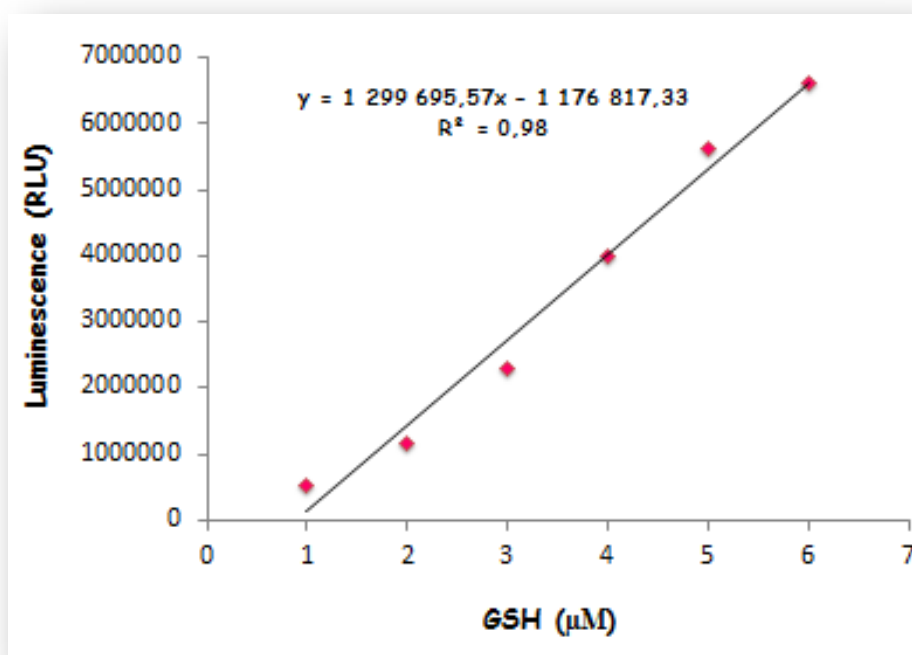


**Figure 1:** Standard curve generated from GSH standards.

### APPENDIX 3

#### ELISA standards- TNF- $\alpha$

Standards were prepared using a stock concentration of 116ng.

Standards	Average OD
0	-0.1135
7.8	-0.1145
15.6	-0.0925
31.3	-0.0285
62.5	0.111
125	0.3245
250	0.79
500	1.618

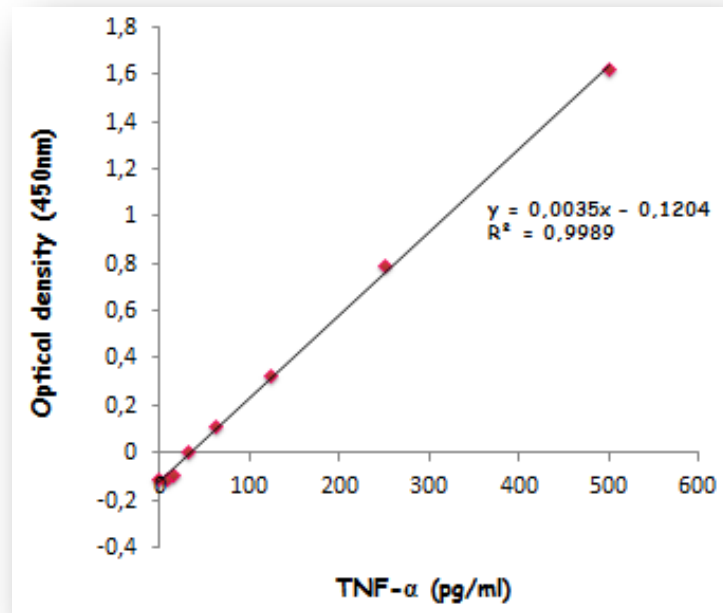


Figure 2: Standard curve generated from TNF- $\alpha$  standards.

## ELISA standards- IL-6

Standards were prepared using a stock concentration of 18ng.

Standards	Average OD
0	-0.654
4.7	-0.6205
9.4	-0.5865
18.8	-0.4935
37.5	-0.4275
75	-0.1705
150	0.1945
300	1.0315

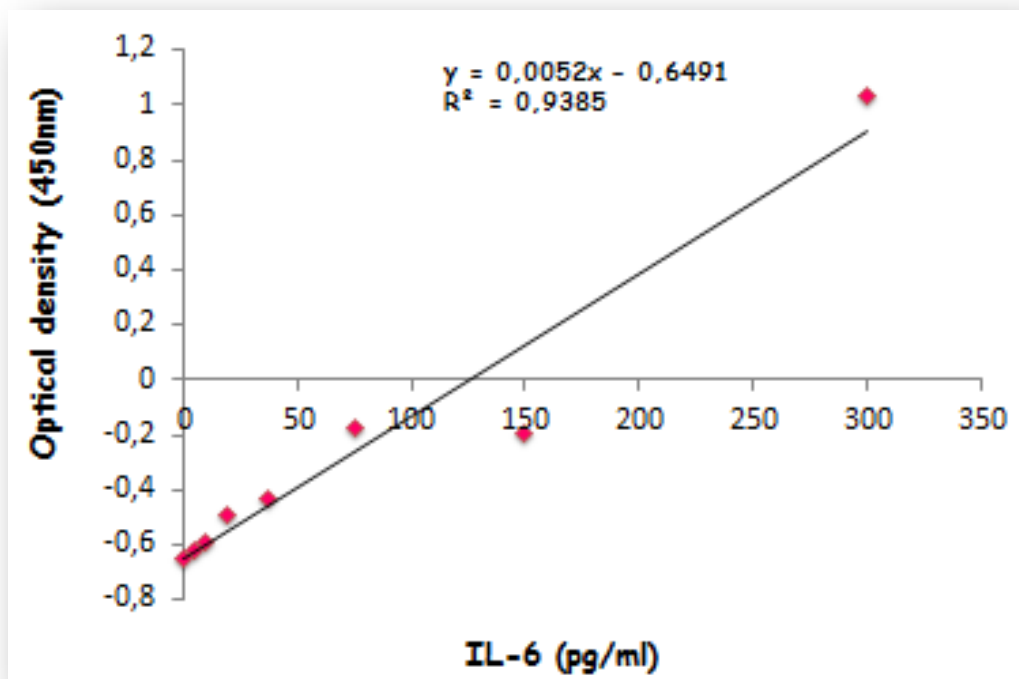


Figure 3: Standard curve generated from IL-6 standards.



## ELISA standards- IL-1 $\beta$

Standards were prepared using a stock concentration of 25ng.

Standards	Average OD
0	-0.1545
3.9	-0.149
7.8	-0.0995
15.6	-0.0425
31.3	0.0905
62.5	0.3335
125	0.773
250	1.56

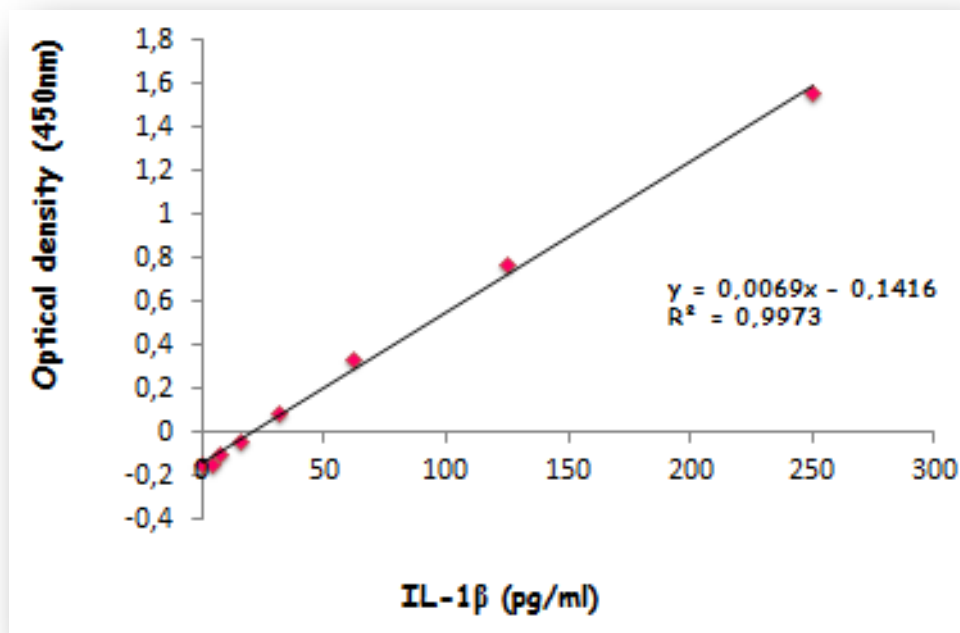


**Figure 4:** Standard curve generated from IL-1 $\beta$  standards.

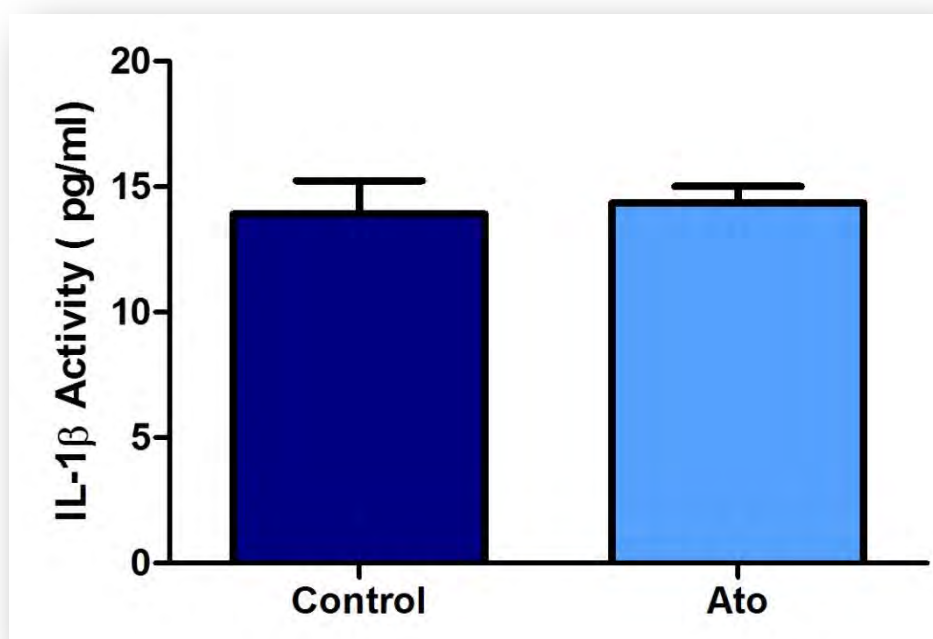


**Figure 5:** No significant change in IL-1 $\beta$  between control and treated cells

#### ELISA standards- IL-10

Standards were prepared using a stock concentration of 13ng.

Standards	Average OD
0	-0.4245
7.8	-0.5055
15.6	-0.386
31.3	-0.4595
62.5	-0.337
125	-0.208
250	0.0915
500	0.331

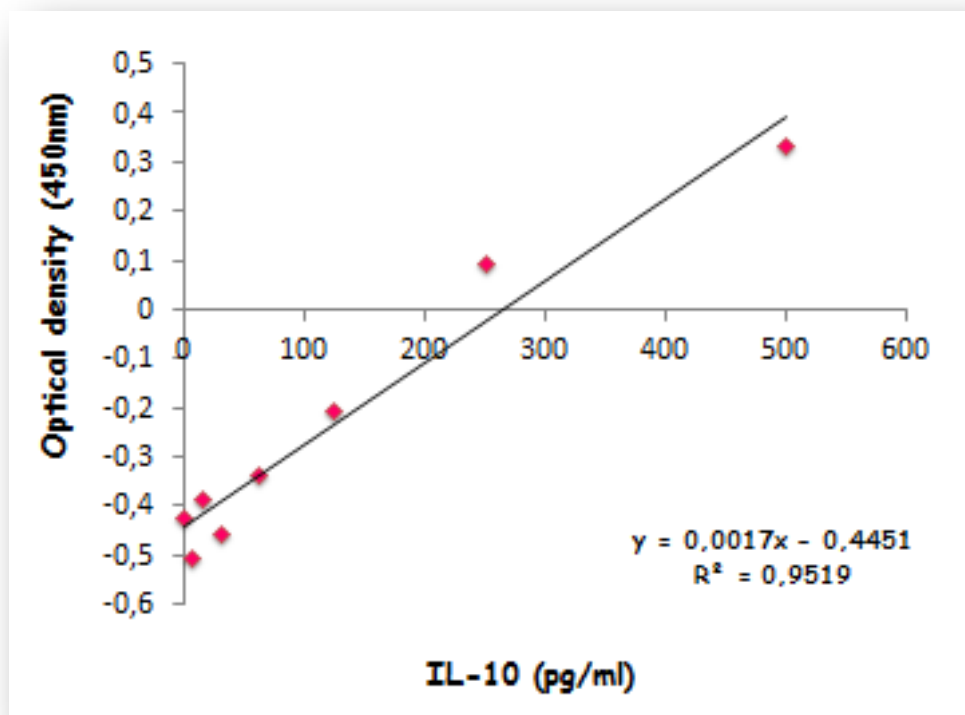


**Figure 6:** Standard curve generated from IL-10 standards.

The concentrations for TNF- $\alpha$ , IL-6, IL-1 $\beta$ , and IL-10 were prepared and used to generate the standard curves above. The curve was extrapolated and the equations displayed on the graphs were used to determine the respective cytokine concentrations of control and Ato-treated cells.

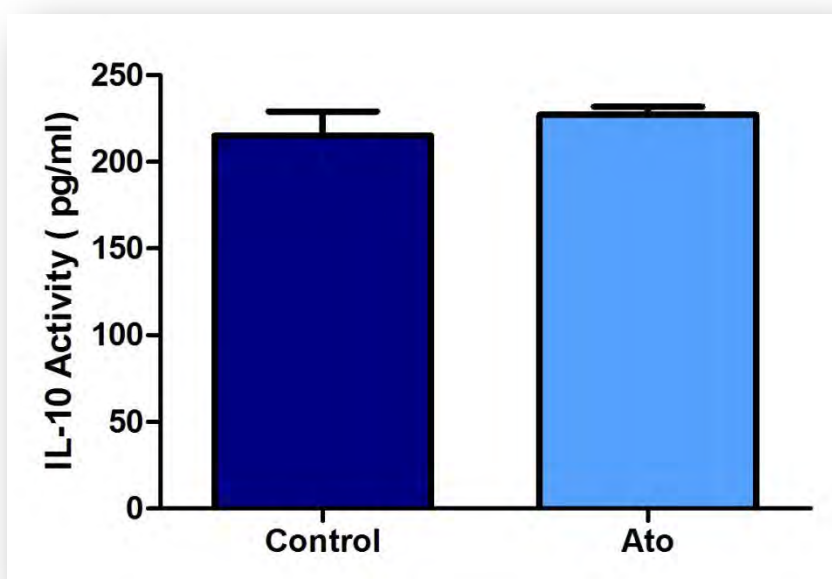
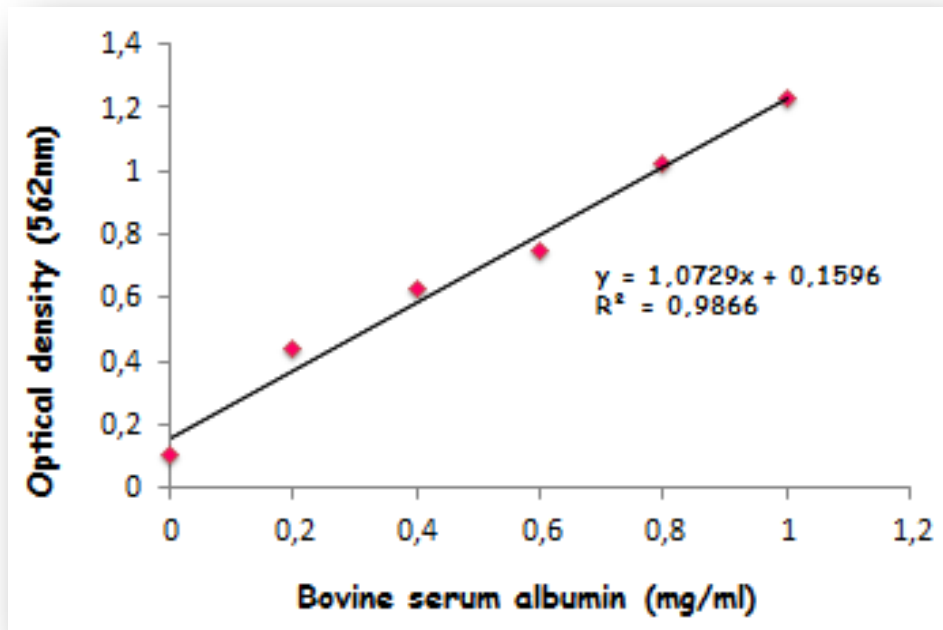


Figure 7: No significant change in IL-10 between control and treated cells

#### APPENDIX 4

##### Protein quantification and standardisation

Standard	Bovine serum albumin (BSA) (mg/ml)					
	0	0.2	0.4	0.6	0.8	1
OD1	0.108	0.412	0.623	0.754	1.099	1.231
OD2	0.105	0.455	0.587	0.746	1.025	1.276
OD3	0.105	0.444	0.670	0.756	0.947	1.186
Average	0.106	0.437	0.627	0.752	1.024	1.231



**Figure 8:** Standard curve generated from BSA standards.